The Intrinsic Caspase Death Pathway in Stroke Neurodegeneration

Nsikan Enekan Akpan

Submitted in partial fulfillment of the
requirements for the degree of
Doctor of Philosophy
in the Graduate School of Arts and Sciences

COLUMBIA UNIVERSITY

2013

ABSTRACT

The Intrinsic Caspase Death Pathway in Stroke Neurodegeneration

Nsikan Enekan Akpan

Stroke has been a major source of morbidity and mortality for centuries. Eight-five percent of all strokes are ischemic in nature, meaning they are caused by the occlusion of a major cerebral artery. Despite extensive research to develop effective treatments for ischemic stroke, therapeutic options remain limited.

Apoptosis (also termed "programmed cell death") is a process by which a stressed or damaged cell commits "suicide". In stroke, runaway apoptosis contributes to stroke neurodegeneration and neurological decline for days to weeks after disease onset.

Cysteine-ASPartic proteASEs (caspases) are key mediators of apoptosis that are activated in distinct molecular pathways, but their impact in stroke is poorly defined. Direct evidence for caspase activation in stroke and the functional relevance of this activity has not been previously characterized.

For this dissertation, we developed an unbiased technique for *in vivo* trapping of active caspases in rodent models of ischemic stroke. We isolated active caspase-9 as a principal contributor to ischemic neurodegeneration in rodents (*Rattus norvegicus* & *Mus musculus*). Caspase-9 is the initiator caspase for the intrinsic cell death pathway.

Intranasal delivery of a novel, cell membrane-penetrating inhibitor for caspase-9 confirmed the pathogenic relevance of caspase-9 activity in stroke. Caspase-9 inhibition provided neurofunctional protection and established caspase-6 as its downstream target. Caspase-6 is an effector caspase and a member of the intrinsic death pathway that has never been implicated in stroke until now.

Coincidentally, we discovered that caspase-6 is specifically activated within the axonal compartment. The temporal and spatial pattern of activation demonstrates that neuronal caspase-9 activity induces caspase-6 activation, which mediates axonal loss in the early stages of stroke (<24 hours). We developed a novel inhibitor for caspase-6, based on a catalytically inactive clone, which demonstrated neuroprotective and axoprotective efficacy against ischemia. Collectively, these results assert that selective inhibition of caspase-9 and caspase-6 is an effective translational strategy for stroke.

The impact of caspase activity is not restricted to neuronal death, as caspases can exacerbate inflammation and alter glial function. Thus, caspases are logical therapeutic targets for stroke. However, they have never been clinically evaluated due to a paucity of ideal drug candidates. This dissertation outlines fresh insights into the mechanisms of stroke neurodegeneration and offers novel caspase-based therapeutic strategies for clinical evaluation.

TABLE OF CONTENTS

LIST OF FIGURES

Chapter 1

Chapter 3

Chapter 4.

Chapter 5.

LIST OF TABLES

Chapter 1.

Chapter 2.

LIST OF ABBREVIATIONS AND ACRONYMS

AD	Alzheimer's disease
BIR	Baculoviral IAP Repeat
BBB	Blood Brain Barrier
bVADfmk	Biotin-Valine-Alanine-Aspartate(OMe)-Fluoromethylketone (bVADfmk
C6-/-	Caspase-6 null
C6DN	Caspase-6 Dominant Negative
CARD	Caspase Activation and Recruitment Domains
CED	Convection-enhanced Delivery
Cl-C3	Cleaved Caspase-3
Cl-C6	Cleaved Caspase-6
CNS	Central Nervous System
Contra	Contralateral
DAB	Diaminobenzidine
DISC	Death-Inducing Signaling Complex

DED	Death Effector Domain
DEVD	Aspartate-Glutamate-Valine-Aspartate
Diablo	Direct IAP Binding Protein With Low pI
ECM	Extracellular Matrix
FADD	Fas-Associated Protein With Death Domain
FG	Fluorogold
GFAP	Glial Fibrillary Acidic Protein
H&E	Hematoxylin and Eosin
HtrA2	High-Temperature-Regulated A2
hpr	Hour Post Reperfusion
HNE	4-hydroxynonenal
IL-1β	Interleukin-1 Beta
IAP	Inhibitor of Apoptosis Protein.
Ipsi	Ipsilateral
LACI	Lacunar Infarct
MCA	Middle Cerebral Artery
MAP-2	Microtubule-Associated Protein 2
MMP	Matrix Metalloproteinase
mRNA	Messenger Ribonucleic Acid
NeuN	Neuronal Nuclear Antigen
NF-L	Neurofilament Light Chain
NGF	Nerve Growth Factor
ONC	Optic Nerve Crush

OMM	Outer Mitochondrial Membrane
PACI	Partial Anterior Circulation Infarct
Pen1	Penetratin1
PA	Plasminogen Activator
POCI	Posterior Circulation Infarct
RGC	Retinal Ganglion Cell
RNAi	Ribonucleic Acid Interference
siRNA	Small/Short Interfering Ribonucleic Acid
miRNA	microRibonucleic Acid
SDS-PAGE	Sodium Dodecyl Sulfate Polyacrylamide Gel Electrophoresis
siCASP2	Caspase-2 Small/Short Interfering Ribonucleic Acid
SMAC	Second Mitochondria-derived Activator Of Caspases
SMA	Smooth Muscle Actin
TJ	Tight Junction
TIMP-1	Tissue Inhibitor Of Metalloproteinases 1
TIA	Transient Ischemic Attack
tMCAo	Transient Middle Cerebral Artery Occlusion
TNF-R1	Tumor Necrosis Factor Receptor 1
TACI	Total Anterior Circulation Infarct
TTC	2,3,5-Triphenyltetrazolium chloride
Tuj1	βIII-tubulin
VEID	Valine–Glutamate–Isoleucine–Aspartate
XIAP	X-linked inhibitor of apoptosis protein

XBIR3	X-linked Inhibitor of Apoptosis Protein Baculoviral IAP Repeat Domain 3
zVAD	benzyloxycarbonyl-Valine-Alanine-Aspartate

ACKNOWLEDGEMENTS

While my name is the only one on the front of this dissertation, it would be specious to believe that this project was performed on my own.

First, I would like to thank my doctoral advisor, Carol Troy, for accepting me as your student and trusting me with such a wonderful project. I have learned a great deal under your tutelage, and I am extremely proud and grateful for what we have been able to accomplish together. Thank you.

Thank you to my undergraduate advisor at Bard College, Michael Tibbetts. You established my scientific foundation. I find myself constantly referring to your sage advice and emulating your ethos as a scientist, a mentor, a writer, and an adult, so thank you.

Special thanks to my former research mentors at Tufts University. To Marina Chuenkova and Mercio PereiraPerrin, thank you for nurturing my confidence and scientific acumen. To Henry Wortis and Diana Pierce, thank you for all of your support over the years. Also Di, thanks for picking up all of those tabs.

I owe an enormous amount of gratitude to my scientific collaborators for aiding the execution of this multifaceted project.

To Esther Serrano-Saiz, thank you for training me when I first joined Dr. Troy's lab and for your friendship over the years.

To E. Sander Connolly and the medical fellows in your neurosurgical unit, Brad Zacharia, Andrew Ducruet, and Marc Otten, you have my sincerest gratitude. I must add a special thanks to my "strokers": Greg Cohen, Sergey Sosunov, and Richard Hwang. This project completely relied on your deft hands.

To Guy Salvesen and Scott Snipas at the Sanford-Burnham Institute, thank you for your guidance and expertise with caspase inhibitors. To Zubair Ahmed, thank you for testing Pen1-C6DN in your ocular degeneration model.

Many thanks to my thesis committee—Lloyd Greene, Ronald Liem, and Gilbert Di Paolo—for your guidance and helpful suggestions towards the completion of this project. Thank you to Wilma Friedman and Marc Tessier-Lavigne for participating with my defense committee.

To Lloyd Greene, Michael Shelanski, and your lab members, thank you for your comments at lab meeting, general scientific advice, and, most importantly, for your camaraderie.

I would also like to acknowledge my mentors from my first rotation: Ottavio Arancio, Mikako Sakurai, and Elena Leznik.

Tremendous appreciation goes to my student "minions": Jennifer Velloza, Amar Vora, Wen Liu, Danielle Fernandes, Alex Kim, and Erin Glennon. I am not sure how you survived my mentorship, but I hope that you are better people for it. Also, many thanks to the past and present members of the Troy lab: Ying Jean, Maria-Elena Pero, Sha-ron Pierre, Elena Ribe, Rebecca Goldstein, and Nathalie Celcis.

To the Pathology coordinator Zaia Sivo, thank you for supporting me from day 1.

Finally, it would have been impossible to complete this project without the support of my family, to whom this thesis is dedicated, and my close friends. To my parents and sisters, Jacob Backon, Tabitha Guzman, David Valdini, Justin Halsey, Mark Halsey, Joanna Halsey, Trevor Halsey, Rose Lee, Daniel Pacheco, Matthew Cummings, Karin Kram, Dylan Citrin, Belem Bueno, Bri Anne Ryer, Rob Magliaro, Sharon Steiner, Jonathan Mandelbaum, Tiffany Zee, Amitabha "Guppy" Gupta, Julio Pozueta, and Yiorgos Mountoufaris…

…thank you for believing.

DEDICATION

For Hanna, Itoro, Nko, and Enekan

Chapter 1. Introduction [Adapted from [1, 2]]

1.1. Stroke Neurodegeneration

1.1.1. Disease Criteria

A stroke is the sudden loss of neurological function because of a perturbation in the cerebral blood supply. Ischemic stroke accounts for the overwhelming majority (80%) of recorded cases and is the primary focus of this dissertation. The remainder are either hemorrhagic (15%) or idiopathic (5%) [3].

Ischemia is caused by the occlusion of a cerebral artery by either thrombosis or an embolism. Unlike the related condition, transient ischemic attack (TIA), the symptoms caused by an ischemic stroke last for over 24 hours and always result in permanent tissue damage. These symptoms include, but are not limited to: hemiplegia, numbness, aphasia, dysarthria, apraxia, memory loss, and balance disruption.

The location of the stroke, symptom presentation, and survival are dictated by which cerebral artery is occluded (Figure 1-1 & 1-2).

Figure 1-1.
Major Cerebral Blood Vessels

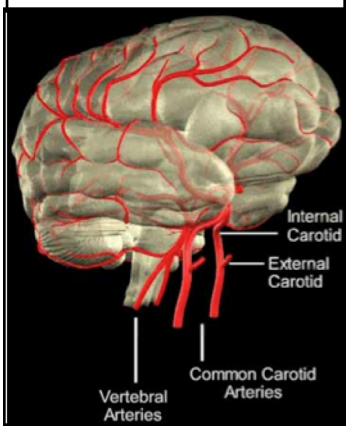

Global ischemia occurs when blood flow to the brain is completely stopped, which is a severe complication of cardiac arrest. In this event, blood flow is halted in the 4 major arteries that supply the brain: the right and left common carotid arteries and the right and left vertebral arteries (Figure 1-1) [4]. Clearly, global ischemia is extraordinarily dangerous as the brain can only survive for a matter of minutes without blood and oxygen.

The long-term consequences of transient ischemic event are dependent on the duration of arterial occlusion or cardiac arrest. With the former, the size of the occlusion also factors into whether the blockage will break into smaller pieces ("embolize") and occlude smaller vessels.

Occlusions in cerebral arteries that are more proximal to the central nervous system (CNS) are far more common and pose various threats to neurological function. In 1991, Bamford et al. classified these strokes into 4 clinical groups (Figure 1-2; adapted from [4]), based on a population study of first-time stroke cases in the Oxfordshire Community Stroke Project (OCSP) [5-7]. These groups along with their prevalence[1] in the OCSP (**blue**) and another large-scale population study, the Perth Community Stroke Project (**red**) [8], are:

1) Total anterior circulation infarcts, TACI (17%, 27%) (Figure 1-2)

2) Partial anterior circulation infarcts, PACI (34%, 30%) (Figure 1-2)

3) Posterior circulation infarcts, POCI (24%, 15%) (Figure 1-2)

4) Lacunar infarcts, LACI (25%, 28%) (Figure 1-2)

Anterior circulation infarction is the most prevalent subtype of ischemia. A "total" versus "partial" classification is dependent on which anterior artery is occluded and the size of the affected region. The middle cerebral artery (MCA) is the largest intracerebral vessel and supplies nearly the entire convex surface of lateral frontal, parietal, and temporal lobes, along with the insula, claustrum, and extreme capsule [9]. MCA occlusion is the most prominent form of ischemia and occurs in nearly 90% of anterior strokes [9].

Symptoms of an anterior stroke typically involve dysfunction in motor and "thought" processes: uncoordinated voluntary motion (ataxia), inability to write (agraphia), inability to calculate (acalculia), unconscious motion (ideomotor apraxia), inability to draw and build (constructional apraxia), and an impairment in understanding language (receptive aphasia).

[1] Cerebral Infarction Cohort Size - OSCP: n = 543; Perth: n = 248

Figure 1-2 Oxfordshire Community Stroke Project [OCSP] Classification and Stroke Syndromes

Anterior Circulation Stroke

Circle of Willis

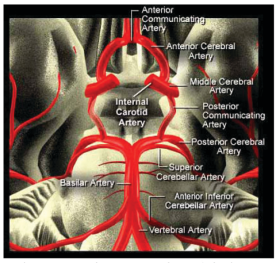

Anterior Arteries

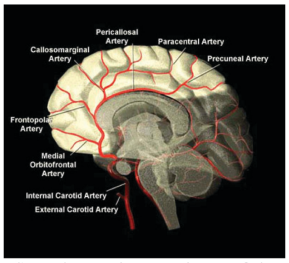

The anterior arteries (right panel) and anterior portions of the circle of Willis (upper half of left panel) are implicated in total and partial anterior ciculation stroke.

Middle Cerebral Artery

Ataxic Hemiparesis
Gerstmann Syndrome (Gerstmann Syndrome)
Middle Cerebral Artery - Inferior Division
Middle Aerebral Artery - Superior Division

Middle Cerebral Artery Branches

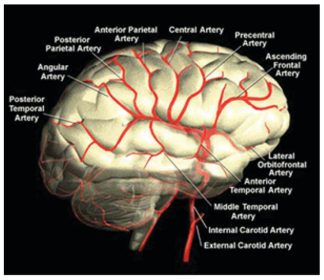

The middle cerebral artery is occluded 90% of the time in anterior circulation strokes.

Posterior Circulation Stroke

Posterior Circulation

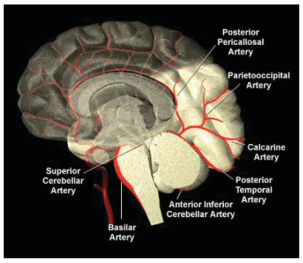

Posterior Cerebral Artery

Alexia without Agraphia
Balint Syndrome (Balint Syndrome)
Claude Syndrome
Cortical Blindness (Anton Syndome)
Posterior Cerebral Artery - Unilateral Occipital
Thalamic Pain Syndrome (Dejerine-Roussy Syndrome)
Weber Syndrome (Weber Syndrome)

Anterior Inferior Cerebellar Artery

Lateral Pontine Syndrome (Marie-Foix Syndrome)

Posterior Inferior Cerebellar Artery

Lateral Medullary Syndrome (Wallenberg Syndrome)

Basilar Artery

Ataxic Hemiparesis
Cortical Blindness (Anton Syndome)
Inferior Medial Pontine Syndrome (Foville Syndrome)
Lateral Pontine Syndrome (Marie-Foix Syndrome)
Locked-in Syndrome
Medial Medullary Syndrome (Dejerine Syndrome)
Ventral Pontine Syndrome (Raymond Syndrome)
Ventral Pontine Syndrome (Millard-Gubler Syndrome)

Anterior Spinal Artery

Medial Sedullary Syndrome (Dejerine Syndrome)

Vertebral Artery

Lateral Medullary Syndrome (Wallenberg Syndrome)
Medial Medullary Syndrome (Dejerine Syndrome)

Lacunar stroke results from an occlusion in a blood vessel that supplies the brain's deeper structures, such as the basal ganglia. Common locations include the lenticulostriate branches of the MCA or the penetrating branches of the Circle of Willis/posterior arteries (vertebral or basilar). Due to the central networking activities of the basal ganglia and the smaller regions of injury, clinical presentation of lacunar infarction is extremely varied and often subtle. Infarcts in

the thalamus can alter pain perception (i.e., cause numbness and burning sensations), while strokes affecting the pons or internal capsule can yield difficulties with swallowing (dysphagia), unilateral paralysis (hemiparesis), and speech dysfunction (dysarthria).

Posterior infarction induces neurodegeneration in the temporal and occipital lobes. As expected, the resulting neurological impairments mainly involve sensory perception, balance, and facial muscle control [4], such as visual loss (hemianopsia), acquired dyslexia (alexia), disabled eye coordination (optic ataxia), impaired pain perception, weakness in upper and lower extremities, vertigo, gait disturbances, and facial weakness [4].

While the population frequencies for these ischemic subtypes varied between the Oxfordshire and Perth studies, mortality rates amongst the various subtypes remained relatively parallel [3, 10-13]. Total anterior circulation infarcts (1-yr mortality: ~60%) are 4 times more lethal than partial anterior (1-yr mortality: ~15%) and posterior (1-yr mortality: ~15%) circulation infarcts. Anterior infarcts are 6 times as lethal as lacunar infarcts (1-yr mortality: 10%).

Following occlusion, several mechanisms contribute to the development of neuronal injury, including oxidative damage, ionic (Na^{2+}, K^{+}, Ca^{2+}) homeostasis, and inflammation. This extensive list of molecular instigators has been thoroughly reviewed elsewhere [14-17], but a relevant overview is provided below.

Stroke injury is morphologically divided into two territories (the core and penumbra), which exhibit two prominent modalities of cell death (necrosis and apoptosis).

Damage in the core is essentially irreversible. In the core, blood perfusion is lowered below the threshold for viability, and neurons become electrically silent because of complete

energy depletion. Necrosis is the prominent mode of cell death in this region, although there is some evidence for apoptosis in the core [1, 17].

The penumbra circumscribes the core and continues to receive blood from collateral arteries after an ischemic event, albeit at lower than physiological levels. Consequently, neurodegeneration in the penumbra is more gradual and dominated by apoptosis, which is an ATP-dependent process. Markers of apoptosis are found in the penumbra for days to weeks after stroke onset.

Thus, a lengthy window of opportunity is available for targeting apoptotic cascades as a means to treat stroke. With timely reperfusion, either spontaneous or therapeutic, this territory may be salvaged. Restoration of blood flow can also induce 'reperfusion injury', which exacerbates inflammation, excitotoxicity, and apoptotic cell injury [16].

Vascular damage accompanies cell death in the stroke infarct [18]. Disruption of the neurovascular unit (i.e., the dynamic interactions between microvessels, neurons, astrocytes, and microglia) permits the infiltration of inflammatory cells and cytokines that are normally excluded from the central nervous system (CNS) by the blood brain barrier. Additionally, stroke induces microvascular permeabilization, which causes the extracellular accumulation of fluid. This process is known as "cerebral edema". Edema is the major cause of mortality within the first 24 hr that follow a stroke, as swelling of the brain leads to herniation and compression of neural centers in the brain stem that govern respiration [19].

1.2. Stroke Therapies

Trends in mortality and morbidity reveal that modern medicine has failed in the arena of stroke. Although 30-day and long-term survival statistics have moderately improved since the 1960s [20, 21], these gains are largely due to innovations in emergency care. There is still no

solution for the progressive neurological destruction that occurs shortly after a stroke. Consequently, stroke remains the 3rd and 10th leading cause of death and chronic disability, respectively, in the U.S [22-24].

Current therapies for stroke can be divided into 2 categories:

1) Preventative Measures
2) Acute Interventions

1.2.1. Preventative Measures

As caspases do not directly factor into preventative measures for stroke, these treatments will be briefly discussed. These measures are divided into two categories based on whether they are counteracting a nascent stroke (primary prevention) or a possible recurring stroke (secondary prevention).

Primary prevention targets risk factors [25] that predispose an individual for having a stroke. Clinical strategies have focused heavily on reducing hypertension [26], but managing smoking habits [27], diabetes [28], cholesterol levels [29], atrial fibrillation [30], and alcohol consumption [31] is advantageous as well.

Secondary prevention strategies overlap with primary methods (e.g., reducing hypertension), but are additionally geared towards improving blood circulation. In this regard, antiplatelet agents and anticoagulants are preferred, although they can slightly increase the risk of cerebral hemorrhage [3].

1.2.2. Acute Interventions

Three acute remedies have proven efficacious for stroke and are widely practiced.

1) Aspirin, a validated primary and secondary preventative drug, also improves short-term mortality (14-day morbidity and mortality [32, 33]) when taken within the first 48 hr after

stroke. The overall benefit is relatively small (4 in 1000), but its low cost and simple administration justify its use.

2) As mentioned in "1.1.1 Disease Criteria", edema is a major cause of mortality during the first 24 hr after a stroke. Hemispheric decompression is utilized to relieve the intracranial pressure generated by brain swelling and prevent herniation of the brain stem. This therapy is highly beneficial in the rare cases (1 – 10%) where it is required [34]. One small study reported 78% versus 29% survival when hemispheric decompression was performed for middle cerebral artery infarcts [35].

3) Tissue plasminogen activator (tPA) is a potent thrombolytic agent ("clot buster") that is used to restore blood flow in the early stages of stroke. It is the only FDA-approved neuroprotective drug for ischemic stroke that reduces consequent disability amongst stroke patients; however, it fails to improve mortality [3]. As stated in "Chapter 1.1.1 Disease Criteria", reperfusion injury can occur when blood flow is restored to the infarcted tissue, and the duration of occlusion directly affects the magnitude of reperfusion injury; i.e. longer occlusions increase the likelihood of reperfusion injury. Unfortunately, the use of tPA is restricted to less than 3% of the patient pool [36] because of a short treatment window (<3 hr). When given later, tPA induces reperfusion injury and can cause hemorrhage. Medical contraindications, such as hypertension, also limit its use.

1.2.3. Neuroprotection: An Argument for Caspase Inhibition

Neuroprotection is one possible answer for stroke, but this idea has encountered repudiation in recent years. It is frequently quoted that over 1000 neuroprotective treatments have been tested and failed in clinical trials for stroke [37]. These nihilistic sentiments are unjust, as these setbacks speak to a variety of issues.

First, selecting a meaningful drug target for stroke has proven difficult because of the myriad mechanisms that are involved with stroke pathogenesis. A majority of the failed interventions targeted molecular pathways that are as beneficial in physiological settings as they are deleterious during stroke. Thus, poor outcomes are to be expected. Major examples of these "Jekyll-Hyde" molecular targets (and their number of failed clinical trials) include glutamate antagonists (16), calcium channel blockers (16), and antioxidants (10) [37].

Second, timing is a critical determinant in the overall effectiveness of any neuroprotective agent. Given that most stroke patients arrive between 5 – 11 hr after stroke onset [38, 39] and that stroke neurodegeneration persists for days and weeks, any possible neuroprotective target must present a large window of activity (i.e., window of therapeutic opportunity) to be effective.

Third, animal models of stroke provide wonderful insight into ischemic mechanisms, but are they accurate facsimiles? Experimental models rely on reproducibility (i.e., inbred rodent lines, identical durations of occlusion, controlled rodent size and diet). In contrast, human stroke patients have different genetic susceptibilities and are exposed to varying environmental factors (i.e., poor diet, hypertension, tobacco exposure, etc.) that contribute to disease outcome. Thus, rigorous preclinical testing in a variety of contexts (e.g., different occlusion times, inbred/outbred rodent strains, non-human primates, poor diet, etc.) is required for any therapy, neuroprotective or otherwise, to be seriously considered for broad use in stroke.

Cysteine-ASPartic proteASEs (caspases) are key mediators of apoptosis (programmed cell death) and neurodegeneration in stroke. The impact of caspase activity is not restricted to neuronal death, as caspases can exacerbate inflammation and alter glial function. Given their diverse roles in degenerative processes, it is surprising that inhibition of caspases has never been

explored in clinical trials for stroke. Apoptosis persists for days to weeks after stroke onset [40, 41], so caspase inhibition offers a broad therapeutic window. Additionally, inhibiting caspases directly targets cell death, rather than targeting broader mechanisms that lead to cell death.

Finally, expression- or activity-based strategies, which can be used in isolation or combination, have demonstrated efficacy in animal models and various preclinical trials. These innovations in caspase inhibition offer new potentials for stroke therapy.

1.3. Caspases: Focused Overview

Emblematic of their importance in stroke, caspases contribute to the inflammatory, apoptotic, and vascular processes that dominate stroke neurodegeneration (Table 1). In humans, apoptotic markers, including cleaved caspases, can be observed in the peri-infarct region from 1 to 26 days following a stroke [40, 41].

Although there are 13 mammalian caspase family members, this section will focus on the caspases that have been implicated in ischemic stroke (Figure 1-3; caspase-1, caspase-2, caspase-3, caspase-6, caspase-7, caspase-8, caspase-9 and caspase-11). For a comprehensive review of caspases and neurodegeneration consult [16].

1.3.1. Caspase Classification

1) *Structure*

2) *Mechanism of Activation*

3) *Cellular Function*

4) *Apoptotic Activation Pathways*

5) *Receptor-mediated Intrinsic Pathway Activation*

1) *Structure*. Caspases possess a prodomain (Figure 1-3) that is either short (caspase-3, caspase-6, and caspase-7) or long (caspase-1, caspase-2, caspase-8, caspase-9, and caspase-11). The size and composition of the prodomain determines whether a caspase requires cleavage for activation (see ”Mechanism of Activation”).

All caspases, except for caspase-2, cleave their substrates at an optimal tetrapeptide motif (denoted P4-P3-P2-P1) [42, 43]. Caspase-2 prefers a pentapeptide motif (denoted P5-P4-P3-P2-P1). P1 is the Asp residue that is molecularly attacked by a caspase’s catalytic Cys. P4-P3-P2 residues interact with corresponding amino acids within the catalytic groove.

In vitro substrate analysis has demonstrated that each caspase prefers a specific sequence of amino acids for P4-P3-P2 [43, 44]. For example, the optimal substrate for caspase-3 is “DEx” (Asp-Glu-x; x symbolizes a promiscuous requirement) [43, 44]. Restrictions also exist for the residue that immediately succeeds P1, which forms the scissile bond (P1-P1′) that is cleaved by the catalytic Cys. P1′ is typically a small, uncharged residue (Gly, Ser, Ala).

It is important to note that *in vitro*-validated motifs do not always translate to substrate specificity *in vivo*, as tertiary protein structure (i.e., loops or folds) influences the proteolysis of natural substrates.

2) *Mechanism of activation*. Caspases are also substrates for caspases. They possess target Asp residues in two regions: 1) between the N-terminal prodomain and the large subunit; 2) between the large subunit and small subunit. Cleavage is required for the activation of some, but not all, caspases.

Activation occurs upon dimerization because structural changes in the longer intersubunit linker allow for the exposure of the catalytic active site. Long prodomains also contain CARD (Caspase Activation and Recruitment Domains) or DED (Death Effector Domain) sequences

(Figure 1-3). These subdomains interact with complementary regions within an adaptor platform molecule (discussed below) to mobilize caspase dimerization/activation. Following proximity-

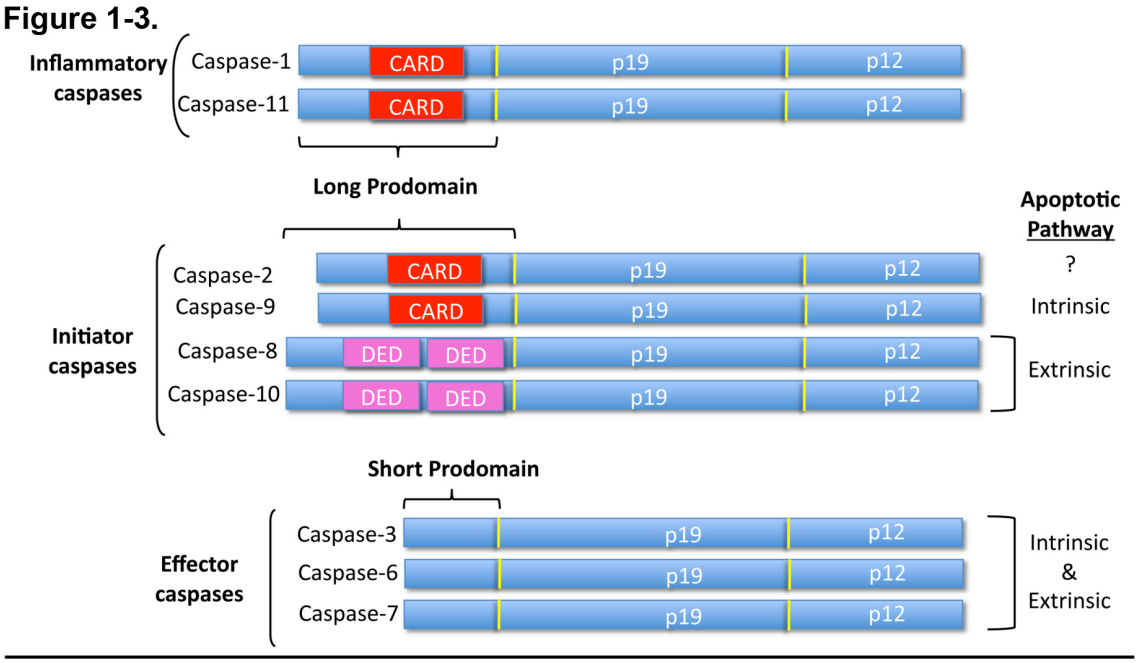

Figure 1-3. Mammalian caspases implicated in stroke.
Caspases are sorted by their roles in inflammation and apoptosis. Structural details are stressed. Yellow lines indicate cleavage sites.

induced dimerization, initiator caspases can autocleave at P1 Asp residues, but cleavage alone does not result in activation [43]. Moreover, cleavage of caspases with long prodomains can stabilize their activity (e.g., caspase-8) or increase their ability to be inhibited (e.g., caspase-9) [45, 46].

In contrast, short prodomain caspases exist as inactive zymogen dimers (Figure 1-4). Proteolytic cleavage initially occurs within the intersubunit linker between the large and small subunits and is an absolute requirement for activation of caspases with short prodomains.

For all caspases, a secondary cleavage between the N-terminal prodomain and large subunit releases the former; this is typically an autocatalytic event.

3) *Cellular Function*. Caspases are further generalized into 3 functional groups: inflammatory, apoptotic initiator, or apoptotic effector.

Caspase-1 contributes to stroke inflammation by processing the proinflammatory cytokine interleukin-1β (IL-1β) into its active form [47]. During ischemic stroke in rodents, IL-1β levels rapidly increase in the CNS. Transgenic expression of a caspase-1 dominant negative mutant prevents IL-1β maturation and reduces ischemic brain injury [48].

Recently, genetic knockout of murine caspase-11 was shown to be protective against lipopolysaccharide exposure [49], suggesting a role in the innate immune response. In a separate study, caspase-11 knockout mice were protected from stroke [50]. Caspase-11 is the probable ortholog of human caspase-4 and caspase-5 (59% and 54% homology, respectively); however, the latter enzymes have not been directly studied in stroke pathogenesis.

Coined "Death by a Thousand Cuts" [51], caspase-mediated apoptosis involves the selective cleavage of a tremendous number of substrates to promote cellular demolition [52]. Apoptotic caspases are classified as either "initiator" or "effector", which is based on their hierarchal nature of activation. Initiators cleave a limited a number of substrates, including effector caspases. In turn, effector caspases are charged with propagating cell death by targeting a wider variety of protein substrates (e.g., cytoskeleton, kinases, organelles, etc.).

Notice that caspase structure (short vs. long prodomain) correlates with apoptotic function (effector vs. initiator). Caspase-2 is the one exception. It possesses a long prodomain but can act as an initiator or effector, depending on the death signal. To add to its uniqueness, caspase-2 is also found in the cell as a zymogen dimer [53].

4) *Activation Pathways*. Apoptotic caspases are organized into two canonical signaling cascades. The "extrinsic" pathway is dependent on the formation of the death-inducing signaling

complex (DISC). Upon ligand binding, a death receptor recruits an adaptor protein, such as the Fas-Associated protein with Death Domain (FADD), to the cell membrane. This adaptor protein sequesters two caspase-8 monomers into close proximity to induce structural changes that free the catalytic site. This trimeric complex (death receptor, adaptor protein, and caspase-8) defines the DISC and proceeds to cleave effector caspases. Autocleavage of caspase-8 occurs, which enhances its activity.

The intrinsic pathway is triggered by a variety of cellular stressors (e.g., genotoxicity, reactive oxygen species, endoplasmic reticulum stress). The first critical event is the permeabilization of the outer mitochondrial membrane (OMM) [54]. Bax and Bak are Bcl-2 family members that trigger OMM permeabilization. In healthy cells, Bak resides in the OMM, while Bax is cytosolic. Death signals cause Bax to translocate to the OMM and induce conformational changes in Bax and Bak that lead to their homo-oligomerization. Although the precise crystal structure of these oligomerized pores is unknown, it is hypothesized that Bax and Bak form pores in the outer membrane that release cytochrome c, the principal killing factor in intrinsic apoptosis, into the cytosol [54]. In an ATP-dependent fashion, cytochrome c forms an activation platform with APAF-1 that recruits caspase-9 monomers, which subsequently dimerize and activate. This caspase 9-based complex, termed the apoptosome, cleaves and activates effector caspases. Although caspase-9 does undergo autocleavage, this action does not appreciably increase caspase-9 activity.

Endogenous inhibitors can modulate the intrinsic mitochondrial pathway. Inhibitor of Apoptosis Proteins (IAPs), particularly XIAP, inhibits active caspase-3, -7, and -9 (discussed below). In turn, Diablo/SMAC or HtrA2/Omi, which are released from permeabilized

mitochondria, are IAP antagonists that block IAP inhibition of caspases. Thus, there are multiple levels of natural regulation for the intrinsic pathway.

5) *Receptor-mediated Intrinsic Pathway Activation*. Evidence is now pointing towards a possible mechanism of receptor-mediated activation for the intrinsic pathway that involves the p75 neurotrophin receptor (p75NTR). Mature neurotrophins (~13 kDa), such as nerve growth factor (NGF) and brain-derived neutrophic factor bind to Trk tyrosine kinase receptors to neuron survival, proliferation, memory and learning, and axon guidance [55-58]. In contrast, their precursor forms—proneurotrophins (e.g., proNGF and proBDNF; 30 – 34 kDa)—are high-affinity ligands for P75NTR and can signal cell death or cell survival.

Figure 1-4.

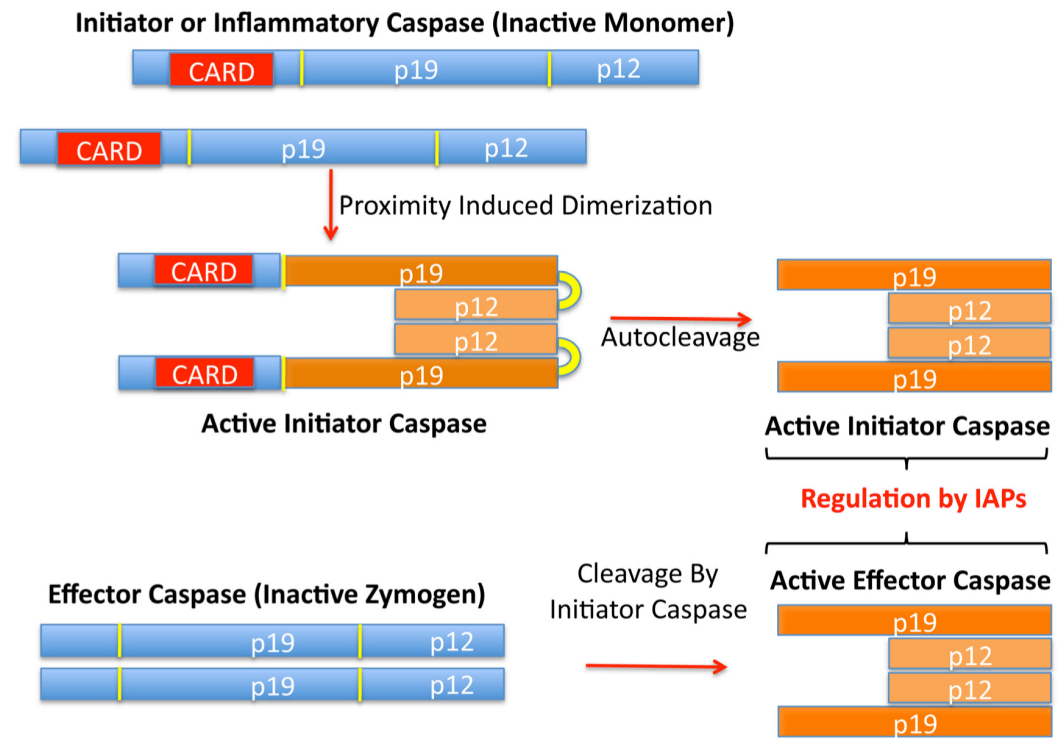

Figure 1-4. Mechanisms of caspase activation.
Activation models for initiator and effector caspases are shown. Blue indicates inactive caspase while orange denotes activated caspase. Some of the activated caspases (i.e., casp-3, casp-7, casp-9) are subject to regulation by IAPs.

P75NTR signals via receptor homodimers as well as heterodimer complexes comprised of various co-receptors. The outcome of p75NTR signaling depends upon the receptor complex [57, 58]: p75 homodimer (survival), p75NTR-NogoR (axon repulsion), p75NTR-Lingo-1 (axon repulsion), and p75NTR-sortilin (neuron and oligodendrocyte death) [59, 60]. P75NTR can also associate with Trks to modify Trk ligand binding and signaling [61].

P75NTR-sortilin induces neuronal apoptosis via a proposed activation pathway [62] that involves the recruitment of p75NTR-binding proteins (NRAGE [63, 64], NRIF [65, 66], and NADE [67, 68], the activation of c-Jun N-terminal kinases (JNK), the induction of p53/p63, and eventual Bax-mediated mitochondrial permeabilization.

Neurotrophin **R**eceptor–interacting m**AGE** homolog (NRAGE) promotes cell death by preventing p75NTR from associating with Trk receptors [63] and activating the JNK pathway [64]. **N**eurotrophin **R**eceptor **I**nteracting **F**actor (NRIF) is a zinc finger protein that is ubiquitinated after p75NTR stimulation and translocates to the nucleus [69] where is it believed to function as transcriptional repressor [70]. NRIF is necessary for p75-mediated JNK activation and sufficient for inducing cell death via a p53-dependent mechanism in sympathetic neurons [66]. P75**N**TR-**A**ssociated cell **D**eath **E**xecutor (NADE) expression is upregulated during transient ischemia in CA1 hippocampal neurons [71], and one study demonstrated that it binds and prevents SMAC/Diablo from inhibiting the anti-apoptotic actions of XIAP [72]. JNK activation mediates p75NTR-triggered apoptosis [73], which increases the expression of p53 and p63 [74, 75] Subsequently, p53 induces Bax expression [74, 76, 77], which leads to the permeabilization of the mitochondrial outer membrane and caspase-9 activation.

1.3.2. Translational Strategies for Caspase Inhibition

There are three major strategies for inhibiting caspases in stroke.

1) *Death receptor blockade*

2) *Genetic Manipulation*

3) *Catalytic Inhibitors*

1) *Death Receptor Blockade.* Inhibiting death receptors can disrupt the execution of the extrinsic pathway. When administered 30 minutes after stroke, antibodies against tumor necrosis factor-receptor-1 (TNF-R1) and CD95, members of the TNF receptor superfamily, can reduce neural injury [78].

2) *Genetic Manipulation.* Ischemic stroke induces caspase expression (mRNA and/or protein) within the first 24 hr for all of the caspases mentioned above [16] (Table 1). Furthermore, genetic knockout of caspase-1, caspase-3, caspase-6, or caspase-11 is neuroprotective against stroke [1, 16].

Obstacles for an RNAi-based gene therapy for caspases include sufficient distribution of the therapeutic siRNA/miRNA to susceptible CNS regions and efficient delivery into neuronal cells. A proof-of-concept study recently overcame these issues with a nonviral-based RNAi system in a rodent ischemia model [79]. Immediately before the induction of stroke, carbon nanotubes loaded with caspase-3 siRNA were stereotactically delivered into motor cortices. Neurons in the treated regions were protected against stroke, and neurological function was preserved.

Viral delivery is another option [80], but this strategy is hampered by the fact that viral vectors are immunogenic [81] and have limited capacity for DNA/RNA payloads [80]. Additionally, they can be difficult to mass-produce and have limited stability after production [80].

Certain drugs can also modify caspase expression. Minocycline inhibits caspase-1 expression during stroke [82] and has the additional benefit of inducing the expression of anti-apoptotic Bcl-2 [83]. However, drug-based knockdown often lacks complete molecular and tissue specificity, with compounds like minocycline affecting a variety of gene targets and organs. For example, minocycline has anti-inflammatory properties; it can alter T-cell and microglia function [84] and is beneficial in inflammatory diseases like multiple sclerosis [85] and rheumatoid arthritis [86]. However, chronic minocycline therapy can trigger immune disorders like lupus and autoimmune hepatitis [87, 88].

Gene therapy is an effective prophylactic strategy, but the true litmus test for any stroke treatment is potency after ischemia has begun. In this regard, gene therapy might have limited utility even in the best scenarios. Caspases are expressed at modest levels in the CNS, which means there is an available pool of death molecules at stroke onset. Therefore, caspase activation could be appreciable before a gene therapy could significantly curtail expression.

For further review on the potential of gene therapies for stroke consult: [80]

3) *Catalytic Inhibitors.* For nearly 20 years, short peptide inhibitors have been the principle tools for studying and manipulating caspase activity. Based on the optimal substrate motif (P4-P3-P2-P1) of an individual caspase, these synthetic inhibitors can be modified by adding chemical moieties to determine their reversibility and membrane permeability. The pan-caspase inhibitor zVAD (benzyloxycarbonyl-Val-Ala-Asp) and putative caspase-3 inhibitor DEVD confer neuroprotection in rodent models of stroke [89]. Although they have never been tested in clinical trials for stroke, trials are underway for the use of these peptide-based inhibitors for liver injury and psoriasis [42].

However, multiple studies have demonstrated that short peptide inhibitors are highly promiscuous [90, 91]. Given that certain caspases have non-death roles in synaptic plasticity and microglial activation [92, 93], this lack of specificity could potentially reduce the overall usefulness of peptide-based inhibitors in stroke.

Natural protein biologics that inhibit caspases offer higher target specificity and an alternative to short peptide inhibitors. Given their larger size, most biologics require assistance to cross the plasma membrane. Trojan peptides (e.g., Tat or Penetratin1) can be utilized towards this goal.

As discussed in Chapters 3 & 4, we recently applied this delivery strategy to a biologic derived from a metazoan caspase inhibitor [1]. Mammals express a family of cell death inhibiting proteins known as IAPs or Inhibitors of Apoptosis Proteins. IAPs contain baculoviral IAP repeat (BIR) domains, which perform specific functions. One member of this family, X-linked IAP (XIAP), is a potent, specific inhibitor of active caspases-9, -3, -7. IAPs are comprised of baculoviral IAP repeat (BIR) domains. For XIAP, caspase inhibition specificity is dependent on the BIR domains. The BIR3 domain is a specific inhibitor of active caspase-9, while the BIR2 domain inhibits active caspases-3 and -7 [94].

XBIR3 can only inhibit caspase-9 after autocleavage [94]. Rather than target the catalytic site of caspase-9, XBIR3 uses a less conventional method of inhibition. Biochemical and crystal structure analysis demonstrates that XBIR3 inhibits caspase-9 by severing the dimer interface, which functionally separates an active caspase homodimer into inactive monomers [94-96]. XBIR3 accomplishes this feat by binding two IAP-binding motifs (IBM) located in the active caspase-9 dimer. One IBM is generated at the amino-terminus of the small subunit, following its separation from the large subunit. The other IBM is located at the dimer interface.

In Chapters 3 & 4, we show that a Trojan peptide—Penetratin1 (Pen1) —can be linked to XBIR3 via a disulfide bond to deliver this caspase inhibitor into the intracellular compartment. Pen1 is the third homeodomain (16 aa) from the *Drosophila* transcription factor Antennapedia, and due to its charge and small size (see below), it can cross biological membranes [97]. Upon cellular entry, this transient linkage is reduced by the cytoplasmic pH, and the cargo is allowed to act on its intended target. When given intranasally, as a prophylactic or therapeutic, Pen1-XBIR3 prevented the activation of the intrinsic pathway (i.e., subsequent caspase-6 activation) and provided substantial neuroprotection against stroke. Additionally, it was revealed that caspase-9 inhibition reduces cerebral edema. As previously stated, edema is a major cause of mortality within the first 24 hr after stroke.

Trojan peptides could usher in a new era in resolving caspase mechanisms and treating cell death. Examples of Trojan peptides, which are typically short (16-35 aa) and partially hydrophobic, include Pen1, HIV-1 TAT protein, VE-cadherin-derived cell-penetrating peptide, and transportan [98]. Most Trojan peptides are polybasic and retain a net positive charge at physiological pH. All Trojan peptides are lipophilic, and many are also amphipathic. Uptake mechanisms include direct penetration and endocytosis.

Along with intracellular targeting, these transport peptides have other distinct advantages. For example with Penetratin1, the upper limit for the molecular weight of peptide cargo is ~100 kDa. Pen1 can also be adapted to deliver siRNA. Other peptide inhibitors require evaluation with this Trojan peptide delivery. Alternatively, endogenous substrates or catalytic dominant negatives, as shown in Chapter 4, can be attached to Trojan peptides and used as competitive inhibitors.

One disadvantage of using Pen1 is a lack of cellular specificity; i.e., it will deliver to all cell types. For discrete transport to neurons, rabies virus glycoprotein can be used to deliver peptides and siRNA [99, 100]. Similarly conceived Trojan peptides from various tissue-tropic, viral-entry proteins could offer innovative methods for organ-specific drug delivery. Another disadvantage is that the net positive charge of Trojan peptides can generate solubility issues after linkage to cargo.

1.3.3. CNS Delivery Methods

The blood brain barrier (BBB) evolved to protect the CNS from molecular insults, but it also restricts the passage of many neuroprotective agents administered into the bloodstream.

Routes for bypassing the BBB do exist. Intranasal delivery is proving efficacious for accessing the CNS and treating neurodegenerative disease [101]. For example, cognition is significantly improved after intranasal administration of insulin in early clinical trials for Alzheimer's disease and mild cognitive impairment [102]. This method provides 100-fold higher CNS concentrations relative to intravenous administration [103]. Alternatively, more invasive methods that utilize direct injection into the brain (e.g., intracerebral and intraventricular) are clinically viable, although less favorable from a patient's viewpoint.

1.3.4. Axon Degeneration, Caspases, and Stroke

Axon degeneration precedes neuronal death in many neurodegenerative diseases, and is an oft neglected target for therapies [104]. Axon degeneration occurs in humans during stroke with diffusion tensor imaging revealing extensive loss of axonal tracts in the stroke penumbra [105, 106].

However, following a brain insult, preservation of neuronal connections is vital in retaining neuronal functions. In the stroke penumbra in gerbils, Ito *et* al. found that corticofugal

axon and synaptosome density decreased at approximately 12-24 hr post-reperfusion and continued until 4 days post-occlusion [107, 108]. In rats, stroke reduces axon density in the forebrain, midbrain, and brainstem [109]. Large amounts of axonal swelling occur immediately following an ischemic event as well as after traumatic brain injury. While the relationship

Table 1-1. Caspases implicated in stroke pathogenesis.

Caspase	Paradigm (Species)	Measure	Reference
1	tMCAo (mouse)	Genetic Knockout (infarct size, cerebral blood flow, brain edema)	[110]
1	pMCAo (mouse)	Ac-YVAD-AFC (catalytic activity)	[111]
1	pMCAo (rat)	mRNA levels	[2]
2	Global Ischemia (rat)	caspase cleavage (WB, IHC)	[112]
3	tMCAo (mouse)	Genetic Knockout (Infarct Volume, neuron density, TUNEL)	[113]
3	pMCAo (rat)	caspase cleavage (WB)	[114]
3	pMCAo (mouse)	Ac-DEVD-AFC (catalytic activity), caspase cleavage (WB, IHC)	[111]
3	pMCAo (rat)	mRNA levels	[2]
6	pMCAo (rat)	mRNA levels	[2]
6	tMCAo (mouse, rat)	Caspase cleavage (IHC), knockout mice (Infarct volume, motor behavior)	[1]
7	pMCAo (rat)	mRNA levels	[2]
8	pMCAo (rat)	mRNA levels	[2]
	pMCAo (mouse)	Ac-IETD-AFC (catalytic activity), caspase cleavage (WB, IHC)	[111]
	pMCAo (rat)	Caspase cleavage (WB)	[114]
9	tMCAo (rat, mouse)	Caspase cleavage (IHC), biochemical isolation of	[115], [1]

		active caspase 9	
	tMCAo (canine)	Release of caspase 9 from mitochondria	[116]
	Human Stroke tissue	IHC	[117]
11	pMCAo (rat)	mRNA levels	[2]
	pMCAo (mouse)	Genetic Knockout (TUNEL-positive cells)	[50]

Translational Intervention	**Caspase**	**Paradigm**	**Inhibitor**	**Delivery Method**	**Efficacy [Reference]**
Catalytic	Pan-caspase	tMCAo (mouse)	Z-VAD-fmk	Intracerebro-ventricular	Infarct vol. reduced by 64%-71% [89]
Expression	1	tMCAo (mouse)	Dominant-negative caspase 1	Transgenic Expression	Infarct vol. reduced by 44%-70% [48, 118]
Expression	1	tMCAo (rat) /Global (gerbil)	Minocycline	Intraperitoneal	Infarct vol. reduced by 63%-76% [82]
Catalytic	3	tMCAo (mouse)	Z-DEVD-fmk	Intracerebro-ventricular	Infarct vol. reduced by 30%-58% [89]
Expression	3	Endothelin-1 (mouse, rat)	Carbon nanotubes (casp-3 RNAi)	Intracerebral Stereotaxis	53% reduction in apoptotic cells (TUNEL) [79]
Catalytic	9	tMCAo (mouse, rat)	Penetratin1-BIR3	Intranasal	73% reduction in neuron loss [1]

Short Peptide Substrates: Ac-YVAD-AFC, Ac-DEVD-AFC, Ac-IETD-AFC. Short Peptide Enzymatic Inhibitors: Z-VAD-fmk, Z-DEVD-fmk

between caspase activation and axonal swelling has not been evaluated in ischemia, cytochrome c release and caspase activation are present early in axons after traumatic brain injury [119].

Wallerian degeneration is a term applied to the 'dying back' phenomenon observed by axons that have been transected [120]. Transected axons initially degenerate at the distal tip and disintegrate in a retrograde manner. In mutant WldS (slow Wallerian degeneration) mice, axons display significant retardation of Wallerian degeneration following axon transection. WldS mice are often utilized to evaluate the contribution of Wallerian degeneration in neurodegenerative disease models. For example, WldS mice are protected against ischemia, which indicates that Wallerian degeneration contributes to ischemic damage [121], although the molecular mechanisms have not been resolved.

It has been proposed that Ca^{2+}-activated proteases (calpains) mediate Wallerian degeneration of axons, while it is strongly asserted by others that caspases are not involved [122, 123]. Bcl-2 overexpression as well as the deletion of proapototic Bax and Bak fail to rescue retinal and optic nerves from Wallerian degeneration [124, 125]. However, caspases do mediate axon degeneration in the setting of neurotrophin withdrawal [126, 127]. Activated forms of caspase-3 and caspase-6 are found in the axons of dorsal root ganglion neurons following local neurotrophin withdrawal [126, 127]. Interestingly, caspases direct dendrite remodeling, a process similar to Wallerian degeneration, in a non-apoptotic setting in Drosophila [128, 129]. Activated caspase-3 is also found in projections of neurons undergoing developmental apoptosis [130].

1.4. Molecular Mechanisms of Cerebral Edema

A small, but significant, portion of this dissertation focuses on the role of caspases in cerebral edema. We discovered a novel relationship between this vascular pathogenic process and caspases; thus, a discussion on the mechanisms of cerebral edema is warranted.

1.4.1. Types of Cerebral Edema.

Cerebral edema is defined as a pathological increase in the total water content of the brain, which subsequently increases brain volume. If left unchecked, tissue swelling will increase intracranial pressure, compress capillaries (causing local ischemia), and herniate the brain, which is fatal. There are three classes of cerebral edema: **cytoxic**, **vasogenic**, and **interstitial**.

Cytoxic edema is caused by a disruption in cellular homeostasis due to impaired Na^+/K^+-ATPase pumps. As a result the Na^+/K^+ gradient is abolished, and sodium ions along with water are retained within the intracellular compartment. This event disrupts the electrochemical gradient that is required for cellular function, but cytotoxic edema is reversible in some scenarios, such as with transient ischemic attacks [131].

Vasogenic edema results from an increase in vascular permeability in the BBB. Thus, Na^+, water, and serum proteins in the main vascular circulation leak into the brain parenchyma and cause swelling. While conversion from edema into hemorrhage is possible [132, 133], this topic will not be discussed in this dissertation.

Diminished absorption of cerebral spinal fluid is the underlying cause of **interstitial edema**. Either an obstruction within the ventricles or increased production of cerebral spinal fluid can spawn this condition. Interstitial edema is not typically a complication of ischemic stroke, although it is observed with hemorrhage [131], so it will not be discussed further.

Cytotoxic edema contributes to pathogenesis in cerebral ischemia during the early stages of stroke (hours – days) [134]. The connection between ischemia and cytotoxic edema is simple: decreased blood flow means less energy/ATP production in the brain, which impairs Na^+/K^+-ATPase pumps and neuronal function.

However, it is unlikely that cytotoxic edema in isolation can elevate intracranial pressure to the point of brain herniation. Indeed, one can argue that brain water content remains the same; water merely transitions from the extracellular space to the intracellular compartment.

In contrast, brain volume is significantly elevated by vasogenic edema, which occurs on the timescale of days to weeks after stroke onset in humans. While the consequences of vasogenic edema are obvious (e.g., herniation), the cellular and molecular events that trigger pathophysiology are barely understood.

1.4.2. The Blood Brain Barrier and the Neurovascular Unit

The crucial event in vasogenic edema is the breakdown of BBB integrity. The structure of the BBB is comprised of the capillary lumen that is completely defined by an **endothelial cell** monolayer. Endothelial cells are ensheathed in a layer of **basal lamina** on the abluminal side, and the apposing membranes of each adjacent cell are connected and sealed by **tight junctions (TJ)**. Residing on top of the basal lamina are **pericytes**, which are in turn covered by another layer of basal lamina, which separates the pericytic layer from the parenchyma. Finally, **astrocyte end-feet** and **neuronal axon terminals** are within close proximity to the vessel structure; they provide chemical and enzymatic signals that regulate BBB permeability. Given the tremendous metabolic demands of neurons, it is not surprising that neurons and their glial support cells influence BBB, which governs nutrient transport from general vascular circulation. These six components—endothelial cells, basal lamina, TJs, pericytes, astrocytes, and neurons—are known as the neurovascular unit.

1.4.3. Proteases Govern BBB Integrity During Ischemia

During cerebral ischemia, two families of proteases—plasminogen activators (PAs) and matrix metalloproteinases (MMPs)—act in concert to open the BBB by breaking down the

extracellular matrix. Plasminogen activators are serine proteases that cleave the zymogen plasminogen into its active form, plasmin. Plasmin, which is typically associated with fibrinolysis, can only cleave a limited number of targets in the vascular ECM, such as laminin and fibronectin [135].

However, plasmins can directly and indirectly activate MMPs [135], which in turn cleave a larger volume of substrates (see below). Interestingly, when recombinant tPA is given after its recommended window (< 3 hr), it contributes to edema and hemorrhagic transformation, arguably through the activation of MMPs [136].

MMPs are zinc-dependent enzymes that are secreted or membrane bound. Relative to plasmin, MMPs proteolyze a broader range of vascular ECM proteins (e.g., laminin, fibronectin, gelatins, collagens, elastin, and perlecan [135, 137]). Additionally, MMPs can disrupt the BBB by cleaving TJ proteins: claudin-5 and occludin [138, 139].

Two MMPs have been strongly linked with the development of ischemic edema: MMP-2 and MMP-9. In ischemia-reperfusion models (rodent and non-human primates), MMP-2 expression/activity increase in the early stages (within 3 hr of reperfusion) [140-142], which corresponds with an initial opening of the BBB and the loss of TJ proteins by 24 hr [138]. A second wave of edema occurs between 24 – 48 h that correlates with an increase in MMP-9 expression/activity and MMP-9-dependent vascular damage [139, 141, 142]. Elevated MMP-9 expression also correlates with hemorrhagic transformation and intracerebral hemorrhage [143].

MMP-3 has been recently implicated in BBB disruption during ischemia [144, 145]. However, it is unclear whether TJ and ECM proteins are directly targeted by MMP-3 proteolysis or if MMP-3 is an upstream activator of MMP-2 and MMP-9 in this scenario.

MMP-9 is mainly expressed by endothelial cells and pericytes, while astrocytes are a major source of MMP-2 [139]. Pericytes also express MMP-3.

Given that many MMPs are constitutively expressed, it is not surprising that a family of endogenous inhibitors exists to regulate MMP activity. Tissue inhibitors for metalloproteinases (TIMPs) are small proteins (between 21 and 28 kDa) that regulate MMP activity [146].

Of the 4 variants (TIMP 1-4), expression levels of TIMP-1 and TIMP-3 are elevated during ischemia in a timeframe that coincides with MMP induction, which is perceived as a natural attempt to temper BBB opening. TIMP-1 has a preference for MMP-9; however, like TIMP-3 and other TIMPs, it is a broad spectrum MMP inhibitor [139].

MMPs are also known to cleave proneurotrophins in the extracellular milieu, which has implications for neurodegeneration [147, 148]. In particular, MMP-7 is sufficient for the processing of proneurotrophins into their mature forms *in vivo* [147-150]. Proneurotrophins are increased during kainic acid-induced seizures [69, 147], and this event coincides with a decrease in MMP-7 levels and an increase in the expression of its endogenous inhibitor TIMP-1 [147]. Thus, MMPs are dynamic regulators of proneurotrophins, which as discussed earlier are pro-apoptotic in nature.

1.4.4. Pericytes Contribute To Ischemic Cerebral Edema

Pericytes provide contractile support for the brain's vast network of microvessels, where there is a 1:3 pericyte:endothelia ratio[151]. (By contrast in striated muscle, where there are fewer microvessels, the pericyte:endothelia ratio is 1:100.) Along with maintaining capillary blood flow and producing endothelial survival factors (e.g., angiopoetin-1) [45], pericytes are integral players in BBB integrity because they induce TJ protein expression, during embryonic development [152] and in adulthood [153], and are also a major source of MMPs [139].

Additionally, pericytes contract early in rodent models of transient middle cerebral artery occlusion and remain contracted for at least 6 hours after reperfusion [154]. This event restricts blood flow, which exacerbates the ischemic condition. Pericyte contraction in this diseased state has been linked to intracellular Ca^{2+} dysregulation and excess ROS generation [45].

1.5. Significance and Outline

The following chapters are an exploration in the relationship between caspase biology and the pathogenic mechanisms of cell death and edema in ischemia. Caspases significantly contribute to neurodegeneration in stroke; thus, these proteases are ideal therapeutic targets. Transient ischemia is a wonderful *in vivo* model for studying caspase biology (e.g., developing activity assays and studying enzyme inhibition) because there is robust caspase activation.

Chapter 2 outlines the experimental methods that were utilized in the study. Chapter 3 details how initiator caspases are critical mediators of cell death and edema during stroke. New tools for the analysis of caspase activity and innovative caspase inhibitors are discussed. Chapter 4 advances down the caspase hierarchy and deals with the role of executioner caspases in cerebral ischemia. A novel relationship between caspase-6, cerebral ischemia, and axon degeneration is expounded, which was followed by the development of a dominant-negative inhibitor for caspase-6, as discussed in Chapter 5. Chapter 6 provides the conclusions and future directions for the project.

Overall, this dissertation describes previously unknown functions for caspases in stroke pathogenesis and strengthens the argument for caspase-based therapies for stroke neurodegeneration.

Chapter 2. Materials and Methods

2.1. Rodent Husbandry and Handling.

All rodent procedures were approved by the Columbia University Institutional Animal Care and Use Committee.

2.1.1. Mouse Breeding. Caspase-6 null (C6-/-) mice (Jackson Laboratories, Bar Harbor, ME) [155, 156] on C57/Bl6 background were bred with wild-type C57/Bl6 mice to generate C6+/- heterozygotes. Heterozygotes were then bred to generate C6-/- and wild-type littermates for studies.

2.1.2. Transient Middle Cerebral Occlusion. Male C6-/- and wild-type littermate mice (23-30 g; aged 2-3 months) as well as adult Wistar male rats (250-300 g; aged 12 weeks, Taconic Laboratories, Germantown, NY) were subjected to transient middle cerebral artery occlusion (tMCAo) as previously published [157, 158]. Rats and mice were anesthetized using isoflurane delivered in a mixture of nitrous oxide (70%) and oxygen (30%) via facemask. TMCAo was accomplished with a 25 mm 4-0 nylon suture (5 mm silicone rubber tip) to occlude the MCA. Rats received 120 min occlusion, while mice received 45 min or 60 min. To confirm cerebral ischemia, transcranial measurements of cerebral blood flow (CBF) were made using laser Doppler flowmetry (LDF) over the MCA territory (1.5 mm posterior and 5.5 mm lateral to the bregma). A reduction in the LDF reading to at least 40% of baseline was defined as an adequate CBF drop-off. The degree of functional deficit at 1 hour post-occlusion was scored using a modified 5-point Bederson scale, which measures forelimb flexion, resistance to lateral push, and circling behavior. Animals with a Bederson's score less than 1 (no deficit) were excluded from analysis. Rodents were placed in a 37°C post-operation incubator and maintained at

normothermia for an hour. Brains were harvested and processed for western blotting or immunohistochemistry, as described below.

2.1.3. Neonate Hypoxia-Ischemia. Caspase activity was measured in the Rice–Vannucci model of hypoxia-ischemia brain injury adapted to postnatal day 9 (P9) to P10 neonatal mice [159, 160]. P3 C57/BL6/J mice, along with their birth mothers, were purchased from Jackson Laboratories. On P7, mice were anesthetized with isoflurane, while the right carotid artery was permanently ligated. After 1.5 hr of recovery, pups were exposed to 15 min of hypoxia (8% O2 with balanced N2) in a hypoxic chamber. Ambient temperature during hypoxia was maintained at 37.0–37.5°C by placing the hypoxic chamber in a neonatal isolette (Airshield).

To measure caspase activity in pups, bVAD-fmk was stereotactically injected into the predicted area of infarction (0.2 μL/min immediately before permanent ligation of the carotid. Pups were sacrificed 1 hr after hypoxia. Infarcted brain tissue was excised and flash frozen with liquid nitrogen. A corresponding sample (internal control) was also dissected from the contralateral hemisphere.

2.1.4. Stereotactic Injection. Adult male Wistar rats (250-300 g) were anesthetized using isoflurane (2%) delivered via an anesthesia mask for stereotactic instruments (Stoelting, Wood Dale, Illinois) and positioned in a stereotactic frame. Convection-enhanced delivery (CED) was performed as previously described [161]. The scalp was shaved, and the skin was prepped with iodine solution and bupivicaine (0.25 ml of 0.25% solution). A 1.0-1.5 cm incision was made in the midline of the scalp to expose the bregma. A 1 mm burrhole was created at the coordinates 1 mm anterior and 3 mm lateral to the bregma. For the acute stereotactic infusions, a 28-gauge cannula was inserted to a depth of 5 mm below the dura into the caudate nucleus [161]. Infusion of the therapeutic was then instituted at a rate of 0.5 μl/minute. Following infusion, the cannula

was removed at a rate of 1 mm/minute, and the burrhole was sealed with bonewax. The skin incision was closed with skin adhesive. Post-procedure, rats were placed in a 37°C post-operation incubator and maintained at normothermia for an hour.

To inhibit caspase-9 pathways *in vivo*, Pen1-XBIR3 (30 μl of 36.8 μM solution) was infused immediately prior to induction of ischemia. Animals were housed at room temperature until they were euthanized. Brains were processed for immunohistochemistry (see below) or protein isolation (brain tissue dissection followed by snap-freezing in liquid nitrogen). An equivalent volume of saline was infused in negative control animals.

2.1.5. Intranasal Injection. While under isoflurane anesthesia, animals were placed so that they were lying on their backs. For rats, Pen1-XBIR3 (36.8 μM) was delivered by administering 6 μl drops to alternating nares every two minutes for 20 minutes (60 μl in total) [103]. For mice, Pen1-C6DN (31.9 μM) was delivered by administering 2 μl drops to alternating nares every minute for 10 min (20 μl in total) [103]. Pen1-XBIR3 intranasal treatment was done either prior to stroke or 4 hr after reperfusion. Pen1-C6DN was only given prior to stroke. Saline was used as a negative control. For non-stroked controls, animals were given 60 μl of vehicle or Pen1-XBIR3 and anesthetized for the same period of time as stroked animals (~1.25 hr). Brains were harvested for immunohistochemistry or western blotting.

2.1.6. Behavioral Examinations. For rat neurofunctional analysis, a 24-point neurological functional exam was developed by adapting strategies from previous studies [162-165] into a single exam (Table 2-1). Groups were analyzed by ANOVA. For mouse neurofunctional analysis (Table 2-2), a 28-point neurological functional exam was performed as previously described [166], with group comparisons made with Student's *t*-test. Additionally, for the WT vs. C6-/- experiments, a single mouse from each genotype was placed in isolation in a fresh cage, and

short videos (3 min at each time point) of spontaneous activity were recorded at three time points (pre-stroke, 24 hr reperfusion, 7 days reperfusion) to track motor decline.

Table 2-1. Rat Neurofunctional Exam

Neurological Examination Grading Scale for Rats After Middle Cerebral Artery Occlusion		
Signs	**Description**	**Score**
Motility, Spontaneous Activity		
OBSERVE ANIMAL FOR FIVE MINUTES	Normal behavior, rat moved around, explored environment, approached at least three walls of the cage, and rose up	0
	Slightly reduced exploratory behavior, rat moved around the cage but did not approach all sides, hesitated to move, did not rise up	1
	Circling	2
	Moving limbs without proceeding	3
	Moving only to stimuli	4
	Unresponsive to stimulus, with normal muscle tone	5
	Severely decreased tone, pre-mortal signs	6
Response to Vibrissae Touch		
SWIPE PEN ON WHISKERS 7x	Rat reacted by turning head or was equally startled by the stimulus on both sides	0
	Rat reacted slowly to stimulus on left side (3+ touches)	1
	Rat did not respond to stimulus on left side	2
Climbing	Climbed up an incline board (45 degrees), gripped with all limbs	0
	Hanging on to board with affected limbs dangling or not actively climbing	1
	Falling off the board, failing to grip with any limbs	2
Forelimb Placement		
OBSERVE ANIMAL FOR 30 secs	Normal placement, affected forelimb touched the ground at the same speed as the right forelimb, and animal was able to keep it pressed down on the table	0
	Weak placement, animal was unable to place affected forelimb down with the same speed as right forelimb and brushed the limb along the ground several times before able to place it down	1
	No placement, animal was not able to place affected forelimb down at all, brushed it along the ground or failed to outstretch it completely	2
Hindlimb Placement		
SCORE BASED ON THE AVERAGE RESULT OF 3 TRIALS	Normal placement, animal replaced the affected hindlimb quickly	0
	Weak placement, animal was delayed in placing the affected hindlimb but eventually placed it back on the surface	1
	No placement, animal was not able to replace hindlimb at all	2
Grasping Strength		
SCORE BASED ON THE AVERAGE RESULT OF 3 TRIALS	Symmetrical grasping strength on wire cage	0
	Asymmetrical grasping strength on wire cage	1
Grasping reflex of forepaw	Grasping onto tube when touched, able to extend forelimbs and maintain grip when tube is being pulled away, and muscles equally tensed.	0
SCORE BASED ON THE AVERAGE RESULT OF 3 TRIALS	Unable to grasp onto tube when touched, cannot extend forelimbs to hold on to the tube when pulled away, unequal tension	1
Cylindrical Beam	0 or 1 falls off the beam with or without attempt to stay on beam	0
ANIMAL IS PLACED PERPENDICULAR TO BEAM WITH HINDLIMBS HANGING	Two times falling off the beam with an attempt to stay on beam	1
	Two times falling off the beam without an attempt to stay on beam	2
	Three times falling off the beam with an attempt	3
	Three times falling off the beam without an attempt	4
Narrow, Rectangular Beam		
ANIMAL IS PLACED PERPENDICULAR TO BEAM WITH HINDLIMBS HANGING	Staying and walking on the beam	0
	Staying on the beam, with affected limbs hanging	1
	Grasping and hanging on the beam	2
	Falling off within 5 seconds with an attempt to stay on the beam	3
	Immediately falling off with or without attempt	4

Table 2-2. Mouse Neurofunctional Exam

Mouse 28-Point Neurological Function Exam	
Test	**Score**
Muscular Body Symmetry	0-4
Gait	0-4
Climbing	0-4
Circling Behavior	0-4
Front Limb Symmetry	0-4
Compulsory Circling	0-4
Vibrissae Response	0-4
Total Score	0 = Normal Motor Function 28 = Severe Motor & Sensory Deficits

2.2 Peptide Inhibitors for Caspases

2.2.1. Peptides

Penetratin1. The Trojan peptide Penetratin1 (Pen1) was custom made by (NeoMPS, San Diego, CA). Amino Acid Sequence: RQIKIWFQNRRMKWKK (16 AA)

X-linked Inhibitor of Apoptosis Protein BIR3 Domain (XBIR3). The BIR3 domain from X-linked Inhibitor of Apoptosis Protein (XBIR3) was purified by our collaborators Scott Snipas and Guy Salvesen (Sanford-Burnham Institute) as previously described [167]. Stock concentration: 36.8 μM. Amino Acid Sequence: NTLPRNPSMADYEARIFTFGTWIYSVNKEQLARAGFYALGEGDKVKCFHCGGGLTDWR PSEDPWEQHARWYPGCRYLLEQRGQEYINNIHLTHS (94 AA).

Caspase-6 Dominant Negative (C6DN). Mutant Caspase-6 (Cys163Ala) dominant negative (C6DN) was cloned with NdeI/XhoI sites but the NdeI is not unique. C6DN was cloned by partial digestion into pET23b. C6DN was purified in our labs as previously described [168]. Stock concentration: 63.2 μM.

C6DN cDNA insertion sequence (coding in CAPS):

attttgtttaactttaagaaggagatatacatATGGCTAGCTCGGCCTCGGGGCTCCGCAGGGGGCACCC

GGCAGGTGGGGAAGAAAACATGACAGAAACAGATGCCTTCTATAAAAGAGAAATG

TTTGATCCGGCAGAAAAGTACAAAATGGACCACAGGAGGAGAGGAATTGCTTTAAT

CTTCAATCATGAGAGGTTCTTTTGGCACTTAACACTGCCAGAAAGGCGGGGCACCTG

CGCAGATAGAGACAATCTTACCCGCAGGTTTTCAGATCTAGGATTTGAAGTGAAATG

CTTTAATGATCTTAAAGCAGAAGAACTACTGCTCAAAATTCATGAGGTGTCAACTGT

TAGCCACGCAGATGCCGATTGCTTTGTGTGTGTCTTCCTGAGCCATGGCGAAGGCAA

TCACATTTATGCATATGATGCTAAAATCGAAATTCAGACATTAACTGGCTTGTTCAA

AGGAGACAAGTGTCACAGCCTGGTTGGAAAACCCAAGATATTTATCATTCAGGCAG

CCCGGGGAAACCAGCACGATGTGCCAGTCATTCCTTTGGATGTAGTAGATAATCAGA

CAGAGAAGTTGGACACCAACATAACTGAGGTGGATGCAGCCTCCGTTTACACGCTG

CCTGCTGGAGCTGACTTCCTCATGTGTTACTCTGTTGCAGAAGGATATTATTCTCACC

GGGAAACTGTGAACGGCTCATGGTACATTCAAGATTTGTGTGAGATGTTGGGAAAA

TATGGCTCCTCCTTAGAGTTCACAGAACTCCTCACACTGGTGAACAGGAAAGTTTCT

CAGCGCCGAGTGGACTTTTGCAAAGACCCAAGTGCAATTGGAAAGAAGCAGGTTCC

CTGTTTTGCCTCAATGCTAACTAAAAAGCTGCATTTCTTTCCAAAATCTAATCTCGAG

CACCACCACCACCACCACTGAgatccggctgctaacaaagcccgaaag.

C6DN Amino Acid Sequence (Cys to Ala substitution is lower case and bold):

MASSASGLRRGHPAGGEENMTETDAFYKREMFDPAEKYKMDHRRRGIALIFNHERFFW

HLTLPERRGTCADRDNLTRRFSDLGFEVKCFNDLKAEELLLKIHEVSTVSHADADCFVC

VFLSHGEGNHIYAYDAKIEIQTLTGLFKGDKCHSLVGKPKIFIIQA**a**RGNQHDVPVIPLDV

VDNQTEKLDTNITEVDAASVYTLPAGADFLMCYSVAEGYYSHRETVNGSWYIQDLCEM

LGKYGSSLEFTELLTLVNRKVSQRRVDFCKDPSAIGKKQVPCFASMLTKKLHFFPKSNLE HHHHHH (302 AA)

2.2.2. Penetratin1 Linkage. Penetratin1 was mixed at an equimolar ratio with purified peptides (i.e., XBIR3 or C6DN) and incubated overnight at 37°C to generate disulfide-linked Pen1-peptide. Linkage was assessed by 20% SDS-PAGE and western blotting with anti-His antibody.

Alternatively, SDS-PAGE gels were stained with Coomassie or SYPRO Ruby (Sigma-Aldrich). First, gels were soaked with isopropanol fixing solution (10% acetic acid, 25% isopropanol; v/v in ddH2O) for 30 min. They were then incubated with Coomassie Brilliant Blue (0.006% in 10% acetic acid) for 3 hr or overnight, which was followed by destaining (10% acetic acid) for 1-2 hr.

For gels stained with SYPRO Ruby, gels were first soaked with methanol fixing solution (7% acetic acid, 50% isopropanol; v/v in ddH2O) for 30 min. They were then incubated overnight with 1x SYPRO Ruby (Bio-Rad #170-3126), which was followed by destaining (10% methanol, 7% acetic acid) for 1-2 hr.

SYPRO Ruby or Coomassie stained gels were imaged on an UV transilluminator and white light box, respectively.

2.2.3. Rhodamine Labeling of Peptides. C6DN (100 μL of 31.9 μM solution) or XBIR3 (100 μL of 36.8 μM solution) were buffer exchanged with ZebaTM desalt spin columns (Thermo Fisher Scientific, Waltham, MA) into 1x phosphate buffered saline (PBS). Buffer exchange is needed to remove primary amines (e.g., Tris or glycine), which can react with the NHS-ester moiety and compete with the intended reaction. Following buffer exchange, protein concentrations were determined using the Bradford colorimetric protein assay (Bio-Rad, Hercules, CA), according to the manufacturer's protocol. NHS-Rhodamine was added to the

peptide at a 10:1 molar ratio. These reactions were incubated on ice for 2 hr. Non-reacted NHS-Rhodamine was removed with fresh ZebaTM desalt spin columns, and protein concentrations were reanalyzed. Rhodamine-labeled peptides were stored at 4°C and protected from light until the day of Penetratin1 linkage.

2.3. Biochemical

2.3.1. *In Vivo* Caspase Activity Assay. Biotin-Val-Ala-Asp(OMe)-Fluoromethylketone (bVADfmk, MP Biomedicals, Santa Ana, CA; stock dissolved in DMSO) was used as an *in vivo* molecular trap for active caspases. BVADfmk (200 nmoles) was diluted in 30 μl sterile saline and infused by CED either prior to stroke or 3 hr after reperfusion in rats. After treatment with bVADfmk and tMCAo, brain tissue was harvested and flash frozen in liquid nitrogen. Tissue was lysed by pestle disruption in cold CHAPS buffer or bVAD buffer (Appendix I. Cell Lysis Buffers) containing protease inhibitors (Roche, Indianapolis, IN). Protein concentrations were determined using the Bradford colorimetric protein assay (Bio-Rad), according to the manufacturer's protocol.

For bVAD fmk-caspase complex precipitation, protein lysates (100 – 120 μg) were pre-cleared by rocking with Sepharose beads (GE Healthcare, Pittsburgh, PA) for 1.0 hr at 4°C. Pre-cleared lysate was centrifuged, and the supernatant was transferred to 30 μl of Streptavidin-agarose beads (Sigma-Aldrich, St. Louis, MO) and rocked gently overnight at 4°C. Beads were washed and centrifuged (300 μl washes, 5000 rpm for 5 minutes) with lysis buffer. This step was repeated 15 times to remove non-specific binders. After the final wash and pelleting, caspase-bVADfmk complexes were extracted from streptavidin beads by boiling in 1x SDS sample buffer (non-reducing conditions, Appendix I Cell Lysis Buffers). Beads were pelleted at 14,000

rpm for 10 minutes, and the supernatant was transferred to a fresh tube and resolved by SDS-PAGE. Saline was used in vehicle animals to act as a precipitation control for bVADfmk.

2.3.2. Axon Fractionation. Following dissection, brain tissue was dissociated with a Dounce homogenizer in 500 µL of Isolation Buffer (listed below). Homogenate was transferred to 1.5 mL microfuge tubes and centrifuged at 10,000 x *g* for 15 min. The myelin float layer (200 µL) was transferred to a fresh microfuge tube, and Dounce homogenization/centrifugation was repeated twice. The soluble fraction was separated into fresh microfuge tubes and flash frozen; the pellet, which contains unmyelinated axons and nuclei, was discarded.

The myelin float layer was further Dounce homogenized with Demyelination Buffer (listed below). Samples were subsequently incubated while rocking for 1 hr at 4 °C. Axoplasm proteins were pelleted by centrifuging at 10,000 x *g* for 15 min, and supernatant was discarded. The resulting pellet was washed with Wash Buffer (listed below) and centrifuged at 10,000 x *g* for 15 min. This step was repeated 2 additional times. After the final centrifugation step, the pellet was resuspended in 25 – 50 µL of RIPA lysis buffer. Samples were resolved by SDS-PAGE and analyzed by western blotting.

Isolation Buffer (pH 6.6): 100 mM NaCl, 10 mM phosphate buffer (0.0964% NaH2PO4-H2O & 0.0808% Na2HPO4-7H2O), 5 mM EDTA, 0.85 M sucrose. *Demyelination buffer* (pH 6.6): 100 mM NaCl, 10 mM phosphate buffer, 5 mM EDTA, 1% Triton-X. *Wash Buffer* (pH 6.6): 100 mM NaCl, 10 mM phosphate buffer, 5 mM EDTA.

2.3.3. Quantification of Edema by Evans Blue Dye Extravasation. Vascular permeability was quantitatively evaluated by fluorescent detection of extravasated Evans blue dye (Sigma Chemical)[169]. After MCA occlusion in mice, 2% Evans blue dye (w/v in saline) was injected intravenously (4 mL/kg) as a tracer of blood brain barrier permeability. Evans blue dye was

injected and allowed to circulate for 30 minutes, prior to euthanasia with a xylazine/ketamine injection and cervical dislocation. Brains were rapidly dissected into ipsilateral and contralateral hemispheres. The hemispheres were flash frozen in liquid nitrogen and stored at -80°C until analysis was performed. Following a brief thaw, the samples were homogenized in 1 mL of 50% trichloroacetic acid and centrifuged (10,000 rpm, 20 min). Supernatant (200 μL) was removed and diluted fourfold with ethanol. Samples were distributed into a 96-well optical plate (Nunc 165305) and scanned on a fluorescent plate reader (620 nm excitation, 680 nm emission; Infinite M200, Tecan) to quantify the dye concentrations. Concentrations were based on external standards dissolved in the same solvent.

2.4. Histochemistry

2.4.1. Immunofluorescence. Rats and mice were euthanized with 0.3 ml of ketamine (10 mg/ml) and xylazine (0.5 mg/ml). Rats were then transcardially perfused with heparin, which was followed by fixation with 4% paraformaldehyde (PFA) in 1x PBS. Brains were dissected and given serial incubations at 4°C with 4% PFA (24 hr), 1x PBS (24 hr), and 30% sucrose in 1x PBS (until brain sank; ~ 2 days). Brains were then sectioned with a cryostat. Sections were blocked for 1 hr with 10% normal goat serum/1% bovine serum albumin with 0.1% Triton-X100, incubated with primary antibody diluted in blocking buffer (overnight at 4°C), washed with PBS-Triton-X100 (0.1%) (3 times; 5 min each), incubated with the species appropriate Alexa Fluor-conjugated secondary antibody (Invitrogen, Grand Island, NY) (1:1000 in blocking buffer; 2 hr at RT). Slides were also stained with Hoechst 33342 (1 μg/ml in blocking buffer, Invitrogen; 15 min at RT) to visualize nuclei or with NeuroTrace fluorescent Nissl stain (1:300 in blocking buffer, Invitrogen; 30 min at RT) to visualize neuronal ribosomes/endoplasmic reticulum.

Human samples were additionally treated with Sudan Black (1% in 70% ethanol) for 5 min at RT and washed with PBS (3 changes; 3 min each).

For detection of fluorescent staining, sections were imaged with an upright Nikon (Melville, NY) fluorescent microscope using a SPOT digital camera (Sterling Heights, MI) or with a Perkin-Elmer Spinning Disc Confocal Imaging System (Waltham, MA) with a Nikon Eclipse TE200 Inverted Microscope with Hamamatsu 1394 Orca-ER digital camera.

Quantification of neurons and axons was accomplished using the Cell Counter plug-in for ImageJ (NIH). For quantification in the rat brain, images were acquired with a 20X objective (Nikon) of the dorsal motor cortex and the S1 somatosensory cortex forelimb region; both regions are contained within the infarct penumbra. For mice, the same penumbral regions were imaged/analyzed as well as regions from the secondary somatosensory and the granular insular cortex; both constitute the ischemic core. Single blind counts of processes or neurons were made in both regions of interest and then pooled for each individual animal. At least three animals were used per cohort. For mouse brains, 20X magnification images were taken in the S1 somatosensory cortex forelimb region and similar counts were made as described below. Counts were made for neurofilament light chain (NF-L) positive processes and NeuronalN (NeuN) positive cell bodies. Comparisons between groups used the Student's *t*-test or ANOVA, p-value: 0.05.

2.4.2. Immunohistochemistry (DAB staining). Human samples were also analyzed with DAB staining. Samples were incubated with 0.3% H_2O_2 for 30min, followed by blocking with 10% normal goat serum/1% bovine serum albumin in PBS, and primary antibody incubation diluted in blocking buffer overnight at 4°C. After washing with PBS, slides were incubated with a species appropriate biotin-conjugated secondary antibody (Vector Laboratories, Burlingame, CA) for 30

min at RT. Samples were then incubated with ABC reagent (Vector Laboratories) for 30 min and DAB stain for 10 min. Samples were counterstained with hematoxylin, subsequently dehydrated with ethanol, and cleared with 2 washes of xylene.

2.4.3. Infarct Volume. Twenty-four hours after MCA occlusion, rats and mice were euthanized with 0.3 ml of ketamine (10 mg/ml) and xylazine (0.5 mg/ml). Sections were prepared for immunohistochemistry (see 2.4.1.) and stained using a hematoxylin-and-eosin kit from American MasterTech (#KTHNEPT; Lodi, CA). Infarcted brain tissue was classified as an area of hematoxylin negative (pink) tissue in a surrounding background of viable (blue and pink) tissue. Serial sections were photographed and projected on tracing paper at a uniform magnification. Direct and indirect infarct volumes were calculated from three serial sections. Direct stroke volume was expressed as the area of the infarct divided by the area of the ipsilateral hemisphere. Indirect stroke volume was expressed as the area of the infarct divided by the area of the contralateral hemisphere. Comparisons between groups used the Student's *t*-test or ANOVA, p-value < 0.05

2.4.4. Bielschowsky Staining (Axons). Mouse and rat sections were stained with Modified Bielschowsky's Stain (American MasterTech #KTBIE), subsequently dehydrated with 3 changes of ethanol, and cleared with 2 washes of xylene.

For mice, the numbers of Bielschowsky-positive axon tracts in the striatum were hand counted from uncropped images acquired with a 20X objective (Nikon).

2.5. Cell culture

2.5.1. Hippocampal and Cortical Neurons. Hippocampal neurons from E-18 rat embryos were dissected, dispersed in a defined serum free media, and plated on poly-D-lysine coated (0.1 mg/ml) in 6-well Nunc tissue culture dishes (9.6 cm2/well; Thermo Fisher Scientific). Plates for

cortical neurons were also coated with laminin (0.1 μg/ml). The neurons were maintained in a serum free environment with Eagle's MEM and Ham's F12 (Gibco; Gaithersburg, MD) containing glucose (6 mg/ml), insulin (25 μg/ml), putrescine (60 μM), progesterone (20 nM), transferrin (100 μg/ml), selenium (30 nM), penicillin (0.5 U/ml), and streptomycin (0.5 μg/ml). Glial cells make up less than 2% of the culture. All cells were cultured for 8-10 days before treatment.

2.5.2. Neuronal Survival Assays.

4-hydroxynonenal (HNE). To induce caspase-9-mediated death [170], 4-hydroxynonenal (3 μM; Cayman Chemicals, Ann Arbor, MI) was added to cultures in triplicate with and without Pen1-XBIR3 (80 nM). After 1 day of treatment cell number was quantified as previously described [170]. Briefly, the cells were lysed in counting buffer, and intact nuclei were counted using a hemocytometer. Nuclei of the healthy cells appear bright and have a clearly defined nuclear membrane, while nuclei of dead cells disintegrate or appear irregularly shaped. Cell counts were performed in triplicate wells and averaged. Survival is relative to control wells. Comparisons between groups used the Student's *t*-test or ANOVA, p-value: 0.05

Proneurotrophin. To trigger p75NTR-mediated death, cortical neurons were treated with mouse furin-resistant proNGF (ΔproNGF, Alomone Laboratories, Jerusalem, Israel). Cultured rat cortical neurons were treated overnight with mouse ΔproNGF (mΔproNGF; 1 ng/ml & 10 ng/ml).

Cell viability was assessed as described directly above. For western blotting, culture medium was aspirated, and cells were washed once with sterile 1x PBS. Cells were harvested with RIPA lysis buffer (Appendix I – Cell Lysis Buffers).

2.6. Materials

2.6.1. Antibodies.

Immunohistochemistry: anti-Tuj1 (Abcam #ab7751, Cambridge, MA), anti-neurofilament-L (Cell Signaling #2835, Danvers, MA), anti-GFAP (Thermo Scientific #PA1-10004), anti-full-length and cleaved caspase-9 (Abcam #ab28131), anti-cleaved caspase-6 (Cell Signaling #9761), anti-cleaved caspase-3 (Cell Signaling #9661), anti-CD34 (Dako #M7165, Carpinteria, CA), anti-smooth muscle actin (Dako #M0851), and anti-cleaved caspase-7 (MBL #BV-3147-3).

Western blotting: THE™ anti-His (GenScript #A00186), anti-caspase-6 (BD #556581), anti-cleaved caspase-6 (Cell Signaling #9761), anti-cleaved caspase-3 (Cell Signaling #9661), anti-Tau V-20 (Santa Cruz Biotechnology #sc-1996, Santa Cruz, CA), anti-Lamin A/C (MBL International #JM-3267-100, Woburn, MA), anti-full-length and cleaved caspase-9 (Abcam #ab28131), anti-neurofilament-L (Cell Signaling #2835), anti-microtubule-associated protein 2 (Sigma-Aldrich #M9942), anti-TauC3 (Santa Cruz #sc-32240), anti-matrix metalloproteinase-9 (Cell Signaling #3852), anti-ERK (Santa Cruz #sc-93), and anti-α-tubulin (Abcam #ab7750).

Receptor Blocking: anti-mouse NGF (Sigma-Aldrich #N6655).

Chapter 3. Initiator Caspases in Stroke Neurodegeneration

3.1. Introduction

The activity of individual caspases has not been specifically assayed in the setting of stroke. It is not known when caspase activity is initiated during a stroke, and defining the time course of caspase activation is important from a mechanistic and a therapeutic perspective. The participation of individual caspases in stroke is poorly understood, but it is generally accepted that initiator caspases are active first, which leads to effector caspase activation and ultimately to cell death. With 11 individual caspases present in the human or rodent brain, specific measures are required to understand the caspase pathways initiated by stroke.

At present, the caspase activity probe biotin-VAD-fmk (bVAD) is the best method for determining if caspases are active after a death stimulus. Commercial catalytic inhibitors do not provide the specificity that is required to accurately dissect caspase pathways [90, 91]. BVAD is an irreversible pan-caspase inhibitor that has been used in cell culture models to measure caspase activation following various death stimuli [171-173]. This method was recently adapted for use in cultured primary neurons [173]. We now apply it for use *in vivo* in the CNS. BVAD binds irreversibly to all caspases that are active. In other words, if a caspase is active and its active site is available, bVAD will bind to it. Once bVAD is bound, it also inhibits that caspase, blocking any downstream events. Since bVAD is biotinylated, it can be isolated on streptavidin agarose, along with any active caspase that is bound to it. Administration of bVAD prior to induction of death will trap active initiator caspases, and the activation of effector caspases will be prevented. Thus, bVAD is useful for studying the inceptive events related to caspase activation in stroke.

Using bVAD-caspase precipitation, we revealed a previously undefined role for caspase-9 activity in transient ischemia in adult rodents, and similarly novel role for caspase-8 in neonatal stroke (Chapter 3.2.1. and 3.2.5.).

To determine the functional relevance of caspase-9 activity in stroke pathogenesis, we inhibited caspase-9 activity both pre- and post-ischemia. As stated above, commercial inhibitors have limited specificity, so we devised a novel method for modulating caspase activity, based on endogenous metazoan caspase-9 inhibitors. Mammals express a family of cell death inhibiting proteins known as IAPs or Inhibitors of Apoptosis Proteins. IAPs contain baculoviral IAP repeat (BIR) domains, which perform specific functions. One member of this family, X-linked IAP (XIAP), is a potent, specific inhibitor of active caspases-9, -3, -7. IAPs are comprised of baculoviral IAP repeat (BIR) domains. For XIAP, caspase inhibition specificity is dependent on the BIR domains. The BIR3 domain is a specific inhibitor of active caspase-9, while the BIR2 domain inhibits active caspases-3 and -7 [94]. XBIR3 was linked to the Trojan peptide Pen1 to facilitate cellular delivery and administered to the CNS via an intranasal route (. 3.2.3.). The efficacy of Pen1-XBIR3 in the prevention of stroke-induced is reported. Moreover, the use of intranasal delivery is an exciting development for stroke therapy [174, 175]. Intranasal delivery takes advantage of the olfactory and trigeminal pathways to bypass the BBB and directly access the cerebral spinal fluid and ventricular system.

As stated in Chapter 1.1.1. and 1.4., the cerebral vasculature is compromised during stroke, which leads to the passive extravasation of fluid into the tissue parenchyma. This process is termed cerebral edema. While damage to large bloods vessels results in hemorrhage, edema is caused by the breakdown of BBB permeability in capillaries (microvessels).

Previous studies have demonstrated that the p75 neurotrophin receptor (p75NTR) death pathway activates caspase-9 [55-58, 176], and p75NTR activation by proneurotrophins increases edema during cardiac ischemia (Barbara Hempstead personal communication). Based on these collective findings, our lab hypothesized that p75NTR activation by proneurotrophins induces caspase-9-dependent cerebral edema during transient ischemic stroke. To explore this potential mechanism, we conducted a histological study of the components of the neurovascular unit (i.e., pericytes and endothelial cells) along microvessels to assess a possible relationship to edema and caspases (expression and activity) (Chapter 3.2.4.).

As stated in . 1, matrix metalloproteinases (MMPs) play crucial roles in the maintenance of the BBB and are implicated in cerebral edema during stroke. For example, MMP-9 expression is increased during ischemia, and MMP-9-null mice develop less edema after ischemia [177, 178]. MMP-9 is inhibited endogenously by TIMP-1, which has a putative caspase-9 cleavage site. In this chapter, we explore the relationship, if any, between caspase activity and MMP-9 in transient ischemia (Chapter 3.2.4.).

3.2. Results

3.2.1. Measuring Initiator Caspase Activity *In Vivo*

To determine which initiator caspases were activated early in stroke, rats were injected with 200 nmoles bVAD via convection-enhanced delivery (CED) to the rat striatum. Injections were executed immediately prior to transient MCAo (2 hr occlusion), which was followed by reperfusion and sacrifice at 1 hour post reperfusion (hpr). The injected region was dissected, and bVAD-caspase complexes were isolated on streptavidin-agarose beads and analyzed by western blotting. BVAD captured caspase-9 and caspase-8 (Figure 3-1A), which indicates the activation

of these initiator caspases as an early event in stroke. Caspase-1 and caspase-2 were not trapped by bVAD at 1hpr (Figure 3-1C).

Figure 3-1.

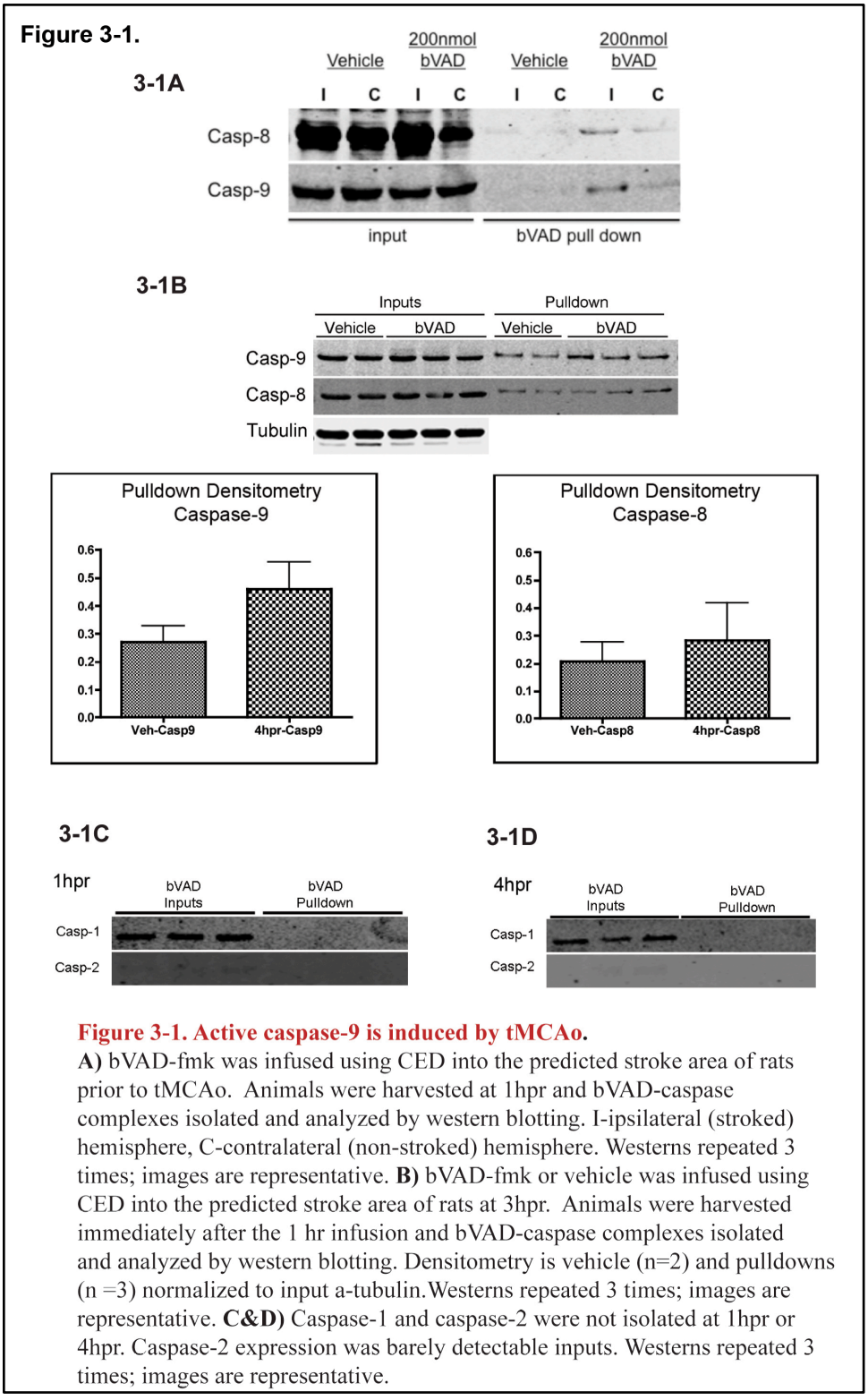

Figure 3-1. Active caspase-9 is induced by tMCAo.
A) bVAD-fmk was infused using CED into the predicted stroke area of rats prior to tMCAo. Animals were harvested at 1hpr and bVAD-caspase complexes isolated and analyzed by western blotting. I-ipsilateral (stroked) hemisphere, C-contralateral (non-stroked) hemisphere. Westerns repeated 3 times; images are representative. **B)** bVAD-fmk or vehicle was infused using CED into the predicted stroke area of rats at 3hpr. Animals were harvested immediately after the 1 hr infusion and bVAD-caspase complexes isolated and analyzed by western blotting. Densitometry is vehicle (n=2) and pulldowns (n =3) normalized to input a-tubulin.Westerns repeated 3 times; images are representative. **C&D)** Caspase-1 and caspase-2 were not isolated at 1hpr or 4hpr. Caspase-2 expression was barely detectable inputs. Westerns repeated 3 times; images are representative.

3.2.2. Temporal Activation of Caspase-9 in Cerebral Ischemia

While caspase-9 can be isolated with bVAD early in the stroke (1hpr, Figure 3-1A), it is still active at 4hpr (Figure 3-1B). Thus, there is extended activation of caspase-9 during stroke. This finding is likely indicative of progressive cell death during stroke. In other words, not every cell dies at once.

The caspase-9 antibody that was used for staining recognizes full-length and cleaved forms of the protease. Therefore, elevated IHC staining in ischemic samples could be indicative of increased caspase-9 expression, increased caspase-9 cleavage into activated forms, or both. The input samples for the western blots in Figure 3-1 demonstrate that full-length caspase-9 expression is not elevated in the ipsilateral versus contralateral hemispheres at 1hpr or 4hpr. Thus, positive caspase-9 staining in Figure 3-2 is potentially due to caspase cleavage and the binding of antibody to neoepitopes.

After stroke, there is a detectable increase in caspase-9 immunofluorescence at 4hpr and 24hpr (Figure 3-2). Caspase-9 co-localized with cleaved forms of effector caspase-6 (cl-C6) in processes and soma. In healthy rodent brains, caspase-9 and cl-C6 are not detected by immunostaining (Chapter 4 Figure 4-8). The co-localization of caspase-9 and cl-C6 supports a mechanism for caspase-9 activating caspase-6 (discussed in Chapter 4).

Interestingly, active caspase-8 was not isolated at 4hpr by bVAD pulldown (Figure 3-1B; densitometry is provided because of considerable background in vehicle samples). This finding implies that caspase-8 mediates cell death in the early, but not late, stages of transient ischemia. Caspase-1 and caspase-2 were not trapped by bVAD at 4hpr (Figure 3-1D).

3.2.3. Caspase-9 Inhibitor: Penetratin1-X-linked Inhibitor of Apoptosis Protein-BIR3 Domain (Pen1-XBIR3)

Figure 3-2.

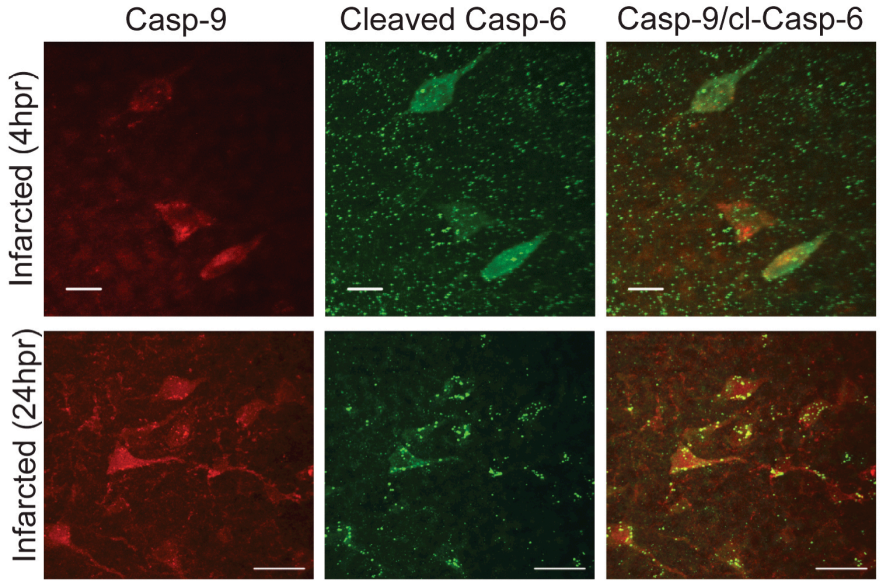

Figure 3-2. Caspase-9 and cleaved caspase-6 are induced in the same cells early in tMCAo.
Rats were subjected to 2hr tMCAo followed by 4hpr or 24hpr. Caspase-9 and cl-C6 immunostaining reveals cells co-labeled with caspase-9 and cl-C6 at both timepoints. Caspase-9 is visible in the processes along with cl-C6. Non-stroked rodent brain does not display caspase-9 or cl-C6 staining (Figure 4-8A). Confocal microscopy; Scale: 25 µm. Cortical penumbra staining.

Therapeutic access of compounds to damaged neurons in the brain requires overcoming several obstacles including the blood brain barrier (BBB) and the plasma membrane of the neuron. To provide intracellular delivery, XIAP-BIR3 was disulfide-linked to Penetratin1, a cell permeating peptide [179] (Figure 3-3A). Upon entry into the cell, the reducing environment of the cytoplasm breaks the disulfide linkage. This event releases the peptide cargo and allows it to act at its target. Functional efficacy of this construct was confirmed using primary hippocampal neuron cultures that were subjected to 4-hydroxynonenal (HNE)-mediated death, which is dependent on caspase-9 [170]. Treatment of HNE-treated cultures with Pen1-XBIR3 abrogated death compared to vehicle treatment alone (Figure 3-3B).

To ensure that a Pen1-peptide could be delivered to cells, Pen1-XBIR3 was labeled with rhodamine and delivered to cortical neurons in culture. After a 30-min incubation, Pen1-XBIR3

was clearly present within the soma (Figure 3-3C). Without a cell transduction peptide, rhodamine collected on the outside of cells (Figure 3-3C).

Figure 3-3.

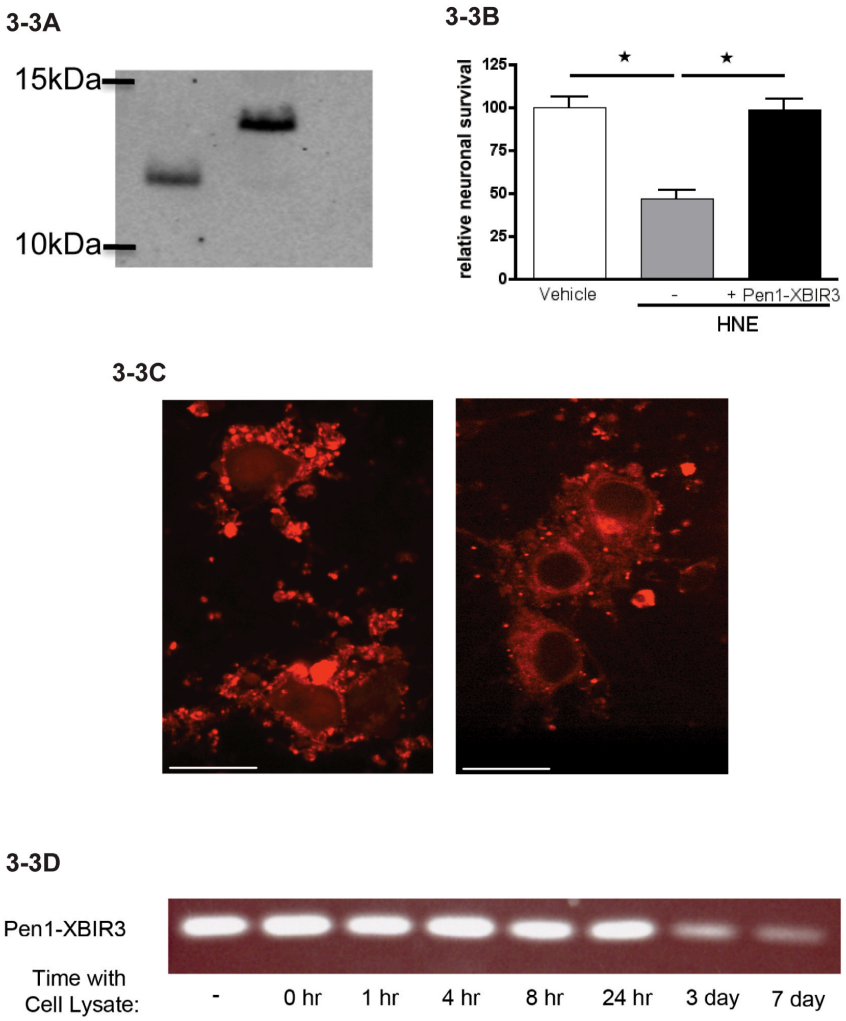

Figure 3-3. Penetratin1 - A Trojan Carrier Peptide for Caspase Inhibitors.
A) Purified BIR3 domain from XIAP (XBIR3) was linked to Penetratin1 (Pen1), a cell transducing peptide. Equimolar amounts of Pen1 and XBIR3 were incubated overnight at 37°C. Linkage is mediated by formation of disulfide bonds. Western blot with anti-6xHIS; recombinant BIR3 peptide has HIS tag. **B)** HNE-induced hippocampal neurodegeneration in vitro is blocked by Penetratin1-linked XBIR3. Primary hippocampal neurons were treated with 3μM HNE with and without 80nM Pen1-XBIR3. Relative neuronal survival was quantified after 1 day treatment, n=3. **C)** Rhodamine-labeled Pen1-XBIR3 readily accesses the neuronal soma within 30min (right panel). Free Rhodamine collects outside of cells (left panel). Scale: 50 μm. **D)** Pen1-XBIR3 (3 μL of 36 μM stock) incubated for the indicated times at 37°C in 50 μL of cortical neuron lysate.

It is valuable for drug design to understand the stability of a compound in a physiological setting. Unfortunately, we could not perform full-fledged half-life studies in cell culture or animal models because we were limited by our supply of recombinant XBIR3 peptide. As an alternative, we incubated aliquots of Pen1-XBIR3 (3 µl of 36 µM stock) in 50 µl of cortical neuron lysate for prescribed periods or time (0 hr, 1 hr, 4 hr, 8 hr, 24 hr, 3 day, 7 day) at 37°C. Pen1-XBIR3 is stable in cortical neuron extracts for at least 24 hr (Figure 3-3D).

To demonstrate peptide delivery in the CNS, Pen1 was linked to a FITC-labeled control peptide (termed "hexapeptide"; 6 aa) that was also labeled with FITC. Pen1-hexapeptide was delivered directly to the striatum using convection-enhanced delivery (CED). Brains were harvested 1 hr after delivery (Figure 3-4). The FITC-hexapeptide entered cells (Figure 3-4 inset) and was distributed throughout the ipsilateral hemisphere.

Figure 3-4.

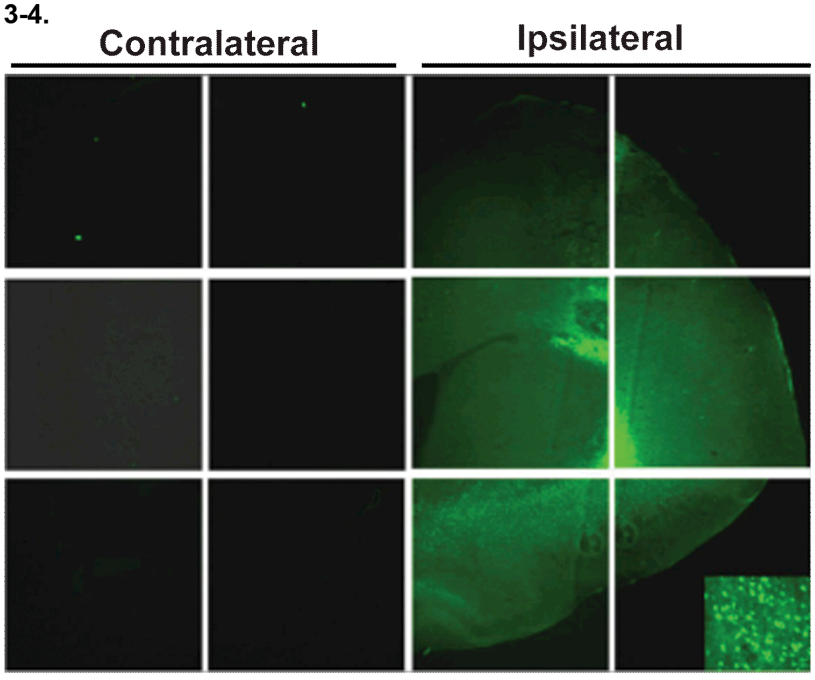

Figure 3-4. Delivery of Pen1-fluorescent peptide to CNS by CED.
Pen1 was linked to a FITC-labeled hexapeptide, which was delivered to the striatum using CED. Diffuse spreading is observed throughout the injected (ipsilateral) hemisphere in the striatum and surrounding cortical matter (4x magnification). Crossover into the non-injected (contralateral) hemisphere was not observed. Inset at higher magnification (20x) shows cellular uptake of FITC. Epifluorescence microscopy.

CED administration provided proof-of-principle that Pen1-peptide can be delivered into the cells in the CNS, but we also utilized a method with greater therapeutic potential: intranasal delivery. Intranasal delivery of neurotrophins and other compounds has been demonstrated to provide access to the CNS to prevent neurodegeneration in a number of disease models [101] including with stroke [174, 175]. This delivery method takes advantage of the olfactory and trigeminal pathways to bypass the BBB and directly access the cerebral spinal fluid and ventricular system. Given that Pen1-cargo indiscriminately crosses biological membranes, systemic administration might result in the cargo being lost in epithelial cells and pericytes as the molecule crosses the BBB or entrapment by non-target organs.

Until now, proteins and compounds delivered intranasally to the rodent CNS have targeted extracellular molecules, such as cell surface receptors. Since we were targeting caspases, which are intracellular proteins, we needed a method for transporting cargo across the plasma membrane. As shown above (Figures 3-3 & 3-4), Penetratin1 provides intracellular uptake of linked peptides. Pen1-XBIR3 was delivered intranasally to rats; brains were sliced coronally; and the presence of XBIR3 in the brain was determined by western blotting (Figure 3-5). Pen1-XBIR3 was delivered to all slices of the brain, similar to the delivery pattern observed with IGF [103].

The effects of Pen1-XBIR3 on ischemia-induced changes in neuron density were assessed by immunostaining for NeuN. Prophylactic intranasal Pen1-XBIR3 provided significant protection against neuron loss at 24hpr, (Figure 3-6). Fluorescent Nissl (NeuroTrace) staining of neuronal ribosomes/endoplasmic reticula yielded similar results (Figure 3-6).

We tested whether Pen1-XBIR3 could prevent sensory-motor disability seen in stroke by administering either a prophylactic (pre-occlusion) or therapeutic (4hpr) intranasal bolus of

vehicle or Pen1-XBIR3. All prophylactic administrations were given immediately prior to the occlusion. Rats were assayed with a 24-point neurofunctional scale beginning at 1 day post-ischemia, with testing every other day for 3 weeks after the ischemic event. Animals treated with Pen1-XBIR3, either prophylactically or at 4hpr, exhibited significantly less stroke-related disability than their vehicle-treated counterparts (Figure 3-7). Therapeutic protection by Pen1-

Figure 3-5.

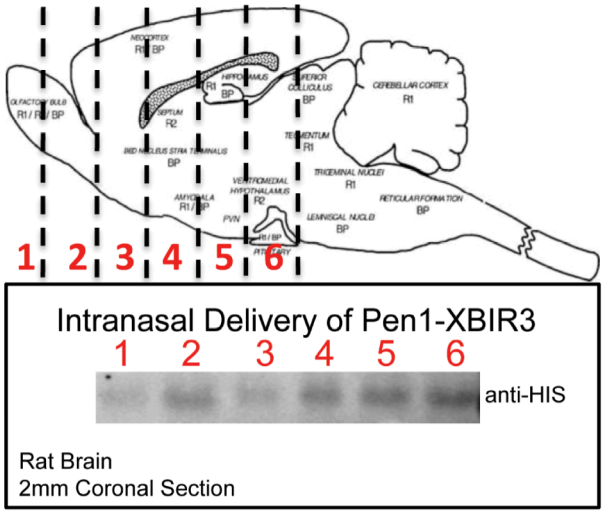

Figure 3-5. Intranasal application delivers Pen1-XBIR3 throughout the rat CNS. The rat was sacrificed 1hr after intranasal delivery of Pen1-XBIR3 (60µl). The brain was sliced into 6 – 2mm coronal sections from anterior (olfactory bulbs) to posterior (occipital pole). Slices were solubilized and protein analyzed by SDS-PAGE and western blotting with anti-HIS. Lanes 1-6: coronal sections anterior (#1) to posterior (#6).

XBIR3 indicates that caspase-9 activation is persistent at least until 4hpr and that this pathway is critical for the acute neurodegeneration elicited by stroke.

3.2.4. Proneurotrophins, Caspase-9, and Cerebral Edema

Direct stroke volume (infarct area:ipsilateral hemisphere area) at 24hpr, as measured by H&E staining, was also reduced in the Pen1-XBIR3 cohort (Figure 3-8; Veh: 55.08 ± 3.546 vs. Pen1-XBIR3: 38.56 ± 4.749). Direct stroke volume automatically corrects the size of the infarct for its level of edema. In contrast, indirect stroke volume (infarct area:contralateral hemisphere area)

does not account for the contribution of edema to infarct size. For vehicle-treated animals, indirect stroke volume was 65.95 ± 4.933, meaning edema accounts for about an 11% expansion in the size of the infarct. For the Pen1-XBIR3 cohort, stroke volume was essentially identical between direct and indirect measurements (38.56 ± 4.749 vs. 39.24 ± 6.276). This finding may indicate that Pen1-XBIR3 reduces edema during MCAo, in addition to decreasing stroke volume. These results show that caspase-9 mediates neuronal death and that intranasally delivered Pen1-XBIR3 is neuroprotective against stroke.

Previous studies have demonstrated that the p75 neurotrophin receptor (p75NTR) death pathway activates caspase-9 [55-58, 176], and p75NTR activation by proneurotrophins increases edema during cardiac ischemia (Barbara Hempstead personal communication). It is possible that p75NTR stimulation by proneurotrophins is connected to the progression of edema development during stroke. In normal tissue, p75NTR stains small blood vessels and co-localizes with the pericyte marker smooth muscle actin (SMA) (Figure 3-9A). Pericytes are contractile cells that surround cerebral capillaries and that govern blood brain barrier integrity in healthy and pathologic scenarios [45]. At early time points of ischemia (1hpr), p75NTR also co-localized with the small vessel endothelial marker CD34 (Figure 3-9B). Thus, p75NTR is spatially primed to induce cell death in brain capillaries.

Caspase-9 staining is also found in the vasculature during the early stages of stroke (1hpr) (Figure 3-9C). In this scenario, caspase-9 co-stains with the endothelial CD34 marker but does not overlap with the pericyte marker SMA (Figure 3-9D). The caspase-9 antibody that was used for staining recognizes full-length and cleaved forms of the protease.

Figure 3-6.

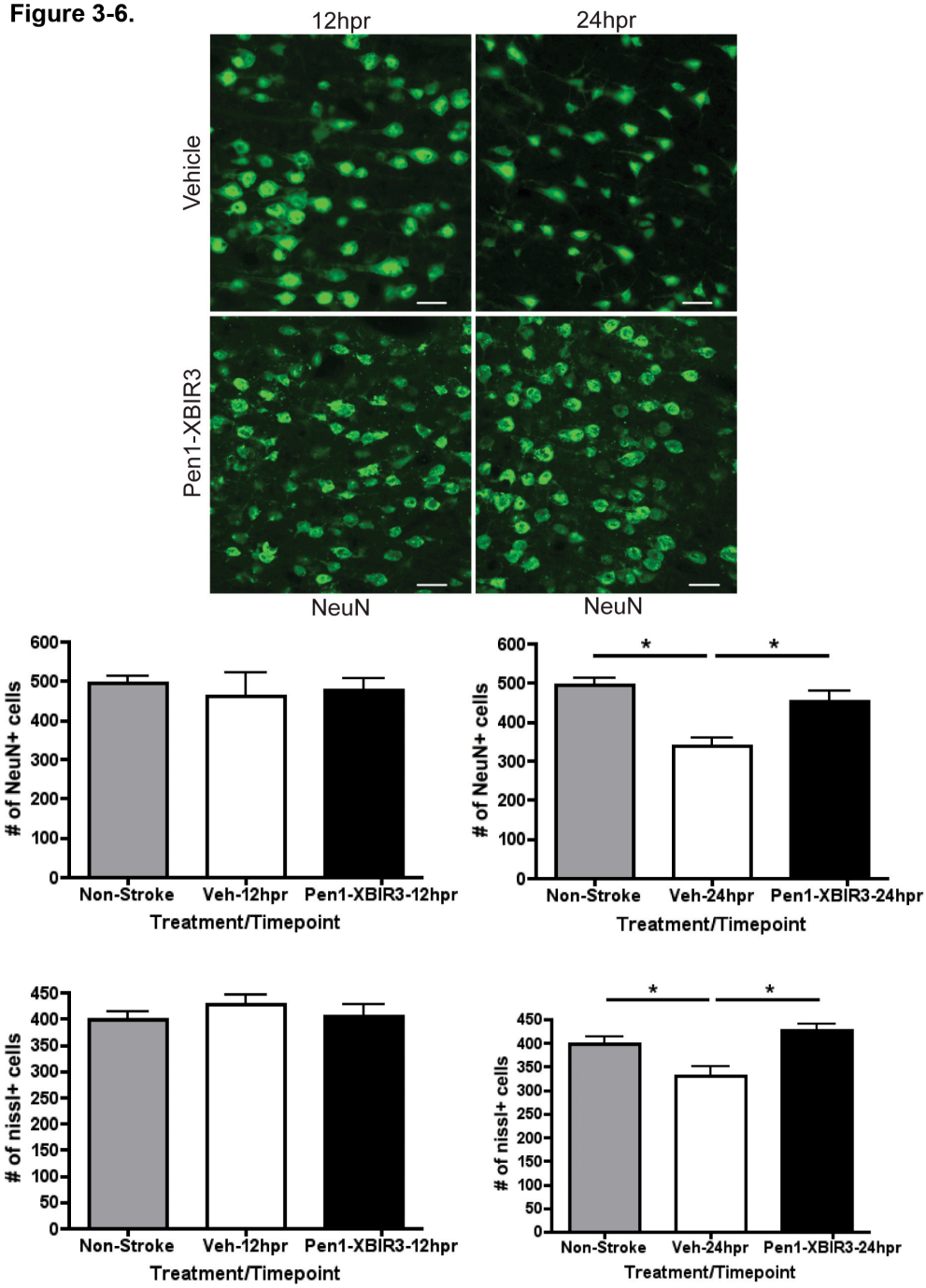

Figure 3-6. Intranasal Pen1-XBIR3 provides short-term protection from tMCAo.
Vehicle or Pen1-XBIR3 was intranasally delivered and rats were harvested at 12hpr (left panels) and 24hpr (right panels). Sections were immunostained for NeuN (green), and NeuN positive cells were quantified. Epifluorescence microscopy. Scale: 50 μm. Graphs are means (with SEM) of neuron counts at 12hpr and 24hpr. Non-stroked: 494.7±18.52, n=3; Vehicle-12hpr: 463.7±57.53, n=3; Pen1-XBIR3-12hpr: 477.3±28.95, n=3; Vehicle-24hpr: 338.0±22.91, n=3; Pen1-XBIR3-24hpr: 453.7±25.44, n=3; (ANOVA, *$p < 0.05$.).

Figure 3-7.

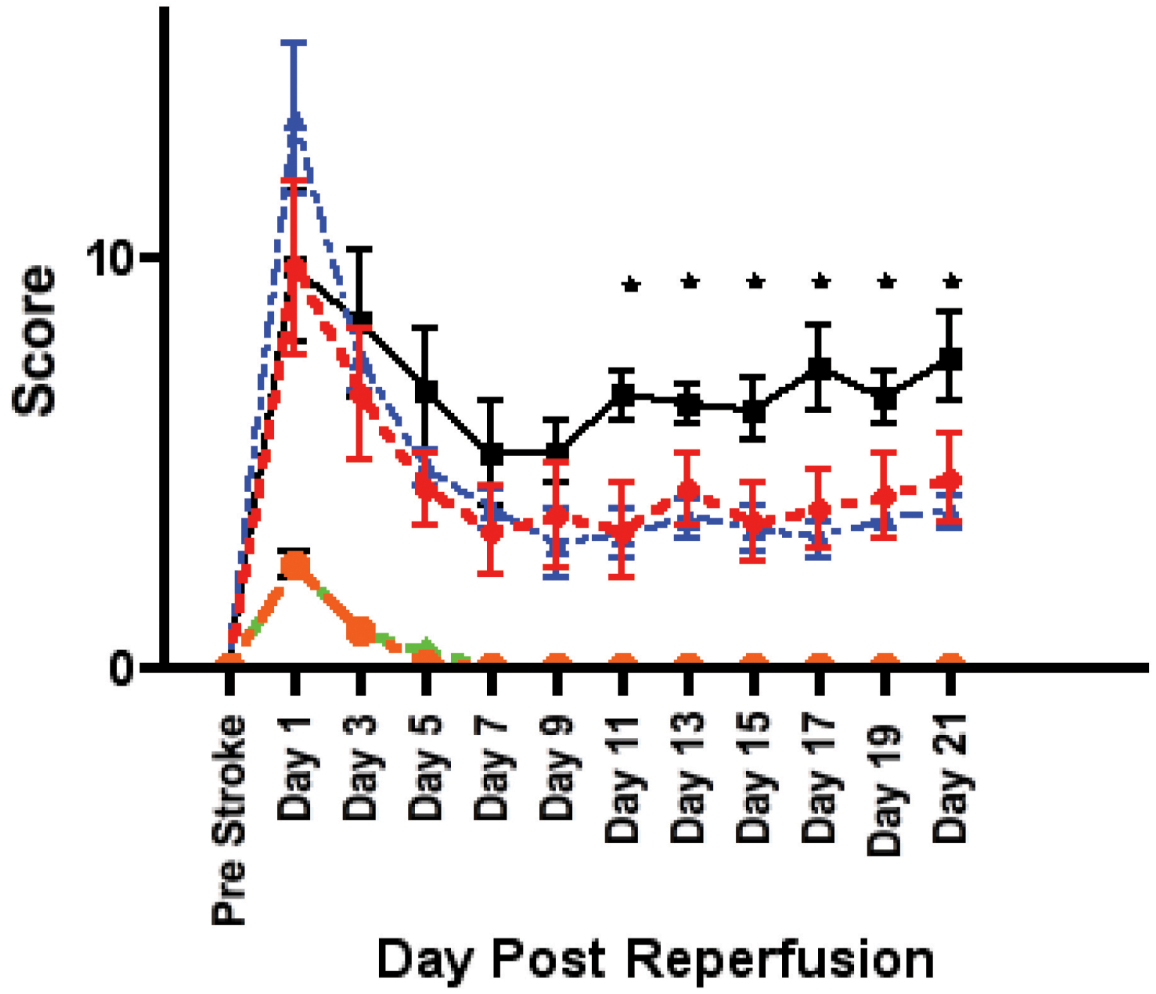

Figure 3-7. Intranasal Pen1-XBIR3 provides long-term protection from tMCAo.
2hr tMCAo was performed on rats given either prophylactic (pre-stroke) intranasal vehicle (black squares) or prophylactic Pen1-XBIR3 (blue triangles) or therapeutic Pen1-XBIR3 (red circles). Prophylactic: immediately prior to occlusion; Therapeutic: post-stroke at 4hpr. Rats were monitored for 21 days. Means (with SEM) of neurofunctional score. Control vehicle (green diamond) and Pen-XBIR3 (orange circle) animals displayed no loss of neurofunction. (ANOVA, *indicates stroked prophylactic vehicle vs. prophylacticor therapeutic Pen1-XBIR3, n = 8 per group, $p < 0.05$.).

Figure 3-8.

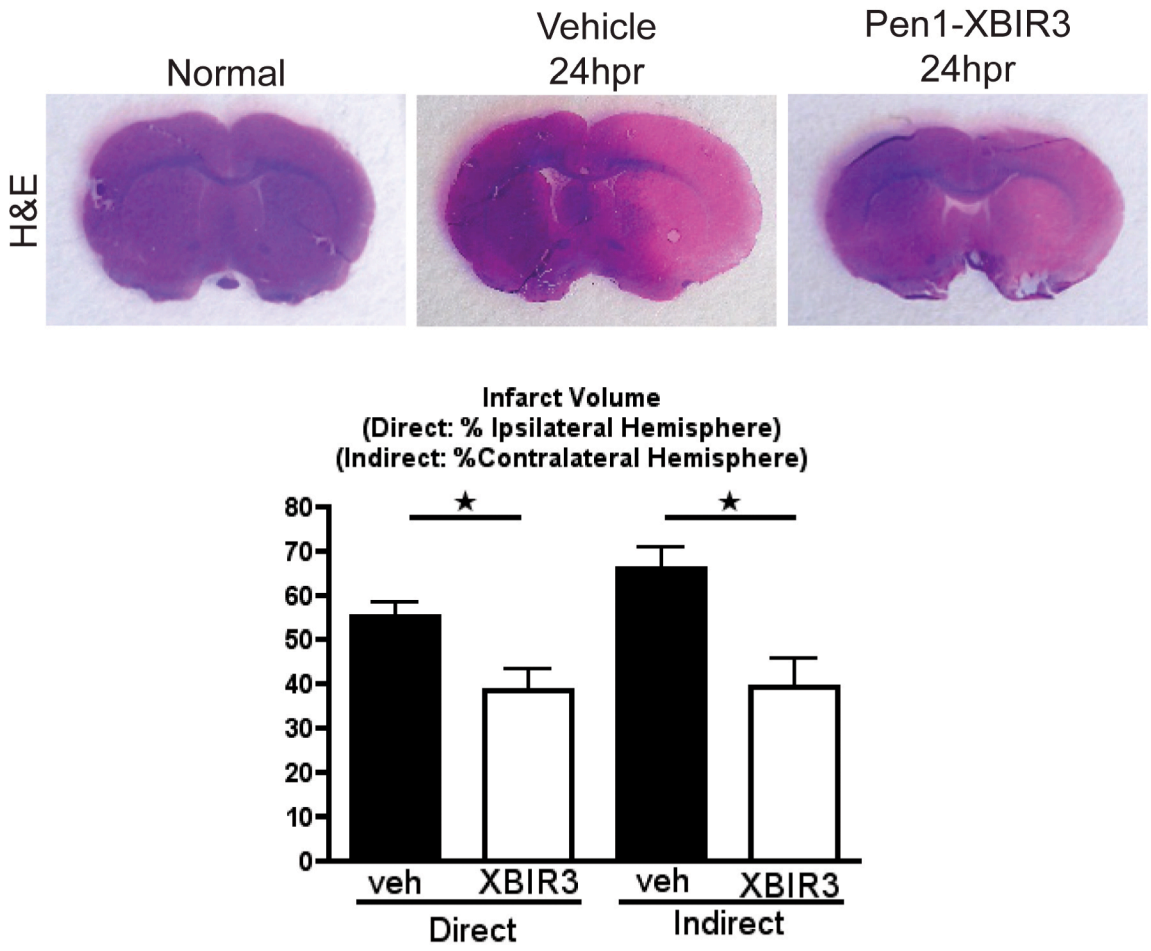

Figure 3-8. Intranasal Pen1-XBIR3 reduces ischemic infarct volume. Vehicle or Pen1-XBIR3 was intranasally delivered in rats as in (Figure 3-6 & 3-7), and animals were harvested at 24hpr (right panels). Sections were stained with hematoxylin and eosin. Direct (infarct area: ipsilateral hemisphere area) and indirect (infarct area: contralateral hemisphere area) stroke volume was quantified. Direct - Vehicle-24hpr: 55.08 ± 3.546, n=3; Pen1-XBIR3-24hpr: 38.56 ± 4.749, n=3 (Student's t-test, *$p < 0.05$). Indirect - Vehicle-24hpr: 65.95 ± 4.933, n=3 Pen1-XBIR3-24hpr: 39.24 ± 6.276, n=3 (Student's t-test, *$p < 0.05$).

Therefore, the rapid increase in caspase-9 staining by 1hpr in ischemic samples could be indicative of increased expression, increased cleavage, or both. Akin to cortical tissue (Chapter 4 Figure 4-8A), vasculature in control animals was negative for capase-9 staining.

We found that Evans blue extravasation was increased by 4hpr in mice given intranasal vehicle (saline) prior to tMCAo (Figure 3-10A). In contrast, intranasal Pen1-XBIR3 treatment of mice immediately before occlusion reversed vascular leakage, as measured by Evans blue (Figure 3-10A; Ipsilateral: control - 0.6517 ± 0.09159; Veh-4hpr - 1.154 ± 0.0626; Pen1-XBIR3-4hpr - 0.7378 ± 0.08593; n = 4 per group; units: ng of Evans blue/mL lysate sample). The contralateral hemisphere was used as an internal control (Figure 3-10A; Contralateral: control - 0.5574 ± 0.1481; Veh-4hpr - 0.7191 ± 0.2125; Pen1-XBIR3-4hpr - 0.5435 ± 0.06621; n = 4 per group; units: ng of Evans blue/mL lysate sample).

We hypothesized that p75NTR and caspase-9 mediate edema through the disinhibition of MMPs. With this regard, expression of the p75NTR-activator proNGF is induced in stroked animals at 12 and 24hpr (Figure 3-10B). When MMP-9 expression was assayed at 24hpr in control, vehicle-treated, and Pen1-XBIR3-treated rats, we found that stroke elevated MMP-9 expression, but Pen1-XBIR3 prevented this induction (Figure 3-10C).

3.2.5. Caspase-8 in Neonatal Hypoxia-Ischemia

In collaboration with Dr. Vadim S. Ten (Columbia University), we investigated whether initiator caspases are active in the early stages of neonate hypoxia-ischemia. Previous studies have demonstrated that neonate Bax-/- mice are resistant to hypoxia-ischemia [46], and broad caspase inhibitors are neuroprotective in this model [44]. Akin to Chapter 3.2.1., we used bVAD to isolate active caspases *in vivo* by injecting this pan-caspase inhibitor into the predicted site of

Figure 3-9.

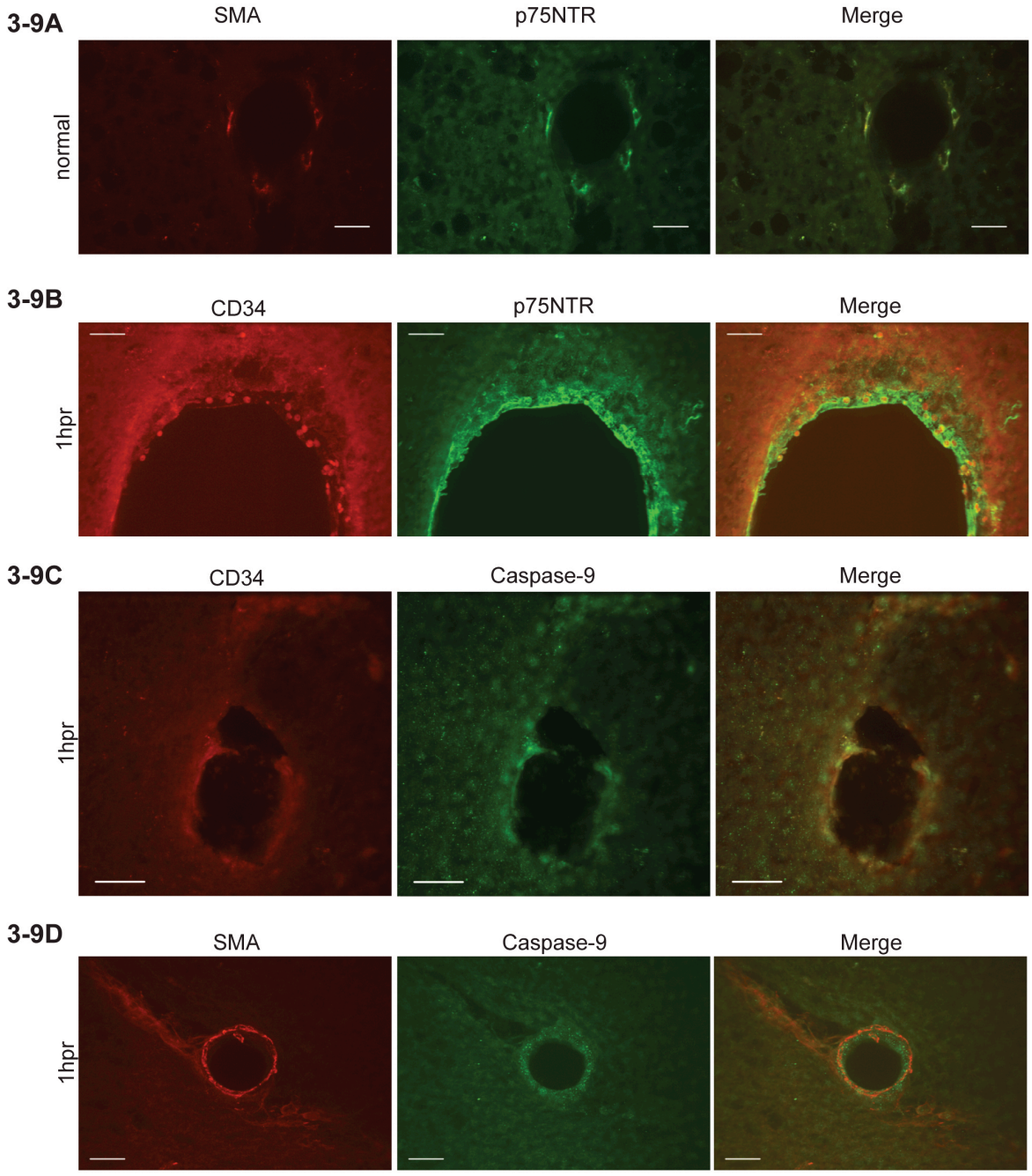

Figure 3-9. Cerebral blood vessels express p75NTR and caspase-9.
A) In normal tissue, pericytes (smooth muscle actin, SMA) express p75NTR. Early in stroke (1 hpr), endothelial cells (CD34) express **B)** p75NTR and **C)** Caspase-9. **D)** At the same ischemic timepoint, SMA sreactivity circumscribes caspase-9 staining, suggesting caspase-9 is restricted to endothelial cells. Confocal microscopy. Scale: 50 μm.

Figure 3-10.

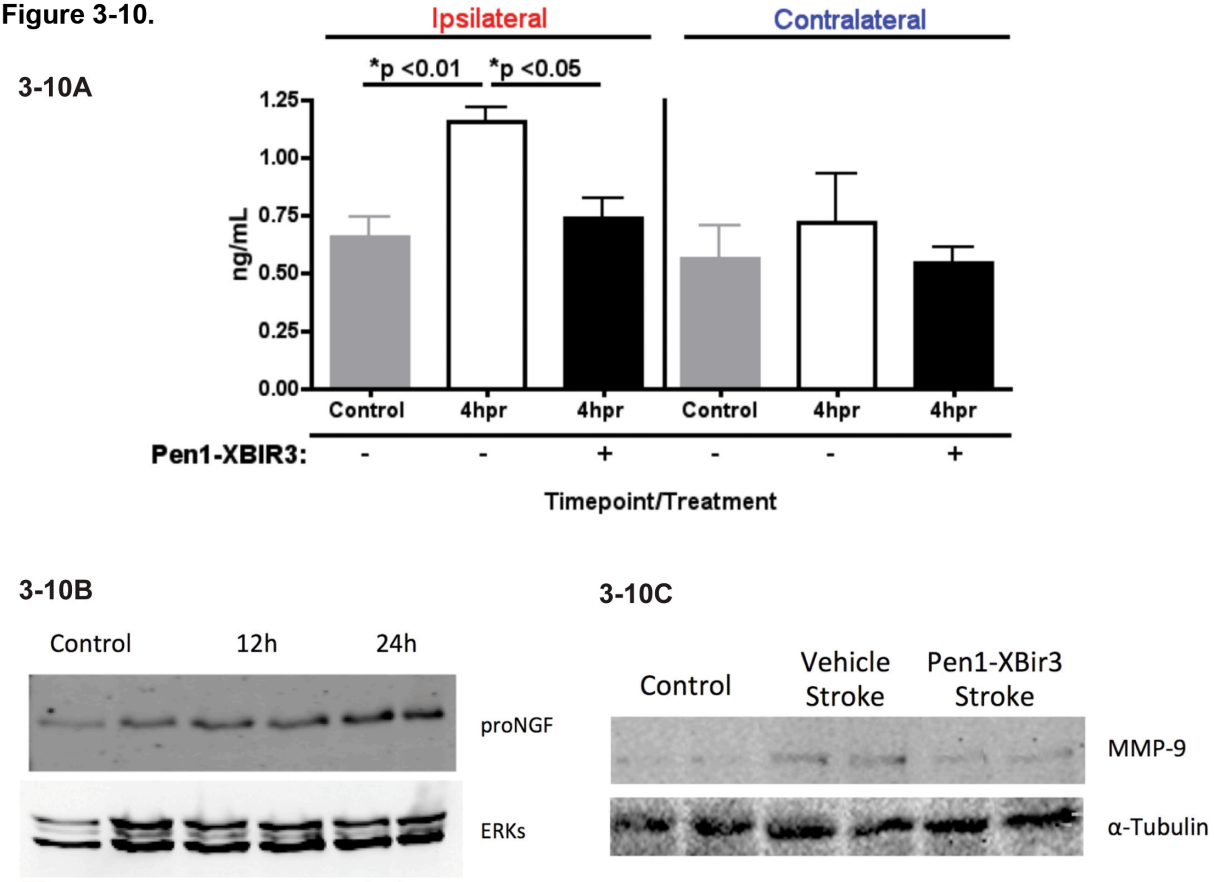

Figure 3-10. Caspase-9 regulates BBB integrity and MMP expression during stroke.
A) Evans blue extravasation was performed to assess cerebreal edema and BBB integrity during stroke. Vehicle or Pen1-XBIR3 were intranasally delivered to mice before tMCAo (45 min occlusion), and Evans blue (2% in saline) was tail-vein injected 30 min prior to sac, harvest, and sample prep. Pen1-XBIR3 reduced etravasation in the ipsilateral (infarcted) hemisphere caused by ischemia. The contralateral hemisphere provides an interanl control. Extrernal standards were used to quantify the ng/mL of Evans blue in each lysate sample (scanned in 96-well opitical plate; 620 nm excitation, 680 emission). Ipsilateral: control - 0.6517 ± 0.09159; Veh-4hpr - 1.154 ± 0.0626; Pen1-XBIR3-4hpr - 0.7378 ± 0.08593. Contralateral: control - 0.5574 ± 0.1481; Veh-4hpr - 0.7191 ± 0.2125; Pen1-XBIR3-4hpr - 0.5435 ± 0.06621. n = 4 per group **B)** ProNGF expression is increased in stroked animals at 12hpr and 24 hpr relative to control animals. Western blot. ERK was used as a loading control. **C)** MMP-9 expression is elevated at 24 hpr in vehicle-treated animals, and this trend is reversed in Pen1-XBIR3-treated animals. Western blot. α-Tubulin was used as a loading control.

injury prior to hypoxia-ischemia. Caspase-bVAD complexes were extracted 1 hour after hypoxia-ischemia.

In contrast to adult tMCAo, caspase-8 was isolated but not caspase-9 (Figure 3-11). Additionally, caspase-2 was not isolated, although genetic ablation of caspase-2 is

neuroprotective against hypoxia-ischemia [95, 96]. It is possible that caspase-2 is not activated at this early stage. Although caspase-1 was not isolated with bVAD, this inhibitor appears to affect the expression level or potentially the processing of this inflammatory caspase (Figure 3-11, inputs). It is possible that bVAD inhibits a caspase that modulates caspase-1. Given the role of caspase-1 in cytokine production, this finding points to a caspase-caspase-1 regulatory pathway for inflammation.

3.3. Discussion

It is common practice to use short peptide caspase substrates, such as DEVD for caspase-3 and IETD for caspase-8, to measure caspase activity. However, these peptides are highly promiscuous [91] and can generate misleading data. Biotin-VAD-fmk, an irreversible pan-caspase inhibitor, provides a reliable measurement of caspase activity, through the biochemical pulldown of active caspases, and has been shown to isolate caspases-1, -2 -8 or -9, depending on the death stimulus utilized. Originally used to assay caspase activity in cell lines [171], and, more recently, in primary neuron cultures [173], we have adapted this procedure for *in vivo* use in the CNS. In the present study, we use this technique to demonstrate that caspase-9 is active early in the progression of the infarct (1hpr). Caspase-8 is also active during the earlier stages of adult tMCAo and in neonate hypoxia-ischemia.

Small peptide caspase inhibitors, such as zVAD and DEVD, have been shown to confer neuroprotection in rodent models of stroke [89]. These inhibitors, as mentioned above, are not specific for individual caspases [91]; therefore, these studies do not specify which caspases are most important.

Given the non-apoptotic functions of caspases in the nervous system, such as with caspase-3 and synaptic plasticity [92], indiscriminately blocking the entire caspase family might

prove detrimental to stroke recovery. For example, axon sprouting and regeneration are common after ischemic attack and are arguably important for recovery [180].

Figure 3-11.

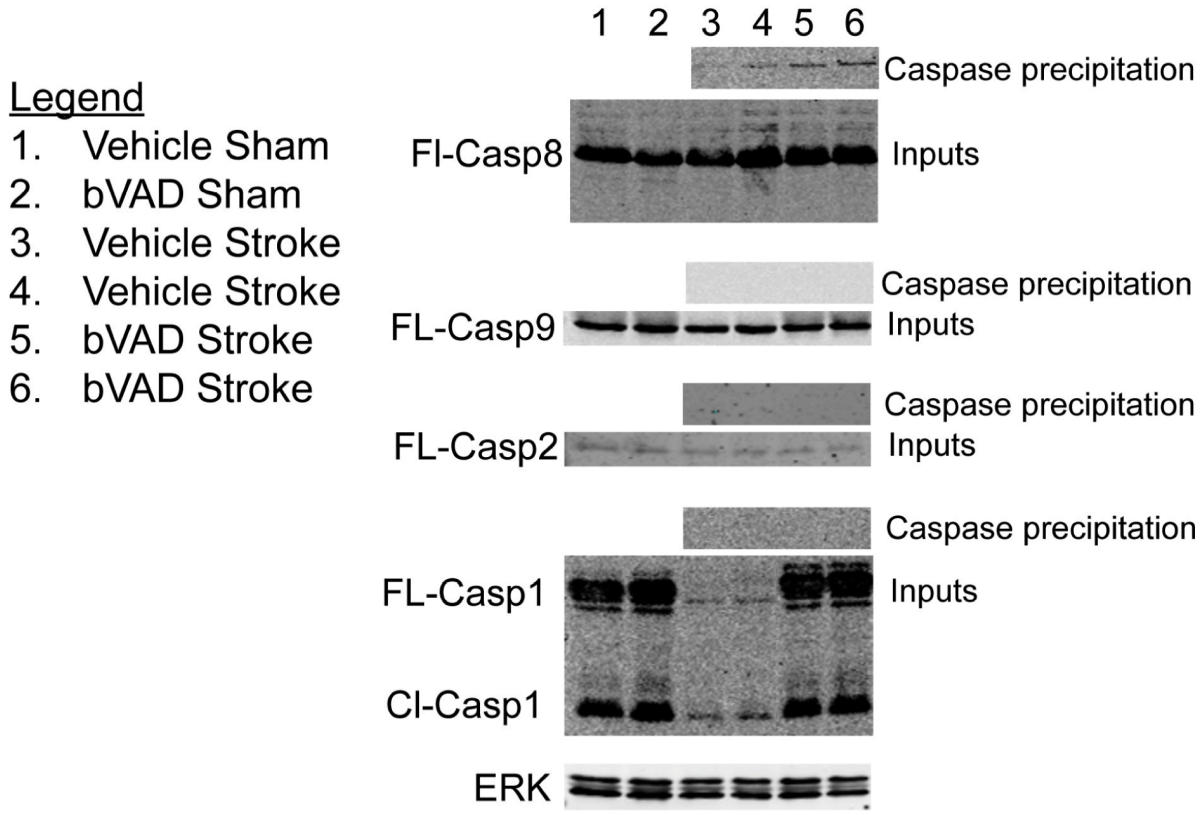

Figure 3-11. Caspase-8 is activated in neonate hypoxia-ischemia. bVAD-fmk was infused using CED into the mice during hypoxia-ischemia. Animals were harvested 1 hr after hypoxia, and bVAD-caspase complexes were isolated. Western blot analysis of ipsilateral samples. Only caspase-8 was isolated. Caspase-1 expression is reduced during hypoxia-ischemia, and this is blocked by bVAD-fmk.

Growing evidence supports a role for caspases in synaptic plasticity [92], dendrite pruning [181], and axon regeneration in the context of retinal injury [182]. Although a relationship between caspases and axon regeneration during stroke has not been investigated, it is possible that non-selective caspase inhibition could impair this recovery mechanism.

Alternatively, rampant cell death might be needed early in stroke to remove terminal cells (i.e., cells past the point-of-no-return), but prolonged apoptotic activity could be unnecessarily detrimental. Defining the best windows of treatment is imperative for the success of caspase-based neuroprotection.

The extrinsic caspase-8 pathway is clearly activated during the early stages of adult tMCAo as well as in neonate hypoxia-ischemia. A specific caspase-8 inhibitor is required to assess the importance of caspase-8 in stroke pathogenesis.

This chapter details a central role for caspase-9 in stroke pathogenesis and possibly ischemic edema. Caspase-9 activity is stimulated early in stroke, and elevated caspase-9 is observed in neurons with cl-C6. Thus, we hypothesized that caspase-9 leads to caspase-6 activation during stroke.

The findings in this chapter show that intranasal Pen1-XBIR3 is neuroprotective against stroke with measurements of short-term (neuron density/stroke volume at 24hpr) and long-term (3-week neurobehavioral assay) outcomes.

The BIR3 domain from XIAP (XBIR3) is a highly specific inhibitor of caspase-9. We linked XBIR3 by a reducible disulfide bond to Penetratin1 (Pen1), a transduction peptide that efficiently delivers cargo across the plasma membrane [179, 183, 184] to inhibit caspase-9 activity in cells. The use of a transient disulfide linkage between Pen1 and the cargo peptide ensures that the cargo peptide can assume its native functional conformation once it is transported into the cell. This method contrasts with cell permeant peptide fusion domains, such as TAT, which can lead to non-functional misfolded cargo protein (G. Salvesen, personal communication). Prior studies showed that Intraperitoneal delivery of a similar caspase-9 inhibitor, a fusion protein of PTD-XBIR3-RING (protein transduction domain with XIAP BIR3

and RING domains), reduces infarct volume following tMCAo [183, 184], but did not explore the downstream mechanisms, which are addressed in the next chapter.

This chapter outlines the previously unknown contribution of the p75NTR-caspase-9 pathway in ischemic edema. Inhibiting caspase-9 prevents Evans blue extravasation at 4hpr (Figure 3-10) along with the expansion in hemispheric swelling and midline shift at 24hpr (Figure 3-8), which signifies a healthier BBB. This is the first demonstration that caspases mediate edema during cerebral ischemia. P75NTR and caspase-9 immunofluorescent staining were observed in neurovascular cells (endothelial and pericytes) before (with p75NTR) and during the early stages (with p75NTR and caspase-9) of ischemia (Figure 3-9). Moreover, p75 expression, as measured by western blot, is increased at 12hpr and 24hpr (Figure 3-10).

MMPs are known to cleave substrates in the vascular basal lamina that regulate BBB integrity. MMP-2 and MMP-9 have been implicated previously in cerebral edema during stroke [139-144], with MMP-9 correlating with a second wave of edema observed approximately 24 hr after stroke onset. We show that inhibiting caspase-9 activity reduces MMP-9 expression at 24hpr, but mechanistic questions remain.

MMPs are secreted or membrane-bound. Thus, it is unlikely that they directly interact with caspase-9, which is restricted to the cytoplasm and is not found in vesicles. It is possible that caspase-9, or one of its downstream effector caspases, prevents the transcription of MMP-9. The transcriptional promoter region for MMP-9 has been characterized [185]. It is comprised of the following binding sites: NF-κB, SP1, PEA3, AP1, TIE, KRE, RCE, and TATA [185]. Caspases have been shown to cleave NF-κB p65 [186, 187] and SP1 [186, 188]. Both are transcriptional activators, so it is counterintuitive that their cleavage, if it occurs during ischemia, would directly lead to an elevation in MMP-9 expression. A brief review of the literature did not

yield any publications on other transcription factors that are implicated in MMP-9 expression. However, it is possible that cleavage of NF- κB, SP1, or other transcription factors alters the function/expression of intermediate(s) that regulate MMP-9.

Chapter 4. Effector Caspases in Stroke Neurodegeneration

4.1. Introduction

Of the effector caspases, only caspase-3 has been implicated in stroke pathogenesis. Genetic knockout of caspase-3 is neuroprotective against stroke (~50% reduction in stroke volume) [111, 113]. Until now, the remaining effectors—caspase-6 & caspase-7—have never been studied in the setting of cerebral ischemia. Experimental observations during my rotation project (Figure 4-1) steered me towards an investigation of caspase-6 function in stroke.

One of the first indications that caspase-6 is involved with neurodegenerative disease came when it was observed that caspase-6 proteolytically cleaves huntingtin in neurons, which is required for disease progression in Huntington's disease [189].

A role for caspase-6 in axon degeneration is now emerging. Caspase-6 cleaves microtubule-associated protein tau, compromising the stability of the cytoskeleton in axons [190]. In Alzheimer's disease (AD), neuropils harbor both caspase-6-cleaved tau and tubulin [191, 192]. In neuronal culture models, caspase-6 mediates neuronal death and axonal degeneration induced by the activation of the p75 neurotrophin receptor [176, 193] or death receptor 6 [127].

With the latter study, axon degeneration was abundant in dissociated dorsal root ganglion (DRG) neurons that were subjected to trophic factor deprivation [127]. The deleterious effects of caspase-6, as measured by genetic knockdown, appeared to be restricted to process degeneration in this context. In contrast, the neuronal soma remained intact with or without caspase-6.

The research presented in Chapter 4 demonstrates for the first time that caspase-6 mediates both neuronal axon and soma loss during ischemia. The temporal activation of caspase-6 in the stroke penumbra corresponds with the progression of axonal degeneration. Axon

degeneration is a major contributor to cell death and might instigate the early stages of apoptosis via the removal of target-derived trophic factors [194-196]. In clinical cerebral ischemia, axon degeneration is observed as early as 2 days post ischemia [106]; however, the molecular events that trigger axon degeneration potentially begin earlier.

4.2. Results

4.2.1. Caspase-6 Is Active In Neuronal Processes And Soma Following Stroke

After identifying which initiator caspases were active early in the stroke, we turned our attention towards effector caspases. The bVAD precipitation method, which worked well for isolating active initiators, blocks the consequent activation of effectors *in vivo*. Unlike initiators, which can be activated by dimerization without cleavage [43], cleavage of effectors is indicative of activation. Thus, we performed immunohistochemical analysis of cleaved effector caspases.

Rats were subjected to tMCAo, and brains were immunostained for cleaved caspase-6 (cl-C6) at increasing time points after reperfusion. The penumbral region in the forebrain, specifically cortical layers I-IV in the granular insular, somatosensory, dorsal motor cortices (Figure 4-1A), revealed a temporal increase in Cl-C6 staining (Figure 4-1B). No cl-C6 immunostaining was detected in control (non-ischemic) animals. Cleaved caspase-3 was detected (discussed in Chapter 4.2.2.), while cleaved caspase-7 was not observed. While there is evidence that caspase-3 causes cell death in stroke [111, 113], a role for caspase-6 has never been reported.

By 4 hours post reperfusion (hpr), there was marginal cl-C6 staining in the penumbra, but by 12hpr, abundant cl-C6 staining was observed in processes and cell bodies (Figure 4-1B).

There was progressive activation of C6 in cell bodies by 24hpr, which continued through

3 days post reperfusion (dpr). At 7dpr, cl-C6 was only observed in cell bodies, which appeared condensed and might have represented apoptotic bodies. In wild-type mice subjected to tMCAo,

Figure 4-1.

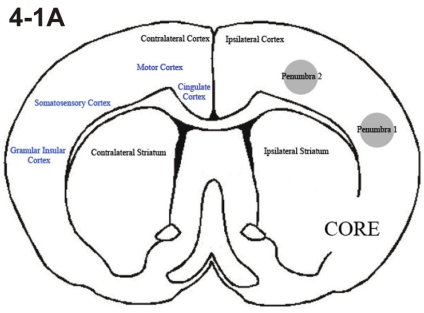

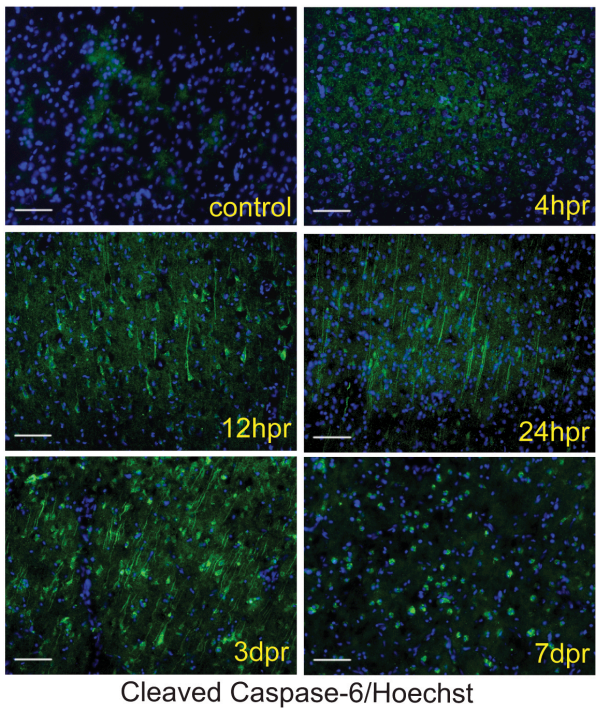

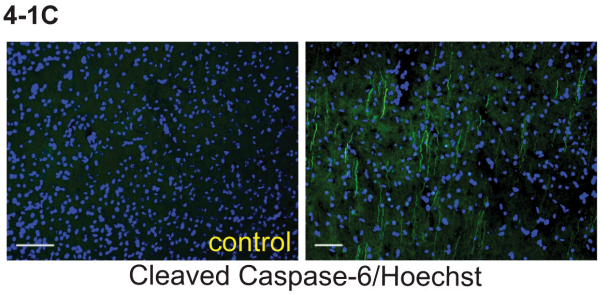

Figure 4-1. Temporal activation of caspase-6 during stroke.
A) Schematic of core and penumbra region in fronto-corticostriatal region. Images shown in panels **B & C** were taken from cortical layers III-IV of the cingulate, primary motor, primary + secondary somatosensory, and granular insular cortices in the penumbra. The MCA to the ipsilateral hemisphere has been transiently occluded whereas the contralateral hemisphere has not been manipulated. **B)** Caspase-6 is activated in cell bodies and processes in stroke penumbra in rat tMCAo. Rats were subjected to 2hr tMCAo followed by reperfusion for the indicated duration. Rodent tissue was immunostained for cleaved caspase-6 (cl-C6, green) and nuclei were stained with Hoechst (blue). Cl-C6 appears in cell bodies and processes at 12hr post-reperfusion (12hpr). Cell body and process staining is observed through 3 days post-reperfusion (3dpr). By 7dpr, nuclei and cell structures that resemble apoptotic bodies are positive for cl-C6. Epifluorescence microscopy. Scale bar: 50 µm. **C)** Caspase-6 is activated in cell bodies and processes in stroke penumbra in mouse tMCAo. Mice were subjected to 1hr tMCAo followed by reperfusion for the indicated duration. Tissue was immunostained for cl-C6 (green) and nuclei stained with Hoechst (blue). Cl-C6 appears in processes. Epifluorescence microscopy. Scale bar: 50 µm.

the pattern of staining was similar, with cell body and process staining detected at 24hpr and 3dpr (Figure 4-1C). This time course neurologically corresponds to both axon degeneration and the progression of the infarct, with expansion of the infarct over the first 3 days.

Co-staining with NeuN showed cl-C6 was present in neurons (Figure 4-2A), whereas there was no co-localization with GFAP, a marker for astrocytes (Chapter 4.2.2. Figure 4-3D).

Figure 4-2.

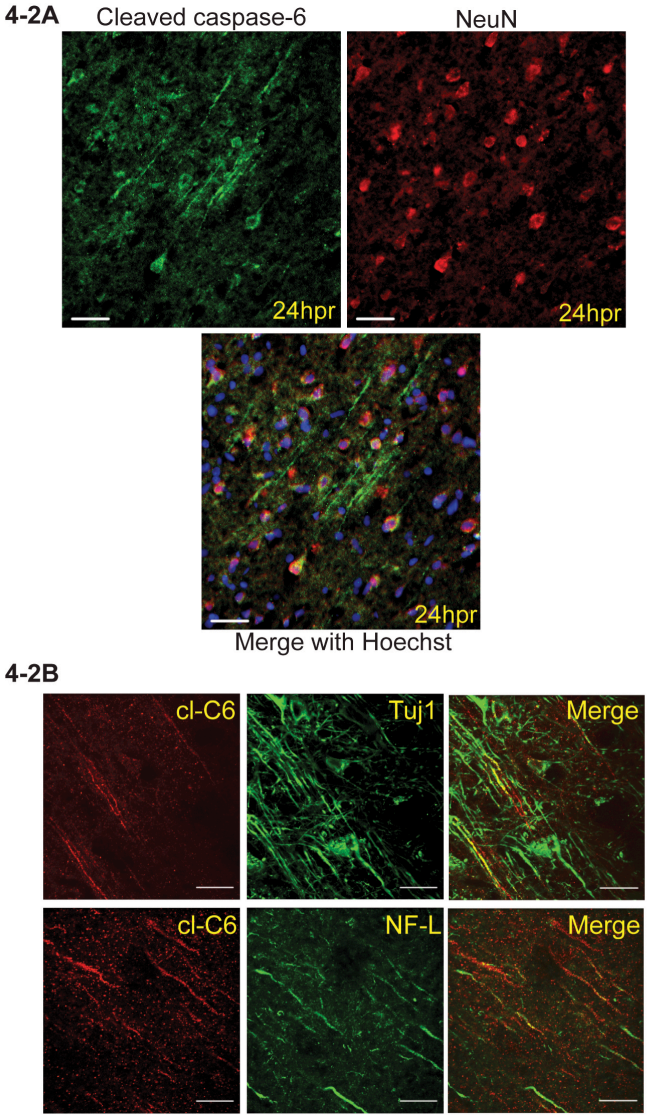

Figure 4-2. Cleaved caspase-6 is neuron specific.
A) Cortical penumbra sections from stroked rats (24hpr) were immunostained for cl-C6 (green), NeuN (red), a neuronal marker, and Hoechst (blue). Left panel shows cl-C6, middle panel shows NeuN and right panel shows the merge of cl-c6, NeuN and Hoechst. Cl-C6 does not co-localize with the astrocyte marker GFAP (data not shown). Epifluorescence microscopy. Scale bar: 50 µm. **B)** Cleaved Caspase-6 is present in axons. Upper panels: Cortical penumbra sections from stroked rats (12hpr) were immunostained for cl-C6 (red) and Tuj1 (green), an axonal marker. Left panel shows cl-C6, middle panel shows Tuj1 and right panel shows a merge of both. Single processes that contain cl-C6 are apparent. Regions of axons with non-fragmented Tuj1 staining do not have cl-C6 staining. In contrast, regions with cl-C6 exhibited fragmented Tuj1 staining. Lower panels: Brain sections were immunostained for cl-C6 (red) and the neurofilament-light chain (NF-L, green), another axon marker. Left panel shows cl-C6, middle panel shows NF-L and right panel shows a merge of both. The staining pattern is similar to cl-C6 and Tuj1: regions of axons with non-fragmented NF-L staining do not have cl-C6 staining. In contrast, regions with cl-C6 exhibited fragmented NF-L staining. Confocal microscopy. Scale bar: 50 µm.

To identify whether caspase-6 is cleaved in axons, sections were co-stained for cl-C6 and axonal markers (Tuj1 or NF-L). At 24hpr, Tuj1 and cl-C6 were found in single neuron processes

(Figure 4-2B). Immunostaining of these processes was not continuous and gaps in the processes were positive for cl-C6. Cleaved C6 is also found in axons containing NF-L (Figure 4-2B), with similarly cl-C6-filled gaps in the process staining. Assuming that the entire diameter of each process was captured in this confocal stack (~20 μm thick, extended focus), one could propose that cl-C6 is possibly responsible for the gaps in cytoskeletal staining. Interestingly, previous work in AD indicates that caspase-6 cleaves tubulin and tau [191, 192], which may disrupt axon stability. Thus, caspase-6 activation might trigger axon degeneration during stroke.

4.2.2. Caspase-3 and Neuronal Cell Type Specification

Immunofluorescent staining for neural cell markers (e.g., astrocytes: GFAP, neurons: NeuN) revealed that activated caspase-3 staining was restricted to astrocytes at 12hpr and 24hpr (Figure 4-3A). Activated caspase-3 exhibited a nuclear staining pattern, as befitting its apoptotic role in chromatin condensation and DNA fragmentation [197].

Nuclear staining of activated caspase-3 did not associate with the neuron marker NeuN or with caspase-9 at 12hpr (Figure 4-3B & C). Interestingly, axonal caspase-6 did not co-stain with GFAP-positive processes (Figure 4-3D).

A previous study [198] reported that activated caspase-3 (cl-C3) is present in reactive astrocytes and microglia during stroke, but cl-C3 co-staining did not correlate with cell death. In contrast, the number of reactive astrocytes and microglia increased in stroked regions, highlighting a possible non-death function for this caspase in glial cells.

Astrocyte density was not measured for this dissertation, so no conclusion can be drawn from our staining towards this regard. Further investigation of caspase-3 function in astrocytes is required and was beyond the scope of this dissertation.

Figure 4-3.

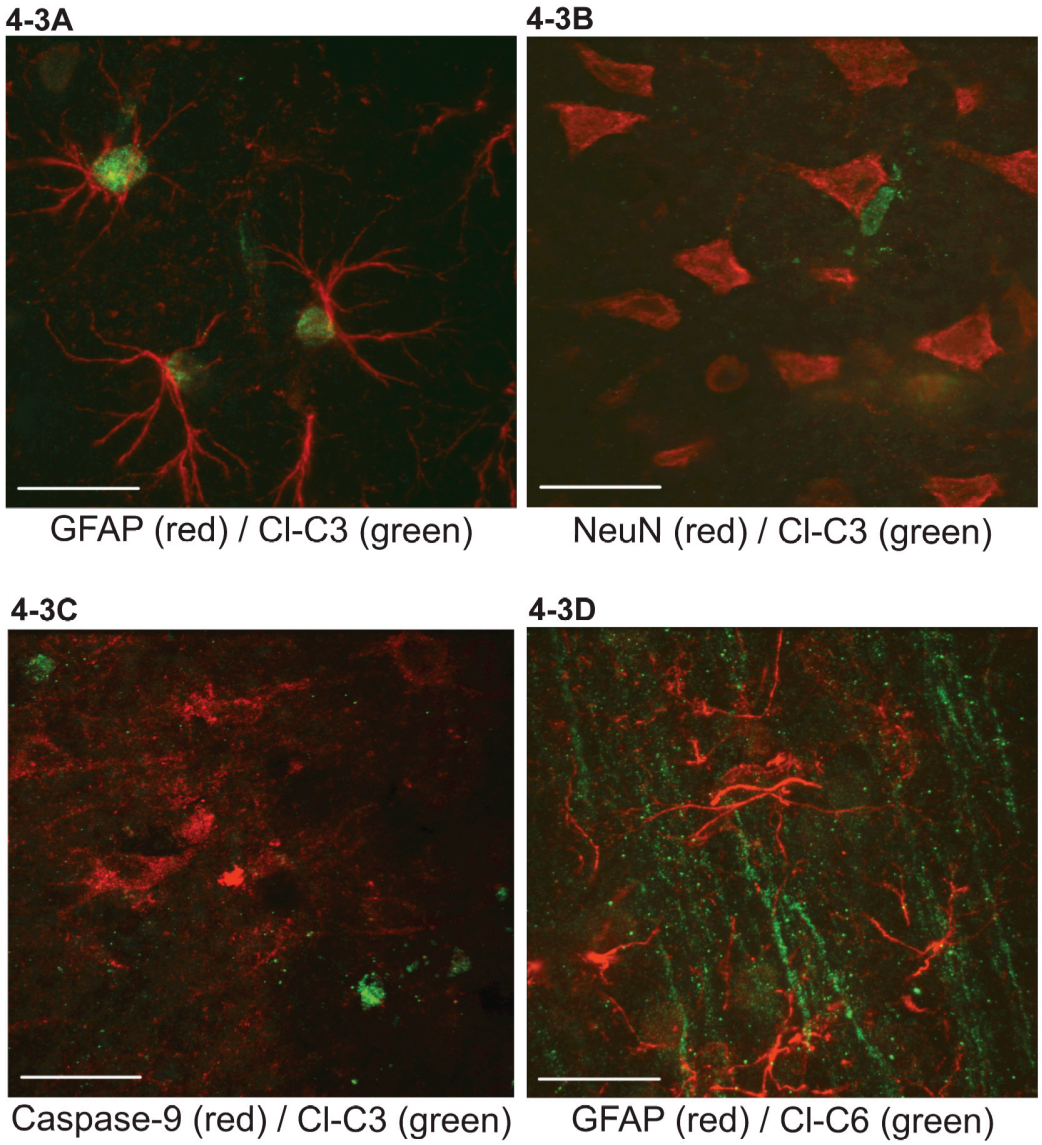

Figure 4-3. Cleaved caspase-3 is glia specific.

A) Cortical penumbra sections from stroked rats (12 hpr) were immunostained for cl-C3 (green) and GFAP (red), an astrocyte marker. Nuclear cl-C3 co-localizes with GFAP. **B)** Nuclear cl-C3 (green) is not observed in neurons (NeuN: red) at 12 hpr or with **C)** Caspase-9 (red). **D)** Cl-C6 (green) does not co-localize with the astrocyte marker GFAP (red). Confocal microscopy. Scale bar: 50 μm.

4.2.3. Caspase-6 Is Enriched In Myelinated Axons

Immunohistochemistry for activated caspase-6 suggests that this effector is preferentially expressed in the axonal compartment. Thus, we performed a neurochemical isolation of myelinated axons from control and ischemic rat brains [34]. This sucrose-based technique yields three fractions: 1) myelinated axons; 2) a soluble layer with cytosolic proteins; and 3) a pellet fraction with nuclei, unmyelinated axons, and insoluble proteins (Figure 4-4). The pellet fraction was not analyzed.

Figure 4-4.

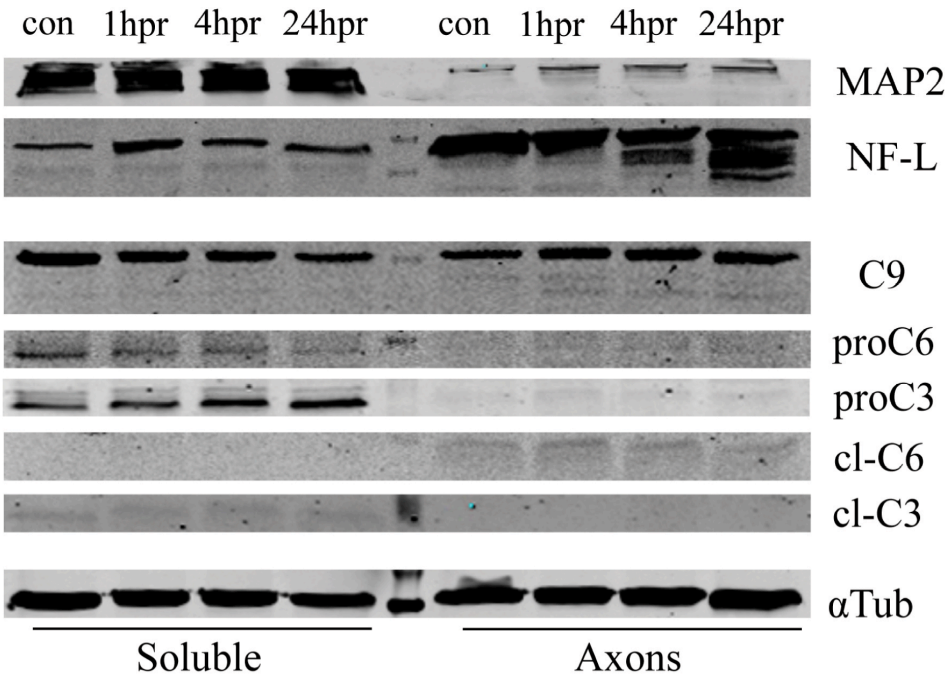

Figure 4-4. Cleaved caspase-6 is temporally enriched in myelinated axons.
Infarcted tissue from the ipsilateral hemisphere, including portions of the corpus callosum, striatum, and cortical matter, were separated on 15% SDS-PAGE gel and analyzed by western blotting. Somatodendritic microtubule-associated protein 2 (MAP-2; top panel) segregates with the soluble fraction, while axonal neurofilament light chain (NF-L) is enriched in the myelinated fraction (second panel). Notice the potential cleavage of NF-L at 4 hpr and 24 hpr, which has a putative caspase-6 cleavage site (VEMD248V). Caspase-9 (C9) is uniformly expressed (third panel). Full-length caspase-6 (proC6) expression decreases over time in the soma (soluble fraction) and increases in axons (fourth panel). Full-length caspase-3 (proC3) demonstrates higher expression in the soluble fraction relative to the axonal fraction (fifth panel). Caspase-6 cleavage is induced in the myelinated axon fraction over time, although there is low constitutive expression in control axons (sixth panel).Cleaved caspase-3 is induced in the soluble fraction during stroke but is not found in myelinated axons (seventh panel). Alph-tubulin was the loading control (eigth panel).

Somatodendritic microtubule-associated protein 2 (MAP-2) [199] and axonal neurofilament light chain (NF-L) [200] fractionate into their predicted compartments (Figure 4-4, top and second panels). Caspase-9 is uniformly expressed in both cell bodies and axons (Figure 4-4, third panel), which agrees with our immunohistochemistry data (Chapter 3 Figure 3-2).

Full-length caspase-6 and caspase-3 (Figure 4-4) were present in the cell body fraction, and the expression of full-length caspase-6 declined during ischemia in the cell body fraction. Activated caspase-6 (Figure 4-4, sixth panel) is induced in the axons over the course of the 24 hours that follow ischemia. This biochemical data supports the concept that caspase-6 activity is compartmentalized within axons during ischemia.

4.2.4. Genetic Knockout Of Caspase-6 Is Neuroprotective

Next, we examined if caspase-6 inhibition is sufficient for neuroprotection against stroke using caspase-6-null mice (caspase-6-/-) [155]. We subjected wild-type and caspase-6-/- mice to tMCAo, and caspase-6-/- mice (Figure 4-5A) showed significantly better neurological function at 24hpr compared to wild-type mice, based on a 28-point exam that measured neurofunctional behavior [166] (wild-type: 19.21 ± 1.931, n=14 vs. caspase-6-/-: 12.64 ± 1.525, n=14). H&E staining showed a significant difference in infarct volume at 24hpr (wild-type: 61.56 ± 2.853, n=3; caspase-6-/-: 45.37 ± 1.482, n=4), which was commensurate with the significant difference in neurofunction.

To determine whether neurofunctional retention was related to the preservation of the neuronal soma and axons, we quantified the density of these structures. Wild-type mice subjected to 1hr tMCAo showed a 47% decrease in neuronal number compared to non-stroked wild-type mice at 24hpr, and this decrease was partially rescued in caspase-6-/- mice (Figure 4-5B; WT-non-stroke: 282.7 ± 32.97; WT-stroke: 148.0 ± 20.22 ; C6-/--non-stroke: 296.3 ± 9.207;

Figure 4-5.

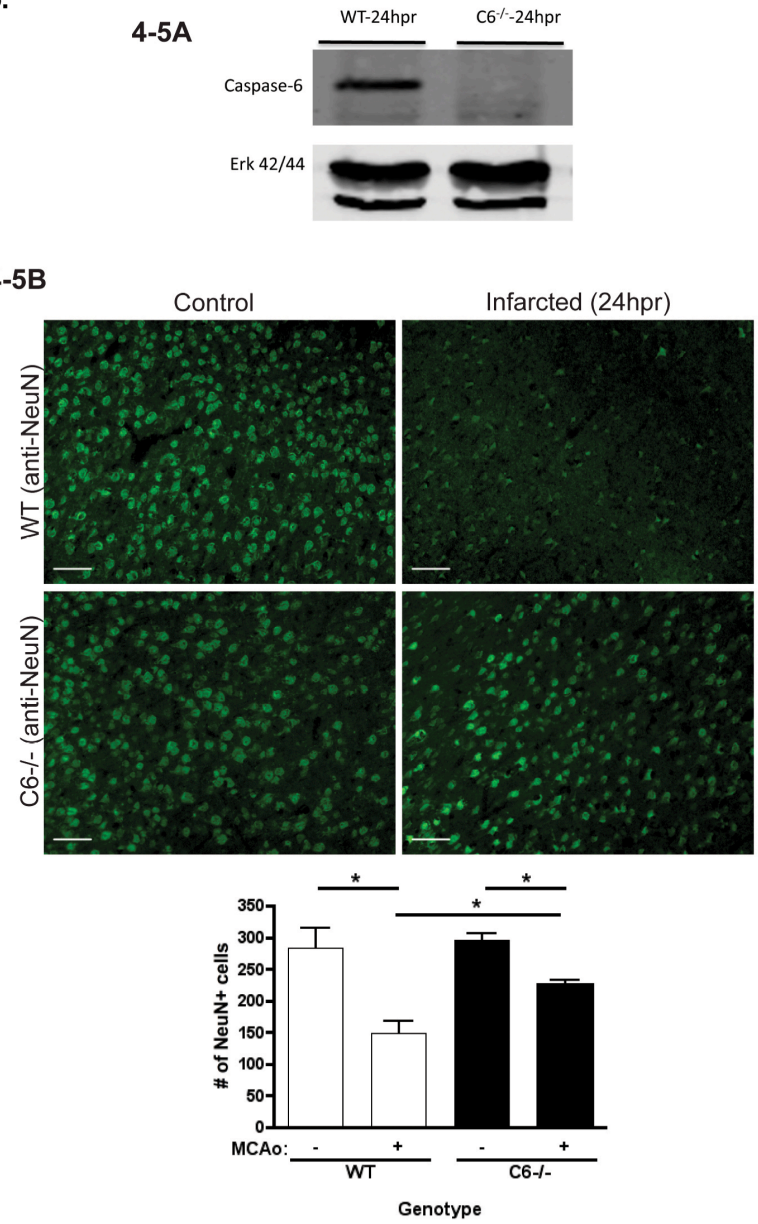

Figure 4-5. Caspase-6 knockout mice retain processes and neurons following tMCAo.
A) Characterization of caspase-6-/- mice. Western blot analysis of caspase-6 expression in wild-type and caspase-6-/- mouse spleen. Erk expression is utilized as a loading control. **B)** Caspase-6 knockout preserves neurons. Wild-type and caspase-6-/- mice were subjected to 1hr tMCAo and sacrificed at 24hpr. NeuN staining of cortical penumbra brain tissue reveals a significant decrease in the number of neurons in stroked wild-type mice (148.0 ± 20.22, n=3) compared to non-infarcted wild-type mice (282.7 ± 32.97, n=3; p=0.0253). Caspase-6-/- mice subjected to tMCAo retain more neurons than stroked wild-type mice (225.0 ± 8.114, n=4 vs. 148.0 ± 20.22, n=3; p=0.0108). Non-stroked wild-type and non-stroked caspase-6-/- mice do not exhibit difference in number of neurons (282.7 ± 32.97, n=3 vs. 296.3 ± 9.207, n=3) (t-test, *$p < 0.05$.). Epifluorescence microscopy. Scale: 50 µm.

C6-/--stroke: 225.0 ± 8.114). Additionally, wild-type mice subjected to tMCAo had fewer NF-L-positive processes compared to caspase-6-/- mice (Figure 4-6A; 47.67 ± 7.219, n=3 vs. 70.00 ± 4.916, n=4). Processes from wild-type mice were shorter and exhibited more fragmented NF-L staining, suggestive of axon degeneration. Tau is a putative axonal substrate for caspase-6 with potential cleavage sites in the N-terminal and C-terminal regions of tau [190, 192].

Figure 4-6.

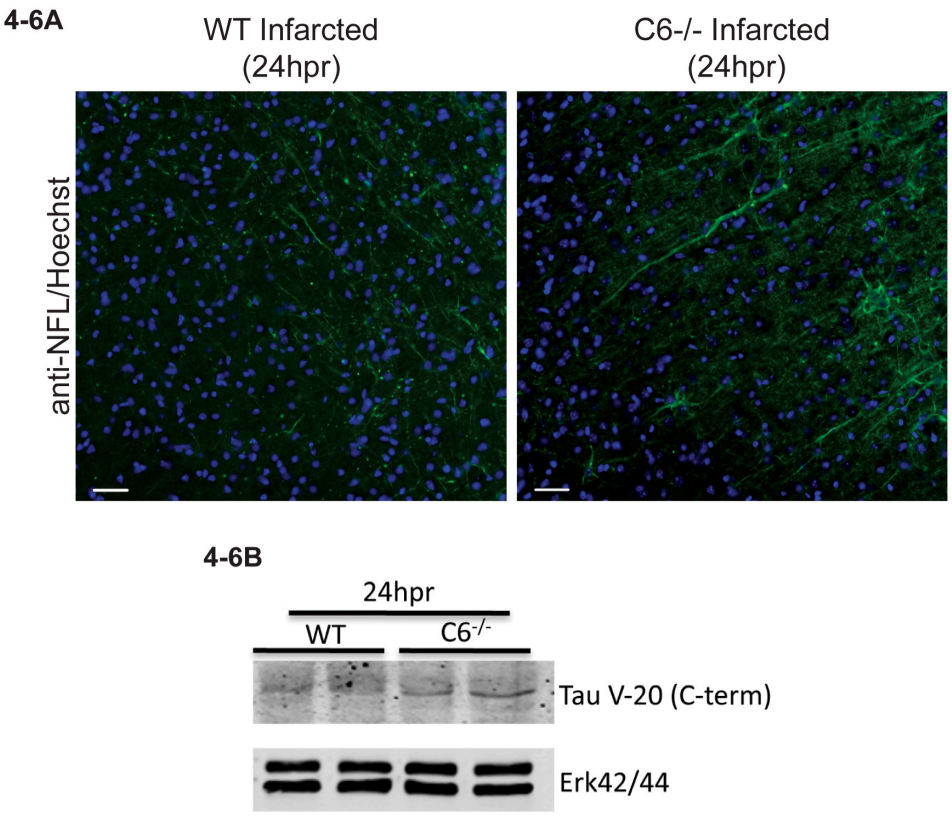

Figure 4-6. Caspase-6 knockout preserves neuronal processes.
A) Brain sections from wild-type and caspase-6-/- mice subjected to 1hr tMCAo and 24hpr were immunostained for NF-L. Stroked wild-type mice have fewer NF-L positive processes compared to stroked caspase-6-/- mice (47.67 ± 7.219, n=3 vs. 70.00 ± 4.916, n=4; p=0.0447) (t-test, *p < 0.05). NF-L positive processes were also shorter and more fragmented in wild-type mice compared to caspase-6-/-. Epifluorescence microscopy. Scale: 50 µm. **B)** Caspase-6 knockout prevents reduction in tau. Brain lysates from wild-type and caspase-6-/- mice subjected to 1hr tMCAo and 24hpr were isolated and analyzed by western blot. Tau expression was analyzed with anti-Tau (V-20), which recognizes the C-terminal end of Tau, the putative location of a caspase-6 cleavage site. Stroked caspase-6-/- mice (density: 1.154 ± 0.08655, n=2) contain more tau than stroked wild-type mice (density: 0.7216 ± 0.03246, n=2). Erk was used for loading control and normalization (n=2). Means (with STD) of densitometry.

Analysis with an antibody specific to the C-terminal region of tau revealed that caspase-6-/- brains retained more intact tau than wild-type brains at 24hpr (Figure 4-6B, densitometry: 0.7216 ± 0.03246 vs. 1.154 ± 0.08655, n=2, mean ± STD). This finding suggests that caspase-6 reduces tau levels during stroke. This loss of tau may lead to microtubule instability and the loss of process integrity.

4.2.5. Caspase-6 Is Activated In Human Stroke

Post-mortem brain tissue from patients who died following ischemic stroke was immunostained for cl-C6. Columbia University's Brain Bank provided human brain samples; details on when the ischemic event occurred relative to fixation and slide preparation were not provided. DAB imaging (Figure 4-7A) of cl-C6 immunostaining showed cell bodies and processes in the infarcted tissue, and NF-L staining of adjacent sections showed a decrease in process density. Using immunofluorescence, we found that cl-C6 immunostaining co-localized with a marker for axons (Figure 4-7B). Cl-C6 was found in a process in the ischemic tissue, and the pattern of co-localization with Tuj1 was very similar to that observed in the rodent models of ischemia.

4.2.6. Caspase-9 Activates Caspase-6 During Ischemia

To determine unequivocally if caspase-9 was activating caspase-6 *in vivo*, we tested whether caspase-9 inhibition could reduce caspase-6 activation. Pen1-XBIR3 was delivered to the striatum 1 hr prior to tMCAo using CED. Animals were harvested at 24hpr, and brain sections were immunostained for caspase-9 and cl-C6. Pen1-XBIR3 completely inhibited the appearance of cl-C6 in cell bodies and axons (Figure 4-8). Co-staining of caspase-9 and cleaved caspas-6 during ischemia was consistently observed for the duration of this project, and it was recorded as early as at 4hpr (Chapter 3 Figure 3-2). Thus, caspase-9 activity is necessary for

activation of caspase-6 in neuronal soma and processes following a transient ischemic event in rats.

Figure 4-7.

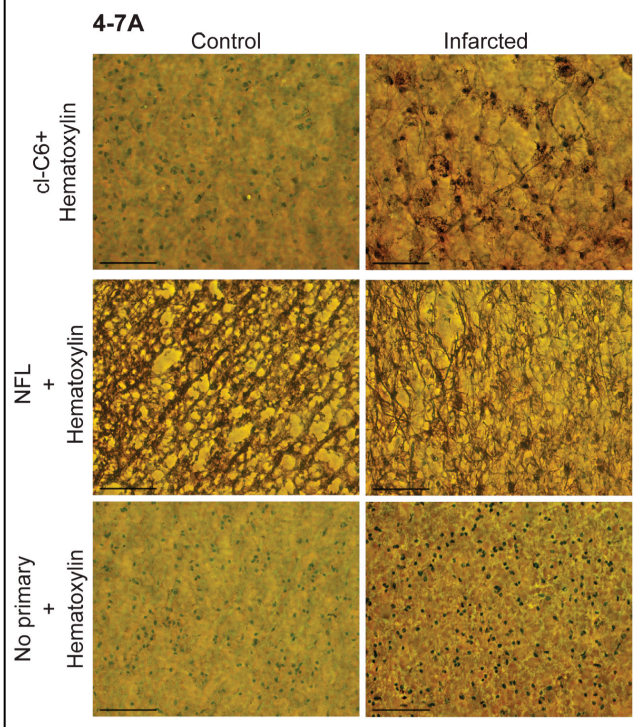

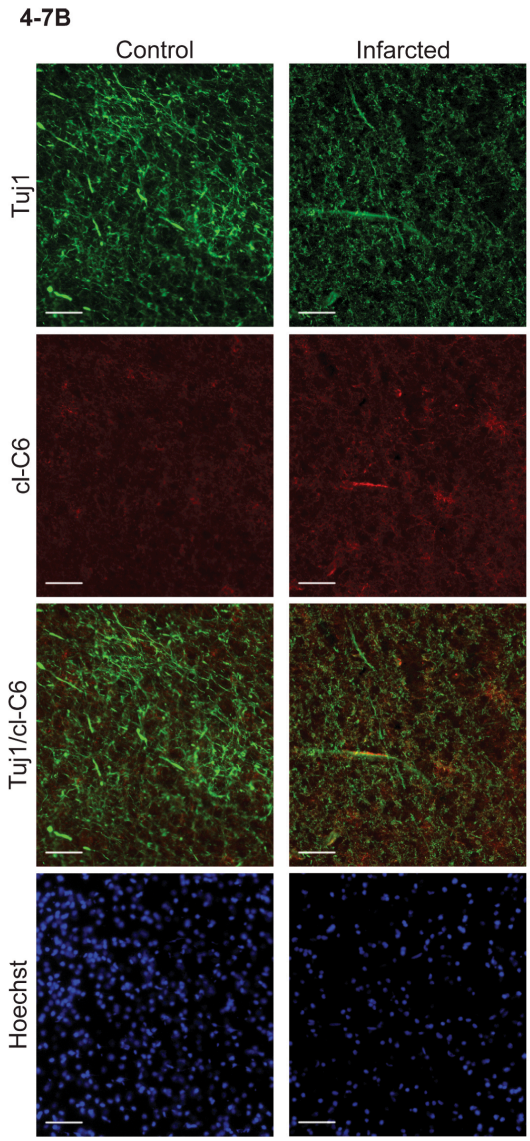

Figure 4-7. Active caspase-6 observed in human ischemia.
Post-mortem brain tissue from a patient who had suffered an infarct and from an age-matched control. **A)** Immunohistological analysis (DAB processing) for cleaved caspase-6. DAB processing for cl-C6 showed cell body and process staining. Sections stained without primary antibody show no cell body or process staining. Cleaved caspase-6 process staining resembles NF-L process staining. Sections from age-matched control brain show no cleaved caspase-6 staining. Scale: 100 µm. **B)** Immunofluorescent staining for cleaved caspase-6 and Tuj1. The infarct area shows the presence of cleaved caspase-6 in a process, Tuj1 appears in the same process. The control brain has no evidence of cleaved caspase-6. Epifluorescence microscopy. Scale: 50 µm.

The preceding findings demonstrate that intraparenchymal delivery of Pen1-XBIR3 prevents activation of caspase-6. To determine if intranasal delivery of Pen1-XBIR3 also altered caspase-6 activity resulting from stroke, animals were treated 1hr prior to tMCAo with Pen1-XBIR3 and harvested at the indicated times of reperfusion. Brains were analyzed for the

expression of activated caspase-6 at 12 and 24hpr. Intranasal Pen1-XBIR3 significantly reduced caspase-6 activation. At 12hpr, there was a trend towards a reduction of caspase-6 activation in

Figure 4-8.

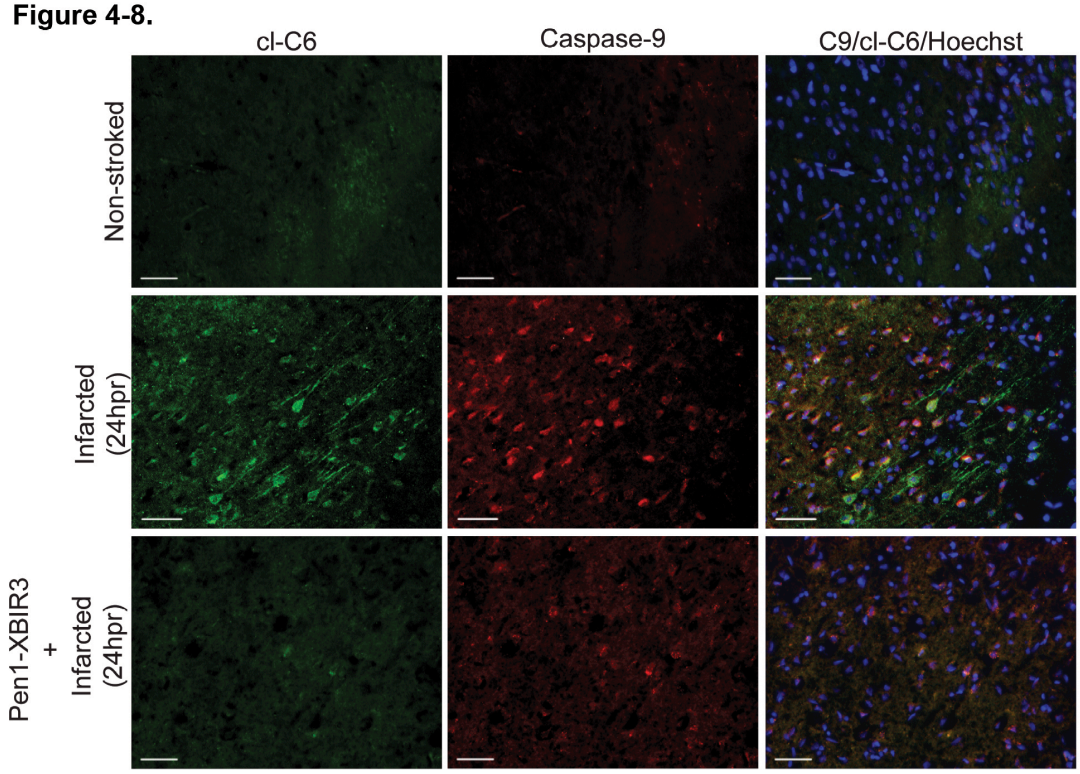

Figure 4-8. Pen1-XBIR3 reduces caspase-6 activation in tMCAo.
Intraparenchymal convection enhanced delivery (CED) of Pen1-XBIR3 blocks tMCAo induction of cleaved caspase-6 in neuronal soma and processes. Pen1-XBIR3 or vehicle was infused with CED into the predicted stroke area of rats prior to tMCAo. Rats were harvested at 24hpr for immunohistochemistry for cl-C6 (green), caspase-9 (red) and Hoechst (blue). Upper panels show a non-stroked animal. Middle panels show vehicle and the lower panels show a Pen1-XBIR3 treated animal. The caspase-9 specific inhibitor, Pen1-XBIR3, blocks the induction of cl-C6 observed at 24hpr. Epifluorescence microscopy. Scales: 50 µm.

processes (Figure 4-9A; Vehicle: 144.0±28.50 vs. Pen1-XBIR3: 102.7±23.15). By 24hpr, the reduction was significant (Figure 4-9A; Vehicle: 109.7±12.73 vs. Pen1-XBIR3: 57.33±10.04) compared to rats treated with saline. Therefore, caspase-9 inhibition using this delivery technique reduced caspase-6 activation. Interestingly, cl-C6 levels at 24hpr inversely correlated with a reduction in NF-L density (Figure 4-9B; Vehicle-24hpr: 138.0±9.074 vs. Pen1-XBIR3-24hpr: 213.7±11.84).

Cleaved caspase-3 was also observed in nuclei after 4hpr. At 24hpr, Pen1-XBIR3 did not alter the presence of cleaved caspase-3 (Vehicle: 89.33±2.333 vs. Pen1-XBIR3: 81.67±7.055). It is probable that other initiators, such as caspase-8, are responsible for caspase-3 activation in stroke.

Figure 4-9.

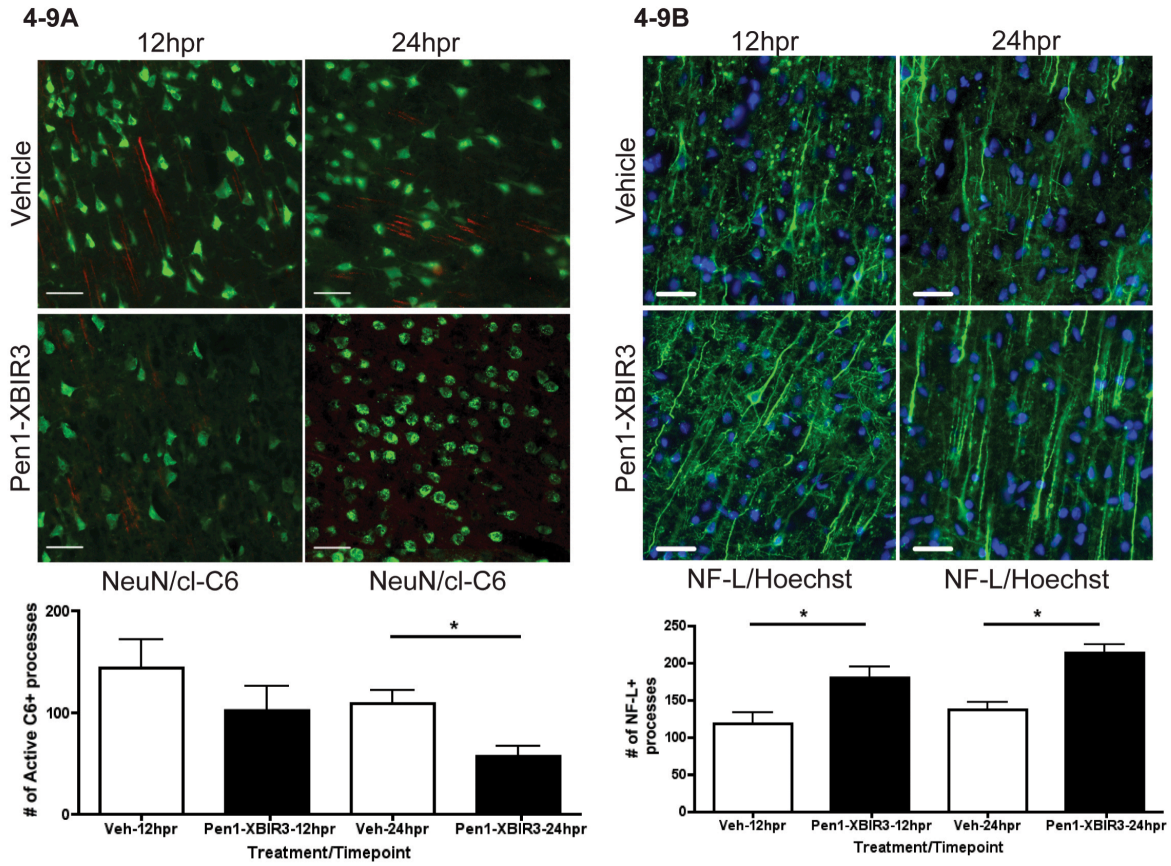

Figure 4-9. Pen1-XBIR3 reduces axon degeneration in tMCAo.

A) Intranasal delivery of Pen1-XBIR3 decreases cleaved caspase-6 expression in processesat 24hpr. Vehicle or Pen1-XBIR3 was delivered intranasally prior to tMCAo and rats were harvested at 12hpr (left panels) and 24-hpr (right panels). Sections were immunostained for cl-C6 (red) and cl-C6 posi-tive processes were quantified. Epifluorescence microscopy. Scale: 50 µm. Graphs are means (with SEM) of axon counts. Vehicle-12hpr: 144.0 ±28.50, n=3 vs. Pen1-XBIR3-12hpr: 102.7±23.15, n=3; p=0.3233. Vehicle-24hpr: 109.7±12.73, n=3 vs. Pen1-XBIR3-24hpr: 57.33±10.04, n=3; p=0.032. (t-test, *p < 0.05.) **B)** Intranasal Pen1-XBIR3 blocks the reduction in NF-L positive processes induced by tMCAo in rats. An intranasal bolus of vehicle or Pen1-XBIR3 was pro-phylactically delivered, and rats were harvested at 12hpr (left panels) and 24hpr (right panels). Sections were immunostained for NF-L (green) and NF-L positive axons were quantified at 12 and 24hpr. Epifluorescence microscopy. Scale: 50 µm. Graphs are means (with SEM) of axon counts. Vehicle-12hpr: 118.7±14.88, n=3; Pen1-XBIR3-12hpr: 179.7±14.89, n=3; Vehicle-24hpr: 138.0±9.074, n=3; Pen1-XBIR3-24hpr: 213.7±11.84, n=3; (t-test, *p < 0.05.).

4.3. Discussion

The last two chapters detail an unbiased approach for identifying caspases that are critical for neurodegeneration in cerebral ischemia. Our data show that caspases-6 and -9 are regulators of neurodegeneration in cerebral ischemia. We have used active caspase trapping and identified caspase-9 as an early stage mediator of cell death in stroke that also promotes caspase-6 activation. We show that caspase-6 is activated in axons, supporting its role in axon degeneration during neuronal death [127]. Inhibiting these caspases, either through peptide inhibition of caspase-9 or genetic knockout of caspase-6, reduced stroke injury and improved sensorimotor outcomes, providing sustained functional neuroprotection out to 3 weeks post-ischemia.

Two different strategies were employed to deliver Pen1-XBIR3 to the brain. Convection-enhanced delivery (CED) provided direct delivery to the region of the infarct and completely abrogated the activation of caspase-6 in neuronal soma and processes. Therefore, caspase-9 activity regulates caspase-6 activity in stroke.

From a therapeutic perspective, intranasal delivery is a very attractive treatment strategy for CNS disorders as it provides direct, non-invasive, access to the brain via the olfactory pathway. Intranasal delivery combined with the cell permeant peptide Penetratin1 provides intracellular delivery to the CNS.

In the present study, intranasal delivery of Pen1-XBIR3 inhibited caspase-6 activation, reduced axon degeneration and was neuroprotective. Pen1-XBIR3-mediated neuroprotection was substantial even 3 weeks after the initial insult.

Our data reveal that caspase-6 activation corresponds to axon degeneration in stroke and provide insights into how this process occurs during ischemia. Since caspase-6 activation is

relatively delayed following ischemic onset, efficacious inhibition of caspase-6 in stroke may provide functional neuroprotection and be a valuable therapeutic strategy for cerebral ischemia.

Previous investigations have employed genetic strategies of caspase inhibition to delineate the post-ischemic function of both initiator and effector caspase activation. Of the initiator caspases, caspase-1-null mice and mice expressing a caspase-1 dominant negative transgene are partially protected from transient Middle Cerebral Artery occlusion (tMCAo) [48, 110]. Caspase-2 null mice do not exhibit neuroprotection [201]. Deletion of caspase-8 or -9 is embryonic lethal; thus, mice lacking these caspases have not been studied in tMCAo. Of the three effector caspases (3, 6, 7), only caspase-3 has been studied extensively in stroke [89, 111]. Caspase-3-null mice are protected from tMCAo, showing a critical role for this caspase [113]. However, caspase-3 gene deletion does not lead to complete protection from stroke. Thus, other effector caspases (or non-caspase death mechanism) might also factor into stroke neurodegeneration.

Moreover, our data and a recent study revealed that caspase-3 is induced in non-apoptotic glial cells (astrocytes and microglia) during stroke [198]. Astrocytes provide biochemical, nutritive, and metabolic support for neurons, while microglia are brain-resident macrophages. Both cell types can regulate neuron survival; thus, the non-apoptotic role of caspase-3 in glial function requires further exploration.

Two studies have proposed that caspase-9 does not directly cleave caspase-6 and that an intermediate, likely caspase-3, is required for activation [34, 202]. However, both of these studies used *in vitro* conditions to measure caspase activation. We did not observe cleaved caspase-3 in mouse or rat axons during stroke. Further investigation is required to determine if caspase-9 can directly cleave caspase-6 *in vivo,* or whether another caspase acts as an

intermediary. Pen1-based inhibitors for the remaining members of the caspase family, if suitable ones can be generated, would be very useful in this regard.

In Chapter 4, we demonstrate that genetic ablation of caspase-6 provides neuroprotection at the structural and functional levels against stroke. Caspase-6 can cleave tau, affecting its ability to stabilize microtubules [190], and caspase-6-mediated cleavage of tau may play a role in AD pathogenesis [191, 192]. In our models of cerebral ischemia, active caspase-6 co-localized with axonal markers, which suggests that caspase-6 causes degeneration of neuronal axons in this disease model. Although present in the same process, some axonal regions with active caspase-6 lacked the process marker, suggesting that caspase-6 was either cleaving the marker or leading to its destabilization. In support of this function for caspase-6 in stroke, we have observed a reduction in tau in wild-type mice subjected to tMCAo relative to caspase-6-/- mice. Further proteomic analysis of tissue lysate from infarcted brains from caspase-6-/- and wild-type mice could be used to reveal a broader spectrum of proteins cleaved by caspase-6 during stroke, potentially many that regulate axon stability.

One study of dissociated DRG neurons subjected to trophic factor deprivation reported that caspase-6 apoptotic process are initially restricted to the axon, and are immediately required for the breakdown of the neuronal soma [127]. We found that caspase-6 mediates both process degeneration and neuronal death during ischemia (Figure 4-5 & 4-6). The temporal activation of caspase-6 in the stroke penumbra corresponds with the progression of axonal degeneration. For other forms of neurodegeneration, axon degeneration is a major contributor to cell death and may instigate death via the removal of target-derived trophic factors [194-196]. In these instances, axon degeneration preceded cell death. In clinical cases of cerebral ischemia, axon degeneration is observed as early as 2 days post ischemia [106]; however, the molecular events triggering

axon degeneration may begin earlier. In the penumbral region, we find that axon loss preceded neuronal loss, which suggests that axon degeneration precedes neuronal loss following an ischemic event.

Our collective results indicate that the caspase-9/caspase-6 pathway is an excellent target for stroke therapy. This pathway is active in the neurons and is responsible for a significant amount of axon loss and neuron death after ischemia. Moreover, the temporal course of activation (present over the first 24 hr) provides a large clinical window for treatment.

Chapter 5. Developing A Caspase-6 Inhibitor For *in vivo* Use

5.1. Introduction

Currently, there are no specific caspase-6 inhibitors. Synthetic molecular substrates/inhibitors have been generated based on canonical caspase cleavage motifs (i.e. for caspase-3: DEVD or for caspase-6: VEID), but these substrates/inhibitors are highly promiscuous [91] and not suitable for specific inhibition *in vivo*.

Our collaborator Guy Salvesen has generated expression vectors containing wild-type and catalytic dominant negative constructs for caspase-3, -6, -7, and -9 [168]. These recombinant proteins contain a 6xHIS-tag; therefore, they can be isolated on Ni^{2+} resin. We have purified the catalytic dominant negative for caspase-6 (C6DN; Cys285Ala) as well as its wild-type active partner [168]. Catalytic dominant negatives have been successfully used to inhibit caspase-1 activity [34, 110, 118].

Caspase-6, an effector caspase, is a dimer zymogen that is activated by cleavage at Asp162 and Asp193. Normally, caspase-6 activation is measured by assessing cleavage, since there are no endogenous inhibitors of caspase-6. However, antibodies for cleaved caspases do not recognize the active site of the caspase, but rather the neoepitope generated by caspase cleavage at Asp162 and Asp193.

In theory, there are two ways that C6DN could inhibit wild-type C6. One is where a monomer of C6DN forms a zymogen with a wild-type C6 monomer. Upon cleavage by upstream caspases, this hybrid zymogen will be unable to form a functional active site

Caspase-6 mediates axon and neuron degeneration [127, 191-193]. To assay the inhibitory capacity of C6DN, I utilized a model where active caspase-6 is abundant and contributes to cell death. In this model, cortical neurons were treated with mutant, furin-resistant

proNGF (ΔproNGF). Proneurotrophins and mature neurotrophins are potent activators of the p75 neurotrophin receptor (p75NTR). Following neurotrophin (pro or mature) binding, p75NTR activation can trigger neuronal apoptosis and axon pruning. P75NTR can also form a complex with sortilin after binding to proneurotrophins, which signals apoptosis [60, 203, 204]. Previous research from our lab and others shows that p75NTR activation induces caspase-6 activity and hippocampal cell death [205].

As proneurotrophins are quickly processed by furin proteases [148], mutated furin-resistant forms of proNGF were used for this study. Both wild-type and furin-resistant proneurotrophins are potent activators of p75NTR that signal cell death [148, 206].

Neurotrophin withdrawal also causes neuron death and axon degeneration, which was recently shown to be caspase-6 dependent [126, 127]. Nikolaev *et* al. 2009 monitored this process in microfluidic chambers [207], which allows for separate treatment conditions for neurons and axons [127]. Local NGF withdrawal at axon tips caused caspase-6-dependent axon degeneration.

5.2. Results

5.2.1. Use in Neuronal Cultures Models of Cell Death

To stimulate p75NTR, we treated cultured rat cortical neurons with mouse ΔproNGF (mΔproNGF ; 1ng/ml & 10ng/ml) overnight, which induced the cleavage/activation of caspase-6 (Figure 5-1A) and cell death (Figure 5-1B). Full-length caspase-6 was also increased. Thus, neurotrophins induce caspase-6 activation in cortical neurons, akin to previous observations with hippocampal neurons [205].

The cleavage of caspase-6-specific substrates was analyzed. Microtubule-associated protein tau is selectively processed by effector caspase-3 and caspase-6 [190]. For western

blotting assays to measure caspase-6 activation, antibodies to that target the tau caspase cleavage site (anti-TauC3) were used. MΔproNGF induced caspase-mediated tau cleavage (Figure 5-1A) as well as cleavage of lamin A/C, a well-established substrate of caspase-6 [202].

Figure 5-1.

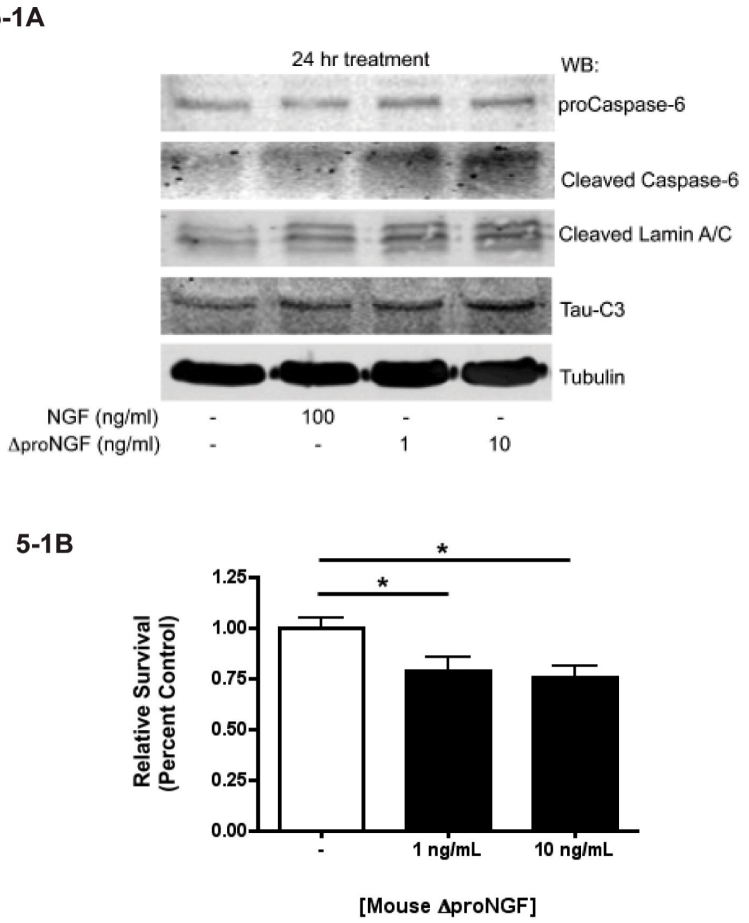

Figure 5-1. Proneurotropins trigger caspase-6 activation.
A) Cultured cortical neurons were treated overnight with nerve growth factor (NGF; 1 ng/ml) or a mutant pro-form of NGF (ΔproNGF; 1 ng/ml & 10 ng/ml). Neurotrophins induced caspase-6 activation. Cleavage of caspase-6 subtrates (lamin A/C and tau) was similarily increased. Representative western blot of 3 independent experiments. **B)** Mutant proNGF (1 ng/ml and 10 ng/ml) induced cortical neuron death. Percentage of healthy nuclei relative to control. Control: 100 ± 4.7% ; 1 ng/ml: 78.6 ± 7.1% ; 10 ng/ml:75.2 ± 5.7%; *p < 0.05 for both comparisons ; n =6 per group.

Caspase-6 catalytic dominant negative (C6DN; C285A) was isolated and purified as described previously [168]. To facilitate intracellular uptake of C6DN, this peptide was disulfide-linked to Penetratin1 [179]. Upon entry into the cell, the disulfide linkage is broken by the reducing environment of the cytoplasm, which allows the peptide cargo to execute its

function. We have successfully used this technique to deliver XBIR3 to neurons (see [1] and Chapters 3 & 4). C6DN can be linked to Pen1, as visualized by a shift in the molecular weight of caspase-6 (Figure 5-2A), and deposited into cells (Figure 5-2B).

Figure 5-2.

5-2A

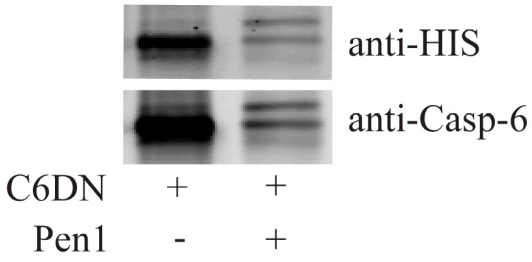

5-2B

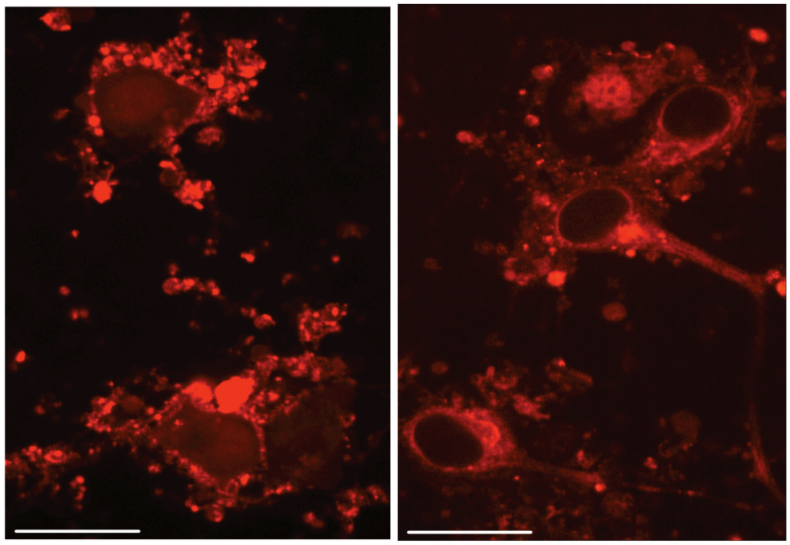

Figure 5-2. Penetratin1-Caspase-6 Dominant Negative (C6DN)
A) Caspase-6 dominant negative (C6DN) was linked to Penetratin1 (Pen1), as indicated by a shift in molecular weight (right lanes). Westerm blotting with anti-caspase-6 and anti-HIS.
B) Rhodamine linked to C6DN was carried into cortical neurons by Pen1 after a 30 incubation (right panel). Free Rhodamine collects on the outside of the cell (left panel).

Along with the regulation of caspase-6 substrate cleavage, we assayed whether Pen1-C6DN can prevent p75NTR-mediated cell death. Cortical neurons were treated overnight with mΔproNGF. Vehicle or Pen1-C6DN was given prior to neurotrophin treatment. Pen1-C6DN

prevented the cleavage of tau (Figure 5-3A), and there was a trend towards reduced neuronal loss (Figure 5-3B).

Figure 5-3.

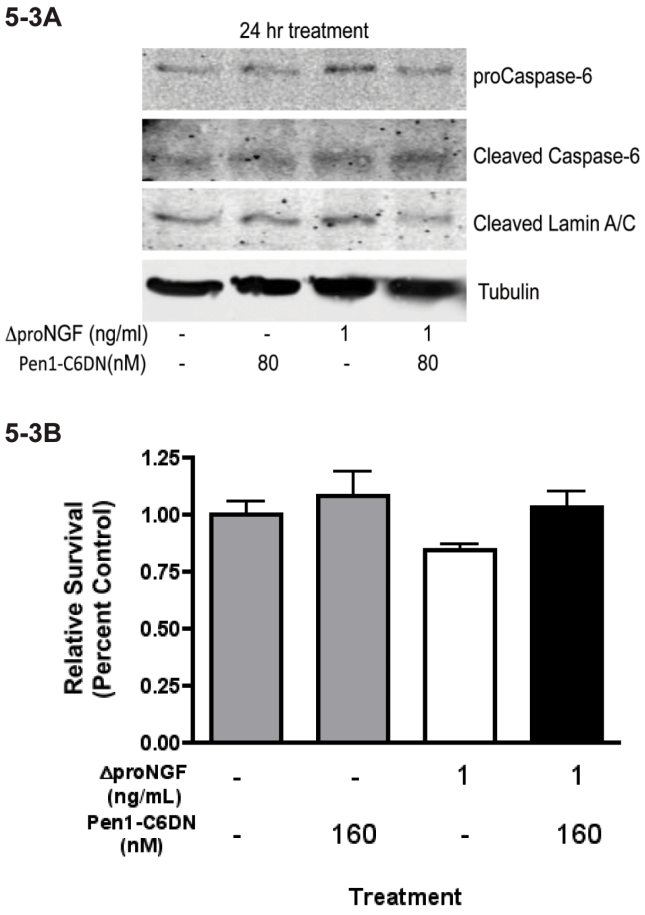

Figure 5-3. Pen1-C6DN prevents proneurotrophin-induced death
A) Pen1-C6DN (80 nM) prevents the cleavage of the caspase-6 substrate lamin A/C after ΔproNGF (1 ng/ml; overnight) treatment. Representative western blot of 3 independent experiments.**B)** Pen1-C6DN (160 nM) protects cortical neurons from ΔproNGF (1 ng/ml; overnight). For ΔproNGF vs. Pen1-C6DN+ΔproNGF, p-value = 0.0731; n = 3 per group.

5.2.2. Use in Cerebral Ischemia

Male C57BL/6 mice (2-3 months old; >25g) were anesthetized using isoflurane (2%) delivered via an anesthesia mask.

Pen1-C6DN (31.9 µM) was delivered by administering 2 µl drops to alternating nares every minute for 10 min (20 µl total delivered) [103]. Intranasal treatment was performed prior

to 1hr transient Middle Cerebral Artery occlusion [157, 158]. Saline was used as a negative control. Brains were harvested for western blotting.

Neuronal death was ameliorated by Pen1-C6DN. Neuron density was quantified by staining brain sections with the neuron marker NeuN and performing hand counts of fluorescent images (20x magnification field of view). In the ischemic core, vehicle-treated groups exhibited a 48% reduction in neuron density in the ipsilateral hemisphere relative to the contralateral hemisphere (85.88 ± 10.36 vs. 165.6 ± 4.903; $p < 0.001$) (Figure 5-4A). In comparison, neuron loss in Pen1-C6DN mice was only 21% (117.9 ± 10.67 vs. 149.8 ± 7.2180). Vehicle versus Pen1-C6DN measurements were significantly different ($p < 0.05$). A similar pattern was observed in the penumbra: Vehicle-ipsi - 122.5 ± 9.943; Vehicle-contra - 174.3 ± 5.978; Pen1-C6DN-ipsi 151.6 ±11.32; Pen1-C6DN-contra 177.4 ±10.18.

Microtubule-associated protein tau has been identified as molecular substrate of caspase-6. We used an antibody that binds to the neoepitope generated by caspase-6 cleavage of tau (anti-TauC3) to measure caspase-6 inhibition by Pen1-C6DN during apoptosis *in vivo*. Pen1-C6DN reduced the cleavage of tau in both the core and the penumbra at 24hpr (Figure 5-4B). Anti-alpha-tubulin was used for a loading control.

Congruent with these biochemical findings, degeneration of axonal tracts in the striatum was prevented by treating mice with Pen1-C6DN prior to stroke. Brain sections were stained using the Bielschowsky method, which labels neurofilaments. The axon tracts were imaged (Figure 5-4C) and counted by hand. A clear demarcation of ischemic injury is apparent (Figure 5-4C). Fewer axon tracts were observed in the ipsilateral (ipsi) hemisphere in vehicle-treated animals relative to Pen1-C6DN-treated animals (93.25 ± 22.5 vs. 178 ± 21.73). Neuron densities

in the non-infarcted contralateral (contra) hemispheres were comparable (vehicle-contra: 238.3 ± 9.05; Pen1-C6DN-contra: 241.7 ± 9.244).

Figure 5-4.

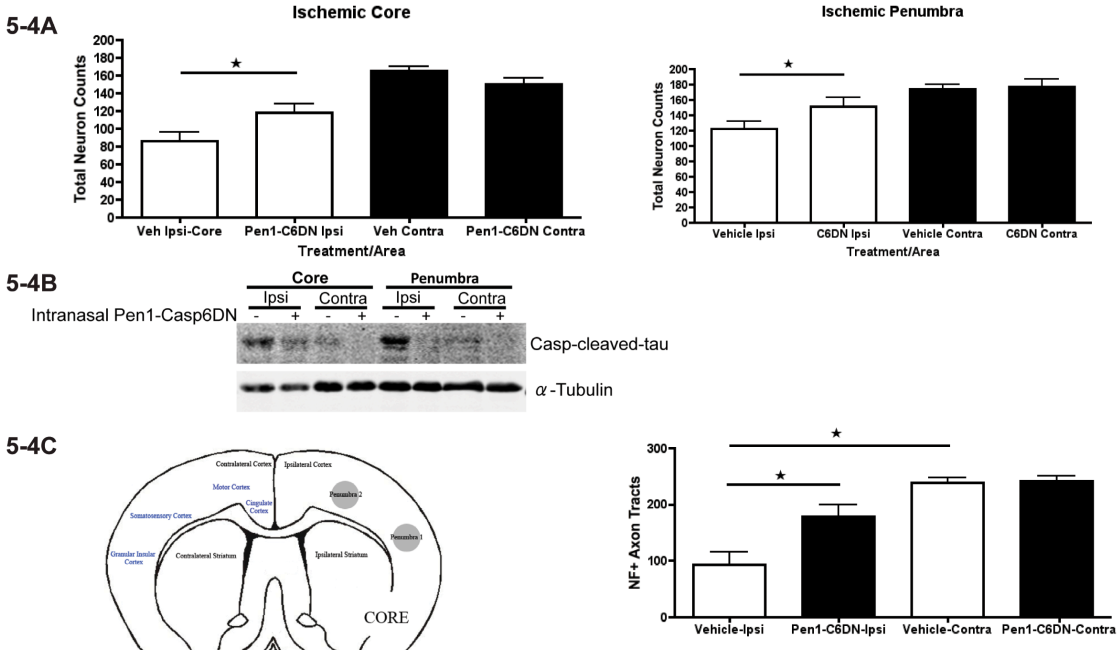

Figure 5-4. Neuroprotection with Pen1-C6DN in stroke. **A)** Intranasal Pen1-C6DN protects neurons. Vehicle or Pen1-XBIR3 was delivered, and mice were harvested at 24-hpr. Sections were immunostained for NeuN, and NeuN-positive cells were quantified in core and penumbra. Graphs are means (with SEM) of axon counts. Graphs are means (with SEM) of neuron counts at 24hpr. For the core, Vehicle-Ipsi: 85.88 ± 10.36, n=8; Pen1-C6DN-Ipsi: 117.9 ± 10.67, n=8; Vehicle-Contra: 165.6 ± 4.903, n=7; Pen1-C6DN-Contra:149.8 ± 7.218, n=8 (ANOVA, overall *$p < 0.0001$; Vehicle-Ipsi vs. Pen1-C6DN: *$p < 0.05$). For the penumbra, Vehicle-Ipsi: 122.5 ± 9.943, n=8; Pen1-C6DN-Ipsi: 151.6 ± 11.32, n=8; Vehicle-Contra: 174.3 ± 5.978, n=8; Pen1-C6DN-Contra: 177.4 ± 10.18, n=8 (ANOVA, overall *$p < 0.01$; Vehicle-Ipsi vs. Pen1-C6DN:*$p < 0.05$). **B)** Intranasal delivery of Pen1-C6DN decreases the amount of tau cleavage that occurs in the core and penumbra during stroke. Alpha-tubulin was used as a loading control. **C)** Intranasal Pen1-C6DN blocks the elimination of axon tracts in the striatum during stroke. The Bielschowsky's method,which stains neurofilament (dark brown), was used to quantify striatal axons. An intranasal bolus of vehicle (upper panel) or Pen1-C6DN (lower panel) was prophylactically delivered, and mice were harvested at 24hpr (right panels). Light microscopy. Scale: 500 µm. Gra-phs are means (with SEM) of axon counts. Vehicle-Ipsi: 93.25 ± 22.50, n=4; Pen1-C6DN-Ipsi: 178.0 ± 21.73,n=3; Vehicle-Contra: 238.3 ± 9.050, n=3; Pen1-C6DN-Contra: 241.7 ± 9.244, n=4 (ANOVA, overall *$p < 0.0003$; Vehicle-Ipsi vs. Pen1-C6DN: *$p < 0.05$; Vehicle-Ipsi vs. Vehicle-Contra: *$p < 0.001$.)

5.2.3. Use in Optic Nerve Crush

To validate Pen1-C6DN with an alternate *in vivo* model of axo- and neurodegeneration, we collaborated with Dr. Zubair Ahmed at the University of Birmingham, UK. His lab studies optic nerve damage, which is a hallmark of ophthalmologic diseases like glaucoma and ocular trauma. One exceptional disease model is optic nerve transection, which is characterized by the selective loss of retinal ganglion cells (RGCs). RGCs are quantified by retrograde labeling with the fluorescent tracer Fluorogold (FG).

Ocular nerve transection or crush impairs retrograde axonal transport of target-derived neurotrophins, which triggers apoptosis. Dr. Ahmed recently demonstrated that ablating caspase-2 expression rescues RGC cell bodies from this injury, but axons continue to degenerate [personal communication and [208].

Dr. Ahmed administered Pen1-C6DN with caspase-2 siRNA (siCASP2) in an optic nerve crush (ONC) model in rats [182]. RGCs were rescued by siCASP2 (Figure 5-5A). Pen1-C6DN did not significantly change the number of cell bodies that remained in ONC (Figure 5-5A); however, more βIII tubulin-positive axons were present after ONC with Pen1-C6DN co-treatment (Figure 5-5B). The remaining axons were also longer with Pen1-C6DN co-treatment relative to siCASP2-alone.

When Pen1-C6DN was given without siCASP2 (Figure 5-5C), there was a slight increase in soma survival that was not as pronounced as with siCASP2/Pen1-6DN. However, axon degeneration was impeded by Pen1-C6DN alone (Figure 5-5D), which showed better efficacy than siCASP2 alone (Figure 5-5B vs. 5-5D). Thus, caspase-6 is a critical mediator of axon degeneration in ONC.

Figure 5-5.

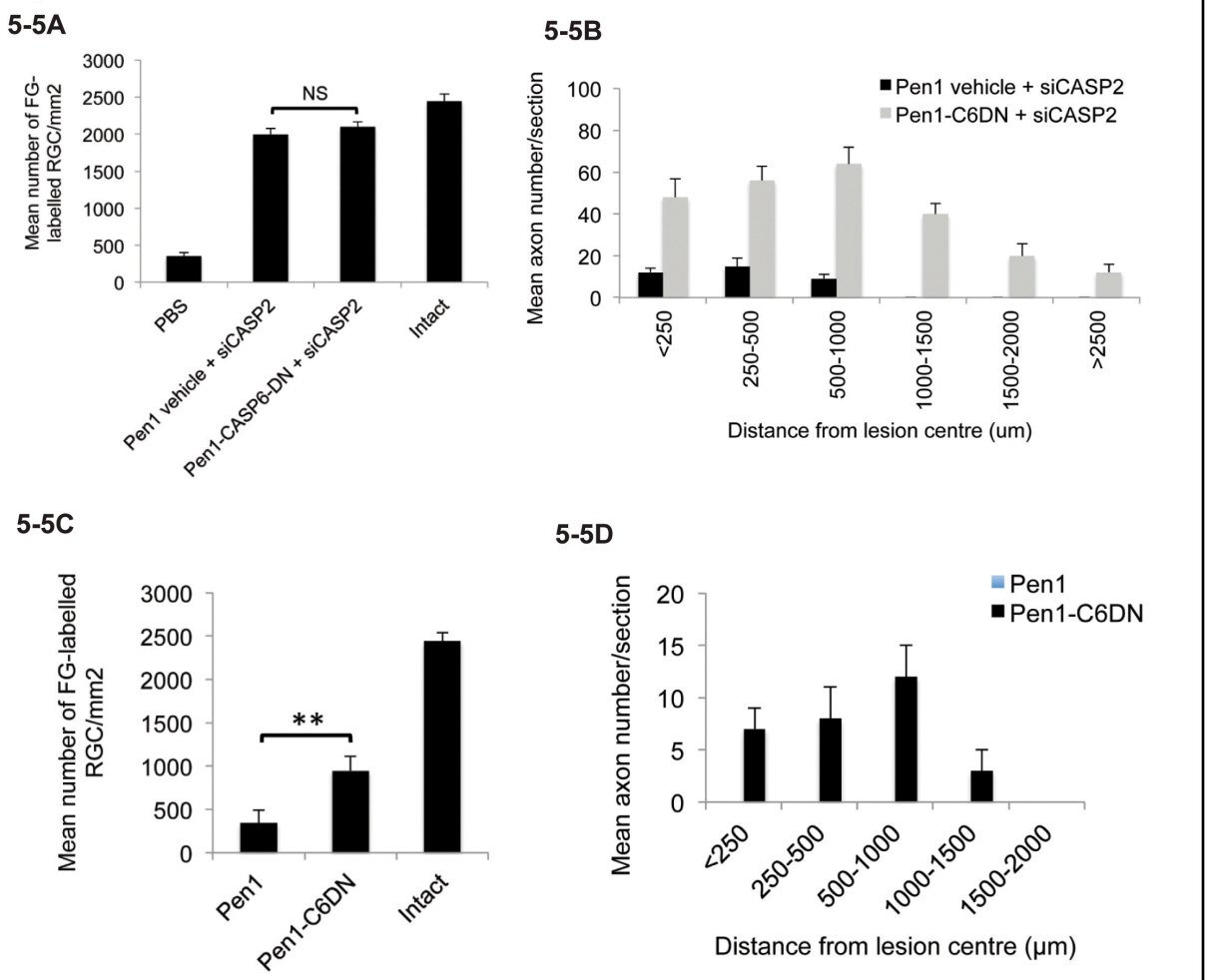

Figure 5-5. Pen1-C6DN in optic nerve crush (ONC).
Optic nerves were crushed in rats, and on day 3 they received an intraocular injection of 1) PBS, 2) Pen1-vehicle siCASP2, 3) siCASP2, or 4) siCASP2 with Pen1-C6DN. Retinal ganglion cells (RGCs) were quantified by retrograde labeling with the fluorescent tracer Fluorogold (FG). **A)** RGC survival siCASP2 and siCASP2 with Pen1-C6DN treatment is relatively equivalent. n = 6 per group. **B)** In contrast , axon loss (βIII tubulin immunofluorescence) is significantly ameliorated by siCASP2 with Pen1-C6DN. For **C)** RGC and **D)** axon survival, Pen1-C6DN by itself is also neuroproective against ONC. n = 6 per group

5.3. Discussion

Chapter 5 establishes Pen1-C6DN as a potent caspase-6 inhibitor in 3 models of neurodegeneration. Small molecule inhibitors lack the specificity to accurately dissect caspase

mechanisms [91], so the prospect of Pen1-C6DN as a first-line caspase-6 inhibitor is valuable from an academic perspective.

For example, one of our collaborators, Dr. Zubair Ahmed, has already found promising results with Pen1-C6DN in the setting of optic nerve transection. Our data suggest that caspase-2 and caspase-6 work synergistically to protect optic axons, but Pen1-C6DN by itself is axoprotective as well.

In Chapter 4, I discussed the delayed nature of caspase-6 activation in cerebral ischemia. Depending on the stage of neurodegeneration in stroke, a caspase-6 inhibitor used in isolation, or in combination with Pen1-XBIR3, might enhance neuroprotection against this disease. Moreover, caspase-6 has been implicated in chronic neuropathologies, like Huntington's disease and Alzheimer's disease. With Huntington's disease, caspase-6 is required for the cleavage of mutant huntingtin into its toxic form, which leads to the selective destruction of motor neurons. Thus, it would be worthwhile to test whether Pen1-C6DN is clinically beneficial in Huntington's disease. However, the use of Pen1-C6DN need not be limited to the context of disease and could reveal the physiological functions for caspase-6 in axon biology.

Chapter 6. Benchmarks: Conclusions and Future Directions

This dissertation exposes the vital nature of the intrinsic caspase death pathway in stroke neurodegeneration. This chapter will outline this project's achievements and future prospects.

6.1. Surveillance Strategy For *in vivo* Caspase Activity

A number of new techniques for measuring caspase activity in living cells or animal models were developed for this project. It has become apparent that older strategies for assessing caspase activity (i.e., short peptide inhibitors/substrates) lack the specificity to resolve caspase mechanisms [90, 91].

6.1.1. Benchmark 1: *In vivo* Active Caspase Precipitation

The biochemical isolation of active caspases from living cells was first performed in the research laboratory of Douglas R. Green [171]. They found that active initiator caspases could be precipitated from cultured neurons by pretreating the cells with bVAD-fmk (bVAD) prior to an apoptotic stimulus. BVAD irreversibly binds to any caspase with an available active site. They also reported that active effector caspases could be isolated if bVAD was given after the death stimulus, but other labs, including ours, have been unable to replicate this finding.

It is now widely accepted that bVAD is an excellent tool for isolating initiator caspases, which do not require cleavage for activation and have no other specific measure for activity. However, this isolation procedure had never been used in animal models until now.

Animal models of cerebral ischemia are arguably the most ideal systems for validating the bVAD-active caspase precipitation method. First, these models have abundant caspase activation. Second, stroke models are highly reproducible, which is important for quantitative assessments in biochemical analysis.

A surveillance strategy based on combining the caspase precipitation assay for active initiators with immunoassays for effector cleavage provides comprehensive *in vivo* analysis of caspase activity during apoptosis. Theoretically, if bVAD is saturated in the injured tissue, it should trap all of the initiator caspases that are active during the early stages of a death paradigm. For effector caspases, cleavage is easily measured by immunoassays (western blotting; WB) and immunohistochemistry (IHC).

However, this strategy is not without limitations. First, because bVAD irreversibly binds caspases, it eliminates any consequent downstream activity. Thus, only incipient events can be measured by bVAD. The second issue involves the endogenous inhibitor XIAP and the fact that we recommend cleavage to represent caspase-3 or caspase-7 activity. Cleavage of caspases-3 and -7, as measured by IHC and WB, would not account for caspase molecules that are possibly bound to endogenous XIAP *in vivo*. XIAP could be bound and inhibiting a cleaved caspase-3 molecule or a cleaved caspase-7 molecule *in vivo*, but this interaction would not prevent an antibody (for IHC or WB) from recognizing the cleaved caspase after the cell is lysed for western blotting or fixed for IHC. XIAP expression is upregulated during stroke, so a windfall scenario likely exists with immunoassays and IHC, where active capase-3 (cleaved and not bound to XIAP) and activated caspase-3 (cleaved, but bound to XIAP) are both counted as active. Although caspase-7 is inhibited by XIAP, it was not detected in our stroke model. Endogenous inhibitors have not been reported for caspase-6. Therefore, any conclusions drawn for caspase-3 in this study while using our strategy should be viewed with "a grain of salt".

XIAP can also inhibit caspase-9, but bVAD-caspase precipitation can only isolate caspase-9 molecules with an available active site; i.e., active caspase-9 that is not bound and inhibited by XIAP.

Overall, combing bVAD precipitation for initiators and immunoassays/IHC for cleaved effectors is a valuable strategy for studying caspase activity *in vivo*.

6.1.2. Benchmark 2: Innovations For Intracellular Peptide Delivery To The CNS

Here, we present another robust partnership: Trojan peptide delivery via the intranasal route.

Trojan peptides—like Penetratin1 (Pen1)—are versatile tools that are ready for widespread use in drug delivery. They provide a simple method for manipulating intracellular targets. For instance, Pen1 provides rapid entry for siRNAs [179] and peptides (Chapter 3.2.3. & Chapter 5.2.1.). Linking peptide cargo to Pen1 is straightforward: overnight incubation at 37°C with equimolar ratios between Pen1 and cargo (e.g., XBIR3 or C6DN). With regards to protein biologics, our results demonstrate that Trojan peptides can rapidly (<30 min) deliver small and large cargo (XBIR3: 16 kDA; C6DN: ~34 kDa). For Pen1, the upper limit for the successful intracellular delivery of protein cargo is as much as 100 kDa (Alain Prochiantz, personal communication).

While Trojan peptides mediate passage across the cell membrane, a method is still required for delivering protein biologics to their intended organs. This is especially a challenge when targeting the brain, where the blood brain barrier (BBB) acts as strict filter for foreign molecules in the peripheral blood circulation.

Intranasal delivery utilizes the porous nature of the cribriform plate, located on the roof of the nasal cavity, to bypass the BBB. This route permits direct access to the CNS by allowing peptides to leak into the CSF/ventricular circulation, which provides diffuse spreading throughout the CNS [1, 101, 175].

There are limitations for both Trojan peptides and intranasal delivery. Choosing the appropriate Trojan peptide is critical for success. For instance, the highly charged nature of Pen1 can lead to solubility issues during peptide linkage.

HIV-TAT is widely used as a carrier protein. However, TAT is permanently linked to its cargo as an expression domain, which can cause protein misfolding or inadvertently block interactions between the cargo and target.

Fewer restrictions exist for intranasal delivery, although the pH and osmolarity of the drug vehicle can affect the permeability of the nasal mucosa [101].

Overall, Trojan peptides and intranasal delivery are innovative tools for elucidating molecular pathways *in vivo.*

6.2. Caspase Biology

Our data show that caspase-9 is an early regulator of neurodegeneration during cerebral ischemia. Additionally, we provide the first evidence that caspase-6 regulates axon degeneration in stroke.

6.2.1. Benchmark 1: The Intrinsic Caspase Pathway In Ischemic Neurodegeneration

In Chapter 3, we used an unbiased approach to identify caspases that are activated by cerebral ischemia. Our data show that caspase-9 is an early regulator of neurodegeneration in cerebral ischemia. In our transient ischemia model, Caspase-9 is highly active during the first 6 hours of ischemia (2 hr of occlusion + 4hpr). BVAD analysis at further time points is required to completely define the window of caspase-9 activity.

In Chapter 4, we link caspase-9 function to the activation of effector caspases, namely caspase-6. This finding relied upon the use of Pen1-XBIR3, a highly specific, membrane-permeable inhibitor for caspase-9. Both prophylactic (immediately prior to stroke) and

therapeutic (at 4hpr) delivery provided long-term neurofunctional protection from cerebral ischemia.

We propose that this beneficial outcome was due to a combination of factors. First, Pen1-XBIR3 prevents neuron loss during the first 24hrs of stroke (at least), which also involves the inhibition of caspase-6-mediated axonal degeneration. Second, BBB damage and cerebral edema are foiled by Pen1-XBIR3 treatment.

Remarkably, only one dose of Pen1-XBIR3 (prophylactic or therapeutic) was needed for significant neuroprotection. Future studies should assess the benefits, if any, of multiple dosing. Additionally, therapeutic windows of treatment must be defined. The average stroke patient reaches the hospital 5.5 hours after the first warning sign [39], but it is common for patients to arrive 24 hr after a stroke [209]. Therefore, future translational studies with Pen1-XBIR3 should focus on determining its efficacy at different stages of stroke.

6.2.2. Benchmark 2: The Intrinsic Caspase Pathway In Ischemic Edema

We report that the p75NTR-caspase-9 pathway is implicated in the regulation of BBB integrity. P75NTR and caspase-9 are expressed at high levels in the cells that comprise the neurovascular unit; i.e., pericytes and endothelial cells. Given that proneurotrophins can stimulate death via p75NTR signaling, the neurovascular unit is possibly more susceptible to proneurotrophin toxicity. This theory requires further investigation.

One possibility is caspase-9 damages the BBB by triggering apoptosis in pericytes and endothelial cells. This hypothesis could be tested by measuring the density of both cell types in blood vessels during ischemia and by then correlating this assessment with the progression of edema.

Alternatively, caspase-9 could modulate the activity of enzymes that breakdown the vascular basal lamina during stroke, namely matrix metalloproteinases (MMPs). We observed that caspase-9 induces the expression of MMP-9 during stroke (Chapter 3.2.4.). MMP-9 has been previously linked to stroke neurodegeneration, specifically through its ability to destabilize the BBB and cause edema [210]. MMP expression is precisely regulated, and a number of transcription factors regulate MMP-9 expression [185]. Some are known targets of caspase cleavage, including NF-κB [186, 187] and SP1 [186, 188], which suggests a regulatory mechanism.

MMPs have recently been shown to regulate proneurotrophin processing. In rodent models of seizure [147] and diabetic retinopathy[150], MMP-7 expression and activity are down-regulated, which leads to an increase in the levels of extracellular proneurotrophins. In turn, proneurotrophins induce further cellular damage via p75NTR signaling in these models. MMP-7 expression was not measured in this study, but if a similar pattern is observed in stroke, it could signal a dynamic regulatory loop between p75NTR signaling, caspase-9 activity, and MMPs.

The complex interplay between the MMP family, proneurotrophins, neuronal apoptosis, and cerebral edema during stroke requires further evaluation and should make for exciting research in the years to come.

6.2.3. Benchmark 3: Axon Compartmentalization Of Caspase-6 Activity

Chapters 4 & 5 demonstrate that caspase-6 and the neuronal axon are intimately acquainted. Recent evidence [126, 127] describes a critical role for caspase-6 in axon health, which is further substantiated by findings in this project.

Here, we reveal that caspase-6 is involved with stroke-induced axon degeneration. One future direction might investigate how caspase-6 mediates axonal destruction. Substrate analysis

could reveal the cytoskeletal molecules that are targeted by caspase-6 during stroke. We have already demonstrated that caspase-6 is required for the proteolysis of tau during ischemia (Chapters 4 and 5). Moreover, staining for cleaved caspase-6 fills axonal regions where cytoskeletal staining is absent (Chapter 4). .

Is caspase-6 always required for axon degeneration or are there unique scenarios for its involvement? The caspase-6 inhibitor developed in this study (Pen1-C6DN) is based on a catalytic dominant negative and provides a new tool for answering this question in other models of axon degeneration. Indeed, Pen1-C6DN has already demonstrated efficacy in models of ocular nerve degeneration, as conducted by our collaborator Dr. Zubair Ahmed (Chapter 5).

6.3. Closing Statement

This dissertation emphasizes the critical role of caspases in stroke neurodegeneration. Given the myriad roles for caspases in stroke neurodegeneration, it is surprising that direct caspase inhibition has never been explored in clinical trials.

We have demonstrated that caspase-based neuroprotection strategies are effective in model systems of stroke. The innovations presented herein highlight new avenues for stroke therapy and new techniques for the dissection of apoptotic pathways.

Bibliography

1. Akpan, N., E. Serrano-Saiz, B.E. Zacharia, M.L. Otten, A.F. Ducruet, S.J. Snipas, W. Liu, J. Velloza, G. Cohen, S.A. Sosunov, W.H. Frey, 2nd, G.S. Salvesen, E.S. Connolly, Jr., and C.M. Troy, *Intranasal delivery of caspase-9 inhibitor reduces caspase-6-dependent axon/neuron loss and improves neurological function after stroke.* J Neurosci, 2011. **31**(24): p. 8894-904.

2. Akpan, N. and C.M. Troy, *Caspase Inhibitors: Prospective Therapies for Stroke.* Neuroscientist, 2012.

3. Donnan, G.A., M. Fisher, M. Macleod, and S.M. Davis, *Stroke.* Lancet, 2008. **371**(9624): p. 1612-23.

4. *Stroke Syndromes*. [cited 2012 May 7]; Available from: http://www.strokecenter.org/professionals/stroke-diagnosis/stroke-syndromes/.

5. Bamford, J., P. Sandercock, M. Dennis, J. Burn, and C. Warlow, *Classification and natural history of clinically identifiable subtypes of cerebral infarction.* Lancet, 1991. **337**(8756): p. 1521-6.

6. Pittock, S.J., D. Meldrum, O. Hardiman, J. Thornton, P. Brennan, and J.T. Moroney, *The Oxfordshire Community Stroke Project classification: correlation with imaging, associated complications, and prediction of outcome in acute ischemic stroke.* Journal of stroke and cerebrovascular diseases : the official journal of National Stroke Association, 2003. **12**(1): p. 1-7.

7. Furie, K.L. and P.J. Kelly, *Handbook of stroke prevention in clinical practice*. Current clinical neurology2004, Totowa, N.J.: Humana Press. xiii, 310 p.

8. Anderson, C.S., B.V. Taylor, G.J. Hankey, E.G. Stewart-Wynne, and K.D. Jamrozik, *Validation of a clinical classification for subtypes of acute cerebral infarction.* Journal of neurology, neurosurgery, and psychiatry, 1994. **57**(10): p. 1173-9.

9. Baird, A.E. and H.L. Lutsep, *Anterior Circulation Stroke*, 2011, Medscape Reference.

10. Cabral, N.L., A.R. Goncalves, A.L. Longo, C.H. Moro, G. Costa, C.H. Amaral, L.A. Fonseca, and J. Eluf-Neto, *Incidence of stroke subtypes, prognosis and prevalence of risk factors in Joinville, Brazil: a 2 year community based study.* Journal of neurology, neurosurgery, and psychiatry, 2009. **80**(7): p. 755-61.

11. Bhatnagar, P., P. Scarborough, N.C. Smeeton, and S. Allender, *The incidence of all stroke and stroke subtype in the United Kingdom, 1985 to 2008: a systematic review.* BMC Public Health, 2010. **10**: p. 539.

12. Anderson, C.S., K.D. Jamrozik, R.J. Broadhurst, and E.G. Stewart-Wynne, *Predicting survival for 1 year among different subtypes of stroke. Results from the Perth Community Stroke Study.* Stroke, 1994. **25**(10): p. 1935-44.

13. Bejot, Y., M. Caillier, D. Ben Salem, G. Couvreur, O. Rouaud, G.V. Osseby, J. Durier, C. Marie, T. Moreau, and M. Giroud, *Ischaemic stroke subtypes and associated risk factors: a French population based study.* Journal of neurology, neurosurgery, and psychiatry, 2008. **79**(12): p. 1344-8.

14. Lipton, P., *Ischemic cell death in brain neurons.* Physiol Rev, 1999. **79**(4): p. 1431-568.

15. Niizuma, K., H. Yoshioka, H. Chen, G.S. Kim, J.E. Jung, M. Katsu, N. Okami, and P.H. Chan, *Mitochondrial and apoptotic neuronal death signaling pathways in cerebral ischemia.* Biochim Biophys Acta, 2010. **1802**(1): p. 92-9.

16. Ribe, E.M., E. Serrano-Saiz, N. Akpan, and C.M. Troy, *Mechanisms of neuronal death in disease: defining the models and the players.* Biochem J, 2008. **415**(2): p. 165-82.

17. Yuan, J., *Neuroprotective strategies targeting apoptotic and necrotic cell death for stroke.* Apoptosis, 2009. **14**(4): p. 469-77.

18. del Zoppo, G.J., *Stroke and neurovascular protection.* N Engl J Med, 2006. **354**(6): p. 553-5.

19. Strbian, D., A. Meretoja, J. Putaala, M. Kaste, and T. Tatlisumak, *Cerebral edema in acute ischemic stroke patients treated with intravenous thrombolysis.* International journal of stroke : official journal of the International Stroke Society, 2012.

20. Boysen, G., J.L. Marott, M. Gronbaek, H. Hassanpour, and T. Truelsen, *Long-term survival after stroke: 30 years of follow-up in a cohort, the Copenhagen City Heart Study.* Neuroepidemiology, 2009. **33**(3): p. 254-60.

21. Carandang, R., S. Seshadri, A. Beiser, M. Kelly-Hayes, C.S. Kase, W.B. Kannel, and P.A. Wolf, *Trends in incidence, lifetime risk, severity, and 30-day mortality of stroke over the past 50 years.* JAMA, 2006. **296**(24): p. 2939-46.

22. CDC, *Prevalence of disabilities and associated health conditions among adults--United States, 1999.* MMWR Morb Mortal Wkly Rep, 2001. **50**(7): p. 120-5.

23. CDC, *Prevalence and most common causes of disability among adults--United States, 2005.* MMWR Morb Mortal Wkly Rep, 2009. **58**(16): p. 421-6.

24. Dhamoon, M.S., Y.P. Moon, M.C. Paik, B. Boden-Albala, T. Rundek, R.L. Sacco, and M.S. Elkind, *Long-term functional recovery after first ischemic stroke: the Northern Manhattan Study.* Stroke, 2009. **40**(8): p. 2805-11.

25. O'Donnell, M.J., D. Xavier, L. Liu, H. Zhang, S.L. Chin, P. Rao-Melacini, S. Rangarajan, S. Islam, P. Pais, M.J. McQueen, C. Mondo, A. Damasceno, P. Lopez-Jaramillo, G.J. Hankey, A.L. Dans, K. Yusoff, T. Truelsen, H.C. Diener, R.L. Sacco, D. Ryglewicz, A. Czlonkowska, C. Weimar, X. Wang, and S. Yusuf, *Risk factors for ischaemic and intracerebral haemorrhagic stroke in 22 countries (the INTERSTROKE study): a case-control study.* Lancet, 2010. **376**(9735): p. 112-23.

26. Bornstein, N., G. Silvestrelli, V. Caso, and L. Parnetti, *Arterial hypertension and stroke prevention: an update.* Clin Exp Hypertens, 2006. **28**(3-4): p. 317-26.

27. Hankey, G.J., *Smoking and risk of stroke.* J Cardiovasc Risk, 1999. **6**(4): p. 207-11.

28. Beckman, J.A., M.A. Creager, and P. Libby, *Diabetes and atherosclerosis: epidemiology, pathophysiology, and management.* JAMA, 2002. **287**(19): p. 2570-81.

29. *Cholesterol, diastolic blood pressure, and stroke: 13,000 strokes in 450,000 people in 45 prospective cohorts. Prospective studies collaboration.* Lancet, 1995. **346**(8991-8992): p. 1647-53.

30. Wolf, P.A., R.D. Abbott, and W.B. Kannel, *Atrial fibrillation: a major contributor to stroke in the elderly. The Framingham Study.* Arch Intern Med, 1987. **147**(9): p. 1561-4.

31. Reynolds, K., B. Lewis, J.D. Nolen, G.L. Kinney, B. Sathya, and J. He, *Alcohol consumption and risk of stroke: a meta-analysis.* JAMA, 2003. **289**(5): p. 579-88.

32. *CAST: randomised placebo-controlled trial of early aspirin use in 20,000 patients with acute ischaemic stroke. CAST (Chinese Acute Stroke Trial) Collaborative Group.* Lancet, 1997. **349**(9066): p. 1641-9.

33. *The International Stroke Trial (IST): a randomised trial of aspirin, subcutaneous heparin, both, or neither among 19435 patients with acute ischaemic stroke. International Stroke Trial Collaborative Group.* Lancet, 1997. **349**(9065): p. 1569-81.

34. Pan, G., E.W. Humke, and V.M. Dixit, *Activation of caspases triggered by cytochrome c in vitro.* FEBS Lett, 1998. **426**(1): p. 151-4.

35. Vahedi, K., J. Hofmeijer, E. Juettler, E. Vicaut, B. George, A. Algra, G.J. Amelink, P. Schmiedeck, S. Schwab, P.M. Rothwell, M.G. Bousser, H.B. van der Worp, and W. Hacke, *Early decompressive surgery in malignant infarction of the middle cerebral artery: a pooled analysis of three randomised controlled trials.* Lancet Neurol, 2007. **6**(3): p. 215-22.

36. ACEP. *Use of Intravenous tPA for the Management of Acute Stroke in the Emergency Department*. Policy Resource and Education Paper 2002 [cited 2012 03/09]; Available from: http://www.acep.org/content.aspx?id=29936.

37. Ginsberg, M.D., *Neuroprotection for ischemic stroke: past, present and future.* Neuropharmacology, 2008. **55**(3): p. 363-89.

38. Azzimondi, G., L. Bassein, L. Fiorani, F. Nonino, U. Montaguti, D. Celin, G. Re, and R. D'Alessandro, *Variables associated with hospital arrival time after stroke: effect of delay on the clinical efficiency of early treatment.* Stroke, 1997. **28**(3): p. 537-42.

39. Maze, L.M. and T. Bakas, *Factors associated with hospital arrival time for stroke patients.* J Neurosci Nurs, 2004. **36**(3): p. 136-41, 155.

40. Broughton, B.R., D.C. Reutens, and C.G. Sobey, *Apoptotic mechanisms after cerebral ischemia.* Stroke, 2009. **40**(5): p. e331-9.

41. Mitsios, N., J. Gaffney, J. Krupinski, R. Mathias, Q. Wang, S. Hayward, F. Rubio, P. Kumar, S. Kumar, and M. Slevin, *Expression of signaling molecules associated with apoptosis in human ischemic stroke tissue.* Cell Biochem Biophys, 2007. **47**(1): p. 73-86.

42. O'Brien, T. *Caspase Inhibitors in Drug Discovery*. in *Apoptosis: Fundamentals, Pathways, Clinical Applications and Role in Disease*. 2007. London: Henry Stewart Talks Ltd.

43. Pop, C. and G.S. Salvesen, *Human caspases: activation, specificity, and regulation.* J Biol Chem, 2009. **284**(33): p. 21777-81.

44. Nicholson, D.W., *Caspase structure, proteolytic substrates, and function during apoptotic cell death.* Cell Death Differ, 1999. **6**(11): p. 1028-42.

45. Boatright, K.M. and G.S. Salvesen, *Mechanisms of caspase activation.* Curr Opin Cell Biol, 2003. **15**(6): p. 725-31.

46. Fuentes-Prior, P. and G.S. Salvesen, *The protein structures that shape caspase activity, specificity, activation and inhibition.* Biochem J, 2004. **384**(Pt 2): p. 201-32.

47. Friedlander, R.M., *Role of caspase 1 in neurologic disease.* Arch Neurol, 2000. **57**(9): p. 1273-6.

48. Friedlander, R.M., V. Gagliardini, H. Hara, K.B. Fink, W. Li, G. MacDonald, M.C. Fishman, A.H. Greenberg, M.A. Moskowitz, and J. Yuan, *Expression of a dominant negative mutant of interleukin-1 beta converting enzyme in transgenic mice prevents neuronal cell death induced by trophic factor withdrawal and ischemic brain injury.* J Exp Med, 1997. **185**(5): p. 933-40.

49. Green, D.R., *Immunology: A heavyweight knocked out.* Nature, 2011. **479**(7371): p. 48-50.

50. Kang, S.J., S. Wang, H. Hara, E.P. Peterson, S. Namura, S. Amin-Hanjani, Z. Huang, A. Srinivasan, K.J. Tomaselli, N.A. Thornberry, M.A. Moskowitz, and J. Yuan, *Dual role of caspase-11 in mediating activation of caspase-1 and caspase-3 under pathological conditions.* J Cell Biol, 2000. **149**(3): p. 613-22.

51. Stroh, C. and K. Schulze-Osthoff, *Death by a thousand cuts: an ever increasing list of caspase substrates.* Cell Death Differ, 1998. **5**(12): p. 997-1000.

52. Luthi, A.U. and S.J. Martin, *The CASBAH: a searchable database of caspase substrates.* Cell Death Differ, 2007. **14**(4): p. 641-50.

53. Schweizer, A., C. Briand, and M.G. Grutter, *Crystal structure of caspase-2, apical initiator of the intrinsic apoptotic pathway.* The Journal of biological chemistry, 2003. **278**(43): p. 42441-7.

54. Westphal, D., G. Dewson, P.E. Czabotar, and R.M. Kluck, *Molecular biology of Bax and Bak activation and action.* Biochim Biophys Acta, 2011. **1813**(4): p. 521-31.

55. Segal, R.A., *Selectivity in neurotrophin signaling: theme and variations.* Annu Rev Neurosci, 2003. **26**: p. 299-330.

56. Huang, E.J. and L.F. Reichardt, *Trk receptors: roles in neuronal signal transduction.* Annu Rev Biochem, 2003. **72**: p. 609-42.

57. Teng, K.K. and B.L. Hempstead, *Neurotrophins and their receptors: signaling trios in complex biological systems.* Cell Mol Life Sci, 2004. **61**(1): p. 35-48.

58. Friedman, W.J., *Proneurotrophins, seizures, and neuronal apoptosis.* Neuroscientist, 2010. **16**(3): p. 244-52.

59. Casaccia-Bonnefil, P., B.D. Carter, R.T. Dobrowsky, and M.V. Chao, *Death of oligodendrocytes mediated by the interaction of nerve growth factor with its receptor p75.* Nature, 1996. **383**(6602): p. 716-9.

60. Beattie, M.S., A.W. Harrington, R. Lee, J.Y. Kim, S.L. Boyce, F.M. Longo, J.C. Bresnahan, B.L. Hempstead, and S.O. Yoon, *ProNGF induces p75-mediated death of oligodendrocytes following spinal cord injury.* Neuron, 2002. **36**(3): p. 375-86.

61. Friedman, W.J. and L.A. Greene, *Neurotrophin signaling via Trks and p75.* Exp Cell Res, 1999. **253**(1): p. 131-42.

62. Song, W., M. Volosin, A.B. Cragnolini, B.L. Hempstead, and W.J. Friedman, *ProNGF induces PTEN via p75NTR to suppress Trk-mediated survival signaling in brain neurons.* J Neurosci, 2010. **30**(46): p. 15608-15.

63. Salehi, A.H., P.P. Roux, C.J. Kubu, C. Zeindler, A. Bhakar, L.L. Tannis, J.M. Verdi, and P.A. Barker, *NRAGE, a novel MAGE protein, interacts with the p75 neurotrophin receptor and facilitates nerve growth factor-dependent apoptosis.* Neuron, 2000. **27**(2): p. 279-88.

64. Salehi, A.H., S. Xanthoudakis, and P.A. Barker, *NRAGE, a p75 neurotrophin receptor-interacting protein, induces caspase activation and cell death through a JNK-dependent mitochondrial pathway.* J Biol Chem, 2002. **277**(50): p. 48043-50.

65. Casademunt, E., B.D. Carter, I. Benzel, J.M. Frade, G. Dechant, and Y.A. Barde, *The zinc finger protein NRIF interacts with the neurotrophin receptor p75(NTR) and participates in programmed cell death.* EMBO J, 1999. **18**(21): p. 6050-61.

66. Linggi, M.S., T.L. Burke, B.B. Williams, A. Harrington, R. Kraemer, B.L. Hempstead, S.O. Yoon, and B.D. Carter, *Neurotrophin receptor interacting factor (NRIF) is an essential mediator of apoptotic signaling by the p75 neurotrophin receptor.* J Biol Chem, 2005. **280**(14): p. 13801-8.

67. Mukai, J., T. Hachiya, S. Shoji-Hoshino, M.T. Kimura, D. Nadano, P. Suvanto, T. Hanaoka, Y. Li, S. Irie, L.A. Greene, and T.A. Sato, *NADE, a p75NTR-associated cell death executor, is involved in signal transduction mediated by the common neurotrophin receptor p75NTR.* J Biol Chem, 2000. **275**(23): p. 17566-70.

68. Mukai, J., P. Suvant, and T.A. Sato, *Nerve growth factor-dependent regulation of NADE-induced apoptosis.* Vitam Horm, 2003. **66**: p. 385-402.

69. Volosin, M., C. Trotter, A. Cragnolini, R.S. Kenchappa, M. Light, B.L. Hempstead, B.D. Carter, and W.J. Friedman, *Induction of proneurotrophins and activation of p75NTR-mediated apoptosis via neurotrophin receptor-interacting factor in hippocampal neurons after seizures.* J Neurosci, 2008. **28**(39): p. 9870-9.

70. Roux, P.P. and P.A. Barker, *Neurotrophin signaling through the p75 neurotrophin receptor.* Prog Neurobiol, 2002. **67**(3): p. 203-33.

71. Park, J.A., J.Y. Lee, T.A. Sato, and J.Y. Koh, *Co-induction of p75NTR and p75NTR-associated death executor in neurons after zinc exposure in cortical culture or transient ischemia in the rat.* J Neurosci, 2000. **20**(24): p. 9096-103.

72. Yoon, K., H.D. Jang, and S.Y. Lee, *Direct interaction of Smac with NADE promotes TRAIL-induced apoptosis.* Biochem Biophys Res Commun, 2004. **319**(2): p. 649-54.

73. Bamji, S.X., M. Majdan, C.D. Pozniak, D.J. Belliveau, R. Aloyz, J. Kohn, C.G. Causing, and F.D. Miller, *The p75 neurotrophin receptor mediates neuronal apoptosis and is essential for naturally occurring sympathetic neuron death.* J Cell Biol, 1998. **140**(4): p. 911-23.

74. Aloyz, R.S., S.X. Bamji, C.D. Pozniak, J.G. Toma, J. Atwal, D.R. Kaplan, and F.D. Miller, *p53 is essential for developmental neuron death as regulated by the TrkA and p75 neurotrophin receptors.* J Cell Biol, 1998. **143**(6): p. 1691-703.

75. Jacobs, W.B., G.S. Walsh, and F.D. Miller, *Neuronal survival and p73/p63/p53: a family affair.* Neuroscientist, 2004. **10**(5): p. 443-55.

76. Cregan, S.P., J.G. MacLaurin, C.G. Craig, G.S. Robertson, D.W. Nicholson, D.S. Park, and R.S. Slack, *Bax-dependent caspase-3 activation is a key determinant in p53-induced apoptosis in neurons.* J Neurosci, 1999. **19**(18): p. 7860-9.

77. Xiang, H., Y. Kinoshita, C.M. Knudson, S.J. Korsmeyer, P.A. Schwartzkroin, and R.S. Morrison, *Bax involvement in p53-mediated neuronal cell death.* J Neurosci, 1998. **18**(4): p. 1363-73.

78. Martin-Villalba, A., M. Hahne, S. Kleber, J. Vogel, W. Falk, J. Schenkel, and P.H. Krammer, *Therapeutic neutralization of CD95-ligand and TNF attenuates brain damage in stroke.* Cell Death Differ, 2001. **8**(7): p. 679-86.

79. Al-Jamal, K.T., L. Gherardini, G. Bardi, A. Nunes, C. Guo, C. Bussy, M.A. Herrero, A. Bianco, M. Prato, K. Kostarelos, and T. Pizzorusso, *Functional motor recovery from brain ischemic insult by carbon nanotube-mediated siRNA silencing.* Proc Natl Acad Sci U S A, 2011. **108**(27): p. 10952-7.

80. Chu, Y., J.D. Miller, and D.D. Heistad, *Gene therapy for stroke: 2006 overview.* Curr Hypertens Rep, 2007. **9**(1): p. 19-24.

81. Wu, T.L. and H.C. Ertl, *Immune barriers to successful gene therapy.* Trends Mol Med, 2009. **15**(1): p. 32-9.

82. Yrjanheikki, J., T. Tikka, R. Keinanen, G. Goldsteins, P.H. Chan, and J. Koistinaho, *A tetracycline derivative, minocycline, reduces inflammation and protects against focal cerebral ischemia with a wide therapeutic window.* Proc Natl Acad Sci U S A, 1999. **96**(23): p. 13496-500.

83. Wang, J., Q. Wei, C.Y. Wang, W.D. Hill, D.C. Hess, and Z. Dong, *Minocycline up-regulates Bcl-2 and protects against cell death in mitochondria.* J Biol Chem, 2004. **279**(19): p. 19948-54.

84. Giuliani, F., W. Hader, and V.W. Yong, *Minocycline attenuates T cell and microglia activity to impair cytokine production in T cell-microglia interaction.* J Leukoc Biol, 2005. **78**(1): p. 135-43.

85. Chen, X., X. Ma, Y. Jiang, R. Pi, Y. Liu, and L. Ma, *The prospects of minocycline in multiple sclerosis.* J Neuroimmunol, 2011. **235**(1-2): p. 1-8.

86. Greenwald, R.A., *The road forward: the scientific basis for tetracycline treatment of arthritic disorders.* Pharmacol Res, 2011. **64**(6): p. 610-3.

87. Gough, A., S. Chapman, K. Wagstaff, P. Emery, and E. Elias, *Minocycline induced autoimmune hepatitis and systemic lupus erythematosus-like syndrome.* BMJ, 1996. **312**(7024): p. 169-72.

88. Krawitt, E.L., *Autoimmune hepatitis.* N Engl J Med, 2006. **354**(1): p. 54-66.

89. Endres, M., S. Namura, M. Shimizu-Sasamata, C. Waeber, L. Zhang, T. Gomez-Isla, B.T. Hyman, and M.A. Moskowitz, *Attenuation of delayed neuronal death after mild focal ischemia in mice by inhibition of the caspase family.* J Cereb Blood Flow Metab, 1998. **18**(3): p. 238-47.

90. Benkova, B., V. Lozanov, I.P. Ivanov, and V. Mitev, *Evaluation of recombinant caspase specificity by competitive substrates.* Anal Biochem, 2009. **394**(1): p. 68-74.

91. McStay, G.P., G.S. Salvesen, and D.R. Green, *Overlapping cleavage motif selectivity of caspases: implications for analysis of apoptotic pathways.* Cell Death Differ, 2008. **15**(2): p. 322-31.

92. Huesmann, G.R. and D.F. Clayton, *Dynamic role of postsynaptic caspase-3 and BIRC4 in zebra finch song-response habituation.* Neuron, 2006. **52**(6): p. 1061-72.

93. Venero, J.L., M.A. Burguillos, P. Brundin, and B. Joseph, *The executioners sing a new song: killer caspases activate microglia.* Cell Death Differ, 2011. **18**(11): p. 1679-91.

94. Eckelman, B.P., G.S. Salvesen, and F.L. Scott, *Human inhibitor of apoptosis proteins: why XIAP is the black sheep of the family.* EMBO Rep, 2006. **7**(10): p. 988-94.

95. Shiozaki, E.N., J. Chai, D.J. Rigotti, S.J. Riedl, P. Li, S.M. Srinivasula, E.S. Alnemri, R. Fairman, and Y. Shi, *Mechanism of XIAP-mediated inhibition of caspase-9.* Mol Cell, 2003. **11**(2): p. 519-27.

96. Srinivasula, S.M., R. Hegde, A. Saleh, P. Datta, E. Shiozaki, J. Chai, R.A. Lee, P.D. Robbins, T. Fernandes-Alnemri, Y. Shi, and E.S. Alnemri, *A conserved XIAP-interaction motif in caspase-9 and Smac/DIABLO regulates caspase activity and apoptosis.* Nature, 2001. **410**(6824): p. 112-6.

97. Derossi, D., A.H. Joliot, G. Chassaing, and A. Prochiantz, *The third helix of the Antennapedia homeodomain translocates through biological membranes.* J Biol Chem, 1994. **269**(14): p. 10444-50.

98. Madani, F., S. Lindberg, U. Langel, S. Futaki, and A. Graslund, *Mechanisms of cellular uptake of cell-penetrating peptides.* J Biophys, 2011. **2011**: p. 414729.

99. Kumar, P., H. Wu, J.L. McBride, K.E. Jung, M.H. Kim, B.L. Davidson, S.K. Lee, P. Shankar, and N. Manjunath, *Transvascular delivery of small interfering RNA to the central nervous system.* Nature, 2007. **448**(7149): p. 39-43.

100. Fu, A., Y. Wang, L. Zhan, and R. Zhou, *Targeted delivery of proteins into the central nervous system mediated by rabies virus glycoprotein-derived peptide.* Pharm Res, 2012. **29**(6): p. 1562-9.

101. Dhuria, S.V., L.R. Hanson, and W.H. Frey, 2nd, *Intranasal delivery to the central nervous system: mechanisms and experimental considerations.* J Pharm Sci, 2010. **99**(4): p. 1654-73.

102. Craft, S., L.D. Baker, T.J. Montine, S. Minoshima, G.S. Watson, A. Claxton, M. Arbuckle, M. Callaghan, E. Tsai, S.R. Plymate, P.S. Green, J. Leverenz, D. Cross, and B. Gerton, *Intranasal insulin therapy for Alzheimer disease and amnestic mild cognitive impairment: a pilot clinical trial.* Arch Neurol, 2012. **69**(1): p. 29-38.

103. Thorne, R.G., G.J. Pronk, V. Padmanabhan, and W.H. Frey, 2nd, *Delivery of insulin-like growth factor-I to the rat brain and spinal cord along olfactory and trigeminal pathways following intranasal administration.* Neuroscience, 2004. **127**(2): p. 481-96.

104. Coleman, M.P. and V.H. Perry, *Axon pathology in neurological disease: a neglected therapeutic target.* Trends Neurosci, 2002. **25**(10): p. 532-7.

105. Lie, C., J.G. Hirsch, C. Rossmanith, M.G. Hennerici, and A. Gass, *Clinicotopographical correlation of corticospinal tract stroke: a color-coded diffusion tensor imaging study.* Stroke, 2004. **35**(1): p. 86-92.

106. Thomalla, G., V. Glauche, M.A. Koch, C. Beaulieu, C. Weiller, and J. Rother, *Diffusion tensor imaging detects early Wallerian degeneration of the pyramidal tract after ischemic stroke.* Neuroimage, 2004. **22**(4): p. 1767-74.

107. Ito, U., T. Kuroiwa, J. Nagasao, E. Kawakami, and K. Oyanagi, *Temporal profiles of axon terminals, synapses and spines in the ischemic penumbra of the cerebral cortex: ultrastructure of neuronal remodeling.* Stroke, 2006. **37**(8): p. 2134-9.

108. Ito, U., E. Kawakami, J. Nagasao, T. Kuroiwa, I. Nakano, and K. Oyanagi, *Restitution of ischemic injuries in penumbra of cerebral cortex after temporary ischemia.* Acta Neurochir Suppl, 2006. **96**: p. 239-43.

109. Iizuka, H., K. Sakatani, and W. Young, *Corticofugal axonal degeneration in rats after middle cerebral artery occlusion.* Stroke, 1989. **20**(10): p. 1396-402.

110. Schielke, G.P., G.Y. Yang, B.D. Shivers, and A.L. Betz, *Reduced ischemic brain injury in interleukin-1 beta converting enzyme-deficient mice.* J Cereb Blood Flow Metab, 1998. **18**(2): p. 180-5.

111. Benchoua, A., C. Guegan, C. Couriaud, H. Hosseini, N. Sampaio, D. Morin, and B. Onteniente, *Specific caspase pathways are activated in the two stages of cerebral infarction.* J Neurosci, 2001. **21**(18): p. 7127-34.

112. Niizuma, K., H. Endo, C. Nito, D.J. Myer, G.S. Kim, and P.H. Chan, *The PIDDosome mediates delayed death of hippocampal CA1 neurons after transient global cerebral ischemia in rats.* Proc Natl Acad Sci U S A, 2008. **105**(42): p. 16368-73.

113. Le, D.A., Y. Wu, Z. Huang, K. Matsushita, N. Plesnila, J.C. Augustinack, B.T. Hyman, J. Yuan, K. Kuida, R.A. Flavell, and M.A. Moskowitz, *Caspase activation and neuroprotection in caspase-3- deficient mice after in vivo cerebral ischemia and in vitro oxygen glucose deprivation.* Proc Natl Acad Sci U S A, 2002. **99**(23): p. 15188-93.

114. Velier, J.J., J.A. Ellison, K.K. Kikly, P.A. Spera, F.C. Barone, and G.Z. Feuerstein, *Caspase-8 and caspase-3 are expressed by different populations of cortical neurons undergoing delayed cell death after focal stroke in the rat.* J Neurosci, 1999. **19**(14): p. 5932-41.

115. Ferrer, I. and A.M. Planas, *Signaling of cell death and cell survival following focal cerebral ischemia: life and death struggle in the penumbra.* J Neuropathol Exp Neurol, 2003. **62**(4): p. 329-39.

116. Krajewski, S., M. Krajewska, L.M. Ellerby, K. Welsh, Z. Xie, Q.L. Deveraux, G.S. Salvesen, D.E. Bredesen, R.E. Rosenthal, G. Fiskum, and J.C. Reed, *Release of caspase-9 from mitochondria during neuronal apoptosis and cerebral ischemia.* Proc Natl Acad Sci U S A, 1999. **96**(10): p. 5752-7.

117. Duan, S.R., J.X. Wang, J. Wang, R. Xu, J.K. Zhao, and D.S. Wang, *Ischemia induces endoplasmic reticulum stress and cell apoptosis in human brain.* Neurosci Lett, 2010. **475**(3): p. 132-5.

118. Hara, H., K. Fink, M. Endres, R.M. Friedlander, V. Gagliardini, J. Yuan, and M.A. Moskowitz, *Attenuation of transient focal cerebral ischemic injury in transgenic mice expressing a mutant ICE inhibitory protein.* J Cereb Blood Flow Metab, 1997. **17**(4): p. 370-5.

119. Buki, A., D.O. Okonkwo, K.K. Wang, and J.T. Povlishock, *Cytochrome c release and caspase activation in traumatic axonal injury.* J Neurosci, 2000. **20**(8): p. 2825-34.

120. Coleman, M.P. and M.R. Freeman, *Wallerian degeneration, wld(s), and nmnat.* Annu Rev Neurosci, 2010. **33**: p. 245-67.

121. Gillingwater, T.H., J.E. Haley, R.R. Ribchester, and K. Horsburgh, *Neuroprotection after transient global cerebral ischemia in Wld(s) mutant mice.* J Cereb Blood Flow Metab, 2004. **24**(1): p. 62-6.

122. Coleman, M., *Axon degeneration mechanisms: commonality amid diversity.* Nat Rev Neurosci, 2005. **6**(11): p. 889-98.

123. Finn, J.T., M. Weil, F. Archer, R. Siman, A. Srinivasan, and M.C. Raff, *Evidence that Wallerian degeneration and localized axon degeneration induced by local neurotrophin deprivation do not involve caspases.* J Neurosci, 2000. **20**(4): p. 1333-41.

124. Burne, J.F., J.K. Staple, and M.C. Raff, *Glial cells are increased proportionally in transgenic optic nerves with increased numbers of axons.* J Neurosci, 1996. **16**(6): p. 2064-73.

125. Whitmore, A.V., T. Lindsten, M.C. Raff, and C.B. Thompson, *The proapoptotic proteins Bax and Bak are not involved in Wallerian degeneration.* Cell Death Differ, 2003. **10**(2): p. 260-1.

126. Vohra, B.P., Y. Sasaki, B.R. Miller, J. Chang, A. DiAntonio, and J. Milbrandt, *Amyloid precursor protein cleavage-dependent and -independent axonal degeneration programs share a common nicotinamide mononucleotide adenylyltransferase 1-sensitive pathway.* J Neurosci, 2010. **30**(41): p. 13729-38.

127. Nikolaev, A., T. McLaughlin, D.D. O'Leary, and M. Tessier-Lavigne, *APP binds DR6 to trigger axon pruning and neuron death via distinct caspases.* Nature, 2009. **457**(7232): p. 981-9.

128. Kuo, C.T., S. Zhu, S. Younger, L.Y. Jan, and Y.N. Jan, *Identification of E2/E3 ubiquitinating enzymes and caspase activity regulating Drosophila sensory neuron dendrite pruning.* Neuron, 2006. **51**(3): p. 283-90.

129. Williams, D.W., S. Kondo, A. Krzyzanowska, Y. Hiromi, and J.W. Truman, *Local caspase activity directs engulfment of dendrites during pruning.* Nat Neurosci, 2006. **9**(10): p. 1234-6.

130. Srinivasan, A., K.A. Roth, R.O. Sayers, K.S. Shindler, A.M. Wong, L.C. Fritz, and K.J. Tomaselli, *In situ immunodetection of activated caspase-3 in apoptotic neurons in the developing nervous system.* Cell Death Differ, 1998. **5**(12): p. 1004-16.

131. Medow, J.E., B.M. Agrawal, and M.K. Baskaya, *Ischemic Cerebral Edema.* Neurosurgery Quarterly, 2009. **19**(3): p. 147-155 10.1097/WNQ.0b013e3181a3630e.

132. Rosenberg, G.A., *Ischemic brain edema.* Prog Cardiovasc Dis, 1999. **42**(3): p. 209-16.

133. Ayata, C. and A.H. Ropper, *Ischaemic brain oedema.* J Clin Neurosci, 2002. **9**(2): p. 113-24.

134. *Edema Formation*. [cited 2012 July 28]; Available from: http://www.strokecenter.org/professionals/brain-anatomy/cellular-injury-during-ischemia/edema-formation/.

135. Lijnen, H.R., *Plasmin and matrix metalloproteinases in vascular remodeling.* Thromb Haemost, 2001. **86**(1): p. 324-33.

136. Candelario-Jalil, E., Y. Yang, and G.A. Rosenberg, *Diverse roles of matrix metalloproteinases and tissue inhibitors of metalloproteinases in neuroinflammation and cerebral ischemia.* Neuroscience, 2009. **158**(3): p. 983-94.

137. Rhodes, J.M. and M. Simons, *The extracellular matrix and blood vessel formation: not just a scaffold.* J Cell Mol Med, 2007. **11**(2): p. 176-205.

138. Yang, Y., E.Y. Estrada, J.F. Thompson, W. Liu, and G.A. Rosenberg, *Matrix metalloproteinase-mediated disruption of tight junction proteins in cerebral vessels is reversed by synthetic matrix metalloproteinase inhibitor in focal ischemia in rat.* J Cereb Blood Flow Metab, 2007. **27**(4): p. 697-709.

139. Yang, Y., J.W. Hill, and G.A. Rosenberg, *Multiple roles of metalloproteinases in neurological disorders.* Prog Mol Biol Transl Sci, 2011. **99**: p. 241-63.

140. Chang, D.I., N. Hosomi, J. Lucero, J.H. Heo, T. Abumiya, A.P. Mazar, and G.J. del Zoppo, *Activation systems for latent matrix metalloproteinase-2 are upregulated*

immediately after focal cerebral ischemia. J Cereb Blood Flow Metab, 2003. **23**(12): p. 1408-19.

141. Heo, J.H., J. Lucero, T. Abumiya, J.A. Koziol, B.R. Copeland, and G.J. del Zoppo, *Matrix metalloproteinases increase very early during experimental focal cerebral ischemia.* J Cereb Blood Flow Metab, 1999. **19**(6): p. 624-33.

142. Rosenberg, G.A., M. Navratil, F. Barone, and G. Feuerstein, *Proteolytic cascade enzymes increase in focal cerebral ischemia in rat.* J Cereb Blood Flow Metab, 1996. **16**(3): p. 360-6.

143. Rosell, A., A. Ortega-Aznar, J. Alvarez-Sabin, I. Fernandez-Cadenas, M. Ribo, C.A. Molina, E.H. Lo, and J. Montaner, *Increased brain expression of matrix metalloproteinase-9 after ischemic and hemorrhagic human stroke.* Stroke, 2006. **37**(6): p. 1399-406.

144. Rosell, A. and E.H. Lo, *Multiphasic roles for matrix metalloproteinases after stroke.* Curr Opin Pharmacol, 2008. **8**(1): p. 82-9.

145. Sole, S., V. Petegnief, R. Gorina, A. Chamorro, and A.M. Planas, *Activation of matrix metalloproteinase-3 and agrin cleavage in cerebral ischemia/reperfusion.* J Neuropathol Exp Neurol, 2004. **63**(4): p. 338-49.

146. Brew, K. and H. Nagase, *The tissue inhibitors of metalloproteinases (TIMPs): an ancient family with structural and functional diversity.* Biochim Biophys Acta, 2010. **1803**(1): p. 55-71.

147. Le, A.P. and W.J. Friedman, *Matrix metalloproteinase-7 regulates cleavage of pro-nerve growth factor and is neuroprotective following kainic acid-induced seizures.* J Neurosci, 2012. **32**(2): p. 703-12.

148. Lee, R., P. Kermani, K.K. Teng, and B.L. Hempstead, *Regulation of cell survival by secreted proneurotrophins.* Science, 2001. **294**(5548): p. 1945-8.

149. Kendall, T.J., S. Hennedige, R.L. Aucott, S.N. Hartland, M.A. Vernon, R.C. Benyon, and J.P. Iredale, *p75 Neurotrophin receptor signaling regulates hepatic myofibroblast proliferation and apoptosis in recovery from rodent liver fibrosis.* Hepatology, 2009. **49**(3): p. 901-10.

150. Ali, T.K., M.M. Al-Gayyar, S. Matragoon, B.A. Pillai, M.A. Abdelsaid, J.J. Nussbaum, and A.B. El-Remessy, *Diabetes-induced peroxynitrite impairs the balance of pro-nerve growth factor and nerve growth factor, and causes neurovascular injury.* Diabetologia, 2011. **54**(3): p. 657-68.

151. Shepro, D. and N.M. Morel, *Pericyte physiology.* FASEB J, 1993. **7**(11): p. 1031-8.

152. Daneman, R., L. Zhou, A.A. Kebede, and B.A. Barres, *Pericytes are required for blood-brain barrier integrity during embryogenesis.* Nature, 2010. **468**(7323): p. 562-6.

153. Bell, R.D., E.A. Winkler, A.P. Sagare, I. Singh, B. LaRue, R. Deane, and B.V. Zlokovic, *Pericytes control key neurovascular functions and neuronal phenotype in the adult brain and during brain aging.* Neuron, 2010. **68**(3): p. 409-27.

154. Yemisci, M., Y. Gursoy-Ozdemir, A. Vural, A. Can, K. Topalkara, and T. Dalkara, *Pericyte contraction induced by oxidative-nitrative stress impairs capillary reflow despite successful opening of an occluded cerebral artery.* Nat Med, 2009. **15**(9): p. 1031-7.

155. Watanabe, C., G.L. Shu, T.S. Zheng, R.A. Flavell, and E.A. Clark, *Caspase 6 regulates B cell activation and differentiation into plasma cells.* J Immunol, 2008. **181**(10): p. 6810-9.

156. Zheng, T.S., S. Hunot, K. Kuida, T. Momoi, A. Srinivasan, D.W. Nicholson, Y. Lazebnik, and R.A. Flavell, *Deficiency in caspase-9 or caspase-3 induces compensatory caspase activation.* Nat Med, 2000. **6**(11): p. 1241-7.

157. Connolly, E.S., Jr., C.J. Winfree, D.M. Stern, R.A. Solomon, and D.J. Pinsky, *Procedural and strain-related variables significantly affect outcome in a murine model of focal cerebral ischemia.* Neurosurgery, 1996. **38**(3): p. 523-31; discussion 532.

158. Komotar, R.J., G.H. Kim, M.E. Sughrue, M.L. Otten, M.A. Rynkowski, C.P. Kellner, D.K. Hahn, M.B. Merkow, M.C. Garrett, R.M. Starke, and E.S. Connolly, *Neurologic assessment of somatosensory dysfunction following an experimental rodent model of cerebral ischemia.* Nat Protoc, 2007. **2**(10): p. 2345-7.

159. Ten, V.S., E.X. Wu, H. Tang, M. Bradley-Moore, M.V. Fedarau, V.I. Ratner, R.I. Stark, J.A. Gingrich, and D.J. Pinsky, *Late measures of brain injury after neonatal hypoxia-ischemia in mice.* Stroke, 2004. **35**(9): p. 2183-8.

160. Ten, V.S., J. Yao, V. Ratner, S. Sosunov, D.A. Fraser, M. Botto, B. Sivasankar, B.P. Morgan, S. Silverstein, R. Stark, R. Polin, S.J. Vannucci, D. Pinsky, and A.A. Starkov, *Complement component c1q mediates mitochondria-driven oxidative stress in neonatal hypoxic-ischemic brain injury.* J Neurosci, 2010. **30**(6): p. 2077-87.

161. Bruce, J.N., A. Falavigna, J.P. Johnson, J.S. Hall, B.D. Birch, J.T. Yoon, E.X. Wu, R.L. Fine, and A.T. Parsa, *Intracerebral clysis in a rat glioma model.* Neurosurgery, 2000. **46**(3): p. 683-91.

162. Garcia, J.H., S. Wagner, K.F. Liu, and X.J. Hu, *Neurological deficit and extent of neuronal necrosis attributable to middle cerebral artery occlusion in rats. Statistical validation.* Stroke, 1995. **26**(4): p. 627-34; discussion 635.

163. Petullo, D., K. Masonic, C. Lincoln, L. Wibberley, M. Teliska, and D.L. Yao, *Model development and behavioral assessment of focal cerebral ischemia in rats.* Life Sci, 1999. **64**(13): p. 1099-108.

164. Reglodi, D., A. Tamas, and I. Lengvari, *Examination of sensorimotor performance following middle cerebral artery occlusion in rats.* Brain Res Bull, 2003. **59**(6): p. 459-66.

165. Wahl, F., M. Allix, M. Plotkine, and R.G. Boulu, *Neurological and behavioral outcomes of focal cerebral ischemia in rats.* Stroke, 1992. **23**(2): p. 267-72.

166. Clark, W.M., N.S. Lessov, M.P. Dixon, and F. Eckenstein, *Monofilament intraluminal middle cerebral artery occlusion in the mouse.* Neurol Res, 1997. **19**(6): p. 641-8.

167. Sun, C., M. Cai, R.P. Meadows, N. Xu, A.H. Gunasekera, J. Herrmann, J.C. Wu, and S.W. Fesik, *NMR structure and mutagenesis of the third Bir domain of the inhibitor of apoptosis protein XIAP.* J Biol Chem, 2000. **275**(43): p. 33777-81.

168. Denault, J.B. and G.S. Salvesen, *Expression, purification, and characterization of caspases.* Curr Protoc Protein Sci, 2003. **Chapter 21**: p. Unit 21 13.

169. Asahi, M., X. Wang, T. Mori, T. Sumii, J.C. Jung, M.A. Moskowitz, M.E. Fini, and E.H. Lo, *Effects of matrix metalloproteinase-9 gene knock-out on the proteolysis of blood-brain barrier and white matter components after cerebral ischemia.* J Neurosci, 2001. **21**(19): p. 7724-32.

170. Rabacchi, S.A., W.J. Friedman, M.L. Shelanski, and C.M. Troy, *Divergence of the apoptotic pathways induced by 4-hydroxynonenal and amyloid beta-protein.* Neurobiol Aging, 2004. **25**(8): p. 1057-66.

171. Tu, S., G.P. McStay, L.M. Boucher, T. Mak, H.M. Beere, and D.R. Green, *In situ trapping of activated initiator caspases reveals a role for caspase-2 in heat shock-induced apoptosis.* Nat Cell Biol, 2006. **8**(1): p. 72-7.

172. Denault, J.B. and G.S. Salvesen, *Human caspase-7 activity and regulation by its N-terminal peptide.* J Biol Chem, 2003. **278**(36): p. 34042-50.

173. Tizon, B., E.M. Ribe, W. Mi, C.M. Troy, and E. Levy, *Cystatin C Protects Neuronal Cells from Amyloid-beta-induced Toxicity.* J Alzheimers Dis, 2009.

174. Liu, X.F., J.R. Fawcett, L.R. Hanson, and W.H. Frey, 2nd, *The window of opportunity for treatment of focal cerebral ischemic damage with noninvasive intranasal insulin-like growth factor-I in rats.* J Stroke Cerebrovasc Dis, 2004. **13**(1): p. 16-23.

175. Liu, X.F., J.R. Fawcett, R.G. Thorne, T.A. DeFor, and W.H. Frey, 2nd, *Intranasal administration of insulin-like growth factor-I bypasses the blood-brain barrier and protects against focal cerebral ischemic damage.* J Neurol Sci, 2001. **187**(1-2): p. 91-7.

176. Troy, C.M., J.E. Friedman, and W.J. Friedman, *Mechanisms of p75-mediated death of Hippocampal neurons: Role of caspases.* J Biol Chem, 2002. **3**: p. 3.

177. Yang, Y. and G.A. Rosenberg, *MMP-mediated disruption of claudin-5 in the blood-brain barrier of rat brain after cerebral ischemia.* Methods Mol Biol, 2011. **762**: p. 333-45.

178. Lee, S.R., K. Tsuji, S.R. Lee, and E.H. Lo, *Role of matrix metalloproteinases in delayed neuronal damage after transient global cerebral ischemia.* J Neurosci, 2004. **24**(3): p. 671-8.

179. Davidson, T.J., S. Harel, V.A. Arboleda, G.F. Prunell, M.L. Shelanski, L.A. Greene, and C.M. Troy, *Highly efficient small interfering RNA delivery to primary mammalian neurons induces MicroRNA-like effects before mRNA degradation.* J Neurosci, 2004. **24**(45): p. 10040-6.

180. Carmichael, S.T., *Themes and strategies for studying the biology of stroke recovery in the poststroke epoch.* Stroke, 2008. **39**(4): p. 1380-8.

181. Feinstein-Rotkopf, Y. and E. Arama, *Can't live without them, can live with them: roles of caspases during vital cellular processes.* Apoptosis, 2009. **14**(8): p. 980-95.

182. Monnier, P.P., P.M. D'Onofrio, M. Magharious, A.C. Hollander, N. Tassew, K. Szydlowska, M. Tymianski, and P.D. Koeberle, *Involvement of caspase-6 and caspase-8 in neuronal apoptosis and the regenerative failure of injured retinal ganglion cells.* J Neurosci, 2011. **31**(29): p. 10494-505.

183. Guegan, C., J. Braudeau, C. Couriaud, G.P. Dietz, P. Lacombe, M. Bahr, M. Nosten-Bertrand, and B. Onteniente, *PTD-XIAP protects against cerebral ischemia by anti-apoptotic and transcriptional regulatory mechanisms.* Neurobiol Dis, 2006. **22**(1): p. 177-86.

184. Fan, Y.F., C.Z. Lu, J. Xie, Y.X. Zhao, and G.Y. Yang, *Apoptosis inhibition in ischemic brain by intraperitoneal PTD-BIR3-RING (XIAP).* Neurochem Int, 2006. **48**(1): p. 50-9.

185. Rosenberg, G.A., *Matrix metalloproteinases and their multiple roles in neurodegenerative diseases.* Lancet Neurol, 2009. **8**(2): p. 205-16.

186. Ravi, R., A. Bedi, E.J. Fuchs, and A. Bedi, *CD95 (Fas)-induced caspase-mediated proteolysis of NF-kappaB.* Cancer Res, 1998. **58**(5): p. 882-6.

187. Kim, H.S., I. Chang, J.Y. Kim, K.H. Choi, and M.S. Lee, *Caspase-mediated p65 cleavage promotes TRAIL-induced apoptosis.* Cancer Res, 2005. **65**(14): p. 6111-9.

188. Rickers, A., N. Peters, V. Badock, R. Beyaert, P. Vandenabeele, B. Dorken, and K. Bommert, *Cleavage of transcription factor SP1 by caspases during anti-IgM-induced B-cell apoptosis.* Eur J Biochem, 1999. **261**(1): p. 269-74.

189. Graham, R.K., Y. Deng, E.J. Slow, B. Haigh, N. Bissada, G. Lu, J. Pearson, J. Shehadeh, L. Bertram, Z. Murphy, S.C. Warby, C.N. Doty, S. Roy, C.L. Wellington, B.R. Leavitt, L.A. Raymond, D.W. Nicholson, and M.R. Hayden, *Cleavage at the caspase-6 site is*

required for neuronal dysfunction and degeneration due to mutant huntingtin. Cell, 2006. **125**(6): p. 1179-91.

190. Horowitz, P.M., K.R. Patterson, A.L. Guillozet-Bongaarts, M.R. Reynolds, C.A. Carroll, S.T. Weintraub, D.A. Bennett, V.L. Cryns, R.W. Berry, and L.I. Binder, *Early N-terminal changes and caspase-6 cleavage of tau in Alzheimer's disease.* J Neurosci, 2004. **24**(36): p. 7895-902.

191. Klaiman, G., T.L. Petzke, J. Hammond, and A.C. Leblanc, *Targets of caspase-6 activity in human neurons and Alzheimer disease.* Mol Cell Proteomics, 2008. **7**(8): p. 1541-55.

192. Guo, H., S. Albrecht, M. Bourdeau, T. Petzke, C. Bergeron, and A.C. LeBlanc, *Active caspase-6 and caspase-6-cleaved tau in neuropil threads, neuritic plaques, and neurofibrillary tangles of Alzheimer's disease.* Am J Pathol, 2004. **165**(2): p. 523-31.

193. Park, K.J., C.A. Grosso, I. Aubert, D.R. Kaplan, and F.D. Miller, *p75NTR-dependent, myelin-mediated axonal degeneration regulates neural connectivity in the adult brain.* Nat Neurosci, 2010. **13**(5): p. 559-66.

194. Stokin, G.B., C. Lillo, T.L. Falzone, R.G. Brusch, E. Rockenstein, S.L. Mount, R. Raman, P. Davies, E. Masliah, D.S. Williams, and L.S. Goldstein, *Axonopathy and transport deficits early in the pathogenesis of Alzheimer's disease.* Science, 2005. **307**(5713): p. 1282-8.

195. Fischer, L.R., D.G. Culver, P. Tennant, A.A. Davis, M. Wang, A. Castellano-Sanchez, J. Khan, M.A. Polak, and J.D. Glass, *Amyotrophic lateral sclerosis is a distal axonopathy: evidence in mice and man.* Exp Neurol, 2004. **185**(2): p. 232-40.

196. Ferri, A., J.R. Sanes, M.P. Coleman, J.M. Cunningham, and A.C. Kato, *Inhibiting axon degeneration and synapse loss attenuates apoptosis and disease progression in a mouse model of motoneuron disease.* Curr Biol, 2003. **13**(8): p. 669-73.

197. Deveraux, Q.L., E. Leo, H.R. Stennicke, K. Welsh, G.S. Salvesen, and J.C. Reed, *Cleavage of human inhibitor of apoptosis protein XIAP results in fragments with distinct specificities for caspases.* EMBO J, 1999. **18**(19): p. 5242-51.

198. Wagner, D.C., U.M. Riegelsberger, S. Michalk, W. Hartig, A. Kranz, and J. Boltze, *Cleaved caspase-3 expression after experimental stroke exhibits different phenotypes and is predominantly non-apoptotic.* Brain Res, 2011. **1381**: p. 237-42.

199. Matus, A., R. Bernhardt, and T. Hugh-Jones, *High molecular weight microtubule-associated proteins are preferentially associated with dendritic microtubules in brain.* Proc Natl Acad Sci U S A, 1981. **78**(5): p. 3010-4.

200. Tytell, M., S.T. Brady, and R.J. Lasek, *Axonal transport of a subclass of tau proteins: evidence for the regional differentiation of microtubules in neurons.* Proc Natl Acad Sci U S A, 1984. **81**(5): p. 1570-4.

201. Bergeron, L., G.I. Perez, G. Macdonald, L. Shi, Y. Sun, A. Jurisicova, S. Varmuza, K.E. Latham, J.A. Flaws, J.C. Salter, H. Hara, M.A. Moskowitz, E. Li, A. Greenberg, J.L. Tilly, and J. Yuan, *Defects in regulation of apoptosis in caspase-2-deficient mice.* Genes Dev, 1998. **12**(9): p. 1304-14.

202. Slee, E.A., M.T. Harte, R.M. Kluck, B.B. Wolf, C.A. Casiano, D.D. Newmeyer, H.G. Wang, J.C. Reed, D.W. Nicholson, E.S. Alnemri, D.R. Green, and S.J. Martin, *Ordering the cytochrome c-initiated caspase cascade: hierarchical activation of caspases-2, -3, -6, -7, -8, and -10 in a caspase-9-dependent manner.* J Cell Biol, 1999. **144**(2): p. 281-92.

203. Teng, K.K., S. Felice, T. Kim, and B.L. Hempstead, *Understanding proneurotrophin actions: Recent advances and challenges.* Dev Neurobiol, 2010. **70**(5): p. 350-9.

204. Teng, H.K., K.K. Teng, R. Lee, S. Wright, S. Tevar, R.D. Almeida, P. Kermani, R. Torkin, Z.Y. Chen, F.S. Lee, R.T. Kraemer, A. Nykjaer, and B.L. Hempstead, *ProBDNF induces neuronal apoptosis via activation of a receptor complex of p75NTR and sortilin.* J Neurosci, 2005. **25**(22): p. 5455-63.

205. Troy, C.M., J.E. Friedman, and W.J. Friedman, *Mechanisms of p75-mediated death of hippocampal neurons. Role of caspases.* J Biol Chem, 2002. **277**(37): p. 34295-302.

206. Volosin, M., W. Song, R.D. Almeida, D.R. Kaplan, B.L. Hempstead, and W.J. Friedman, *Interaction of survival and death signaling in basal forebrain neurons: roles of neurotrophins and proneurotrophins.* J Neurosci, 2006. **26**(29): p. 7756-66.

207. Hengst, U., A. Deglincerti, H.J. Kim, N.L. Jeon, and S.R. Jaffrey, *Axonal elongation triggered by stimulus-induced local translation of a polarity complex protein.* Nat Cell Biol, 2009. **11**(8): p. 1024-30.

208. Ahmed, Z., H. Kalinski, M. Berry, M. Almasieh, H. Ashush, N. Slager, A. Brafman, I. Spivak, N. Prasad, I. Mett, E. Shalom, E. Alpert, A. Di Polo, E. Feinstein, and A. Logan, *Ocular neuroprotection by siRNA targeting caspase-2.* Cell Death Dis, 2011. **2**: p. e173.

209. Kothari, R., E. Jauch, J. Broderick, T. Brott, L. Sauerbeck, J. Khoury, and T. Liu, *Acute stroke: delays to presentation and emergency department evaluation.* Ann Emerg Med, 1999. **33**(1): p. 3-8.

210. Cunningham, L.A., M. Wetzel, and G.A. Rosenberg, *Multiple roles for MMPs and TIMPs in cerebral ischemia.* Glia, 2005. **50**(4): p. 329-39.

211. Taoufik, E., S. Valable, G.J. Muller, M.L. Roberts, D. Divoux, A. Tinel, A. Voulgari-Kokota, V. Tseveleki, F. Altruda, H. Lassmann, E. Petit, and L. Probert, *FLIP(L) protects neurons against in vivo ischemia and in vitro glucose deprivation-induced cell death.* J Neurosci, 2007. **27**(25): p. 6633-46.

Appendices. Detailed Protocols

Appendix I. Cell Lysis Buffers

RIPA Buffer

150 mM	Sodium Chloride
1.0%	NP-40 or Triton X-100
0.5%	Sodium Deoxycholate
0.1%	SDS (sodium dodecyl sulphate)
50 mM	Tris, pH 7.4

CHAPS Buffer

150 mM	KCl
50 mM	HEPES
0.1%	CHAPS
pH 7.4	

bVAD Buffer

10%	Glycerol
150 mM	NaCl
0.2%	NP-40
20 mM	Tris-HCl (pH 7.3)

4x Laemmli Buffer (SDS Sample Buffer)

8%	SDS
40%	glycerol
240 mM	Tris, pH 6.8
0.04%	bromophenol blue

Appendix II. Active Caspase Precipitation

Protocol 1. With CHAPS Lysis Buffer
bVAD administered prior to stroke by clysis (CED) injection.

Materials & Solutions:
a. CHAPS Buffer (pH 7.4)
- 150 mM KCl
- 50 mM HEPES
- 0.1% CHAPS

b. Roche Protease Inhibitor tablet or equivalent.
c. CHAPS w/o protease inhibitors (50 ml)
d. CHAPS w/ protease inhibitors (10 ml)
e. Plain agarose beads (GE Life Science# 17-0120-01)
f. Streptavidin-agarose beads (Invitrogen# SA100-04)
g. 1x Laemmli Sample Buffer without BME (100-200 ml)

Tissue Preparation:
1. Lyse tissue with pestle and 200 ml CHAPS Buffer w/ protease inhibitors
    a. Incubate on ice for 15 min
    b. Transfer 75% of the lysate to a new tube (sol. fraction)
    c. Label remaining 25% as whole cell lysate (WCL) and freeze at -20 °C

2. Isolate soluble fraction by centrifugation @ 13,000 rpm for 10 min
    a. Transfer supernatant to a new tube
    b. Measure protein concentration w/ Bio-Rad Bradford assay

Pre-clearing the lysate:
3. Transfer 30 ml of agarose beads into a fresh 0.5-ml microfuge tube.
    a. Use a cut tip

4. Wash beads with 300 ml cold CHAPS Buffer w/o protease inhibitors; Centrifuge @ 7,000 rpm for 3 min 4 °C; Aspirate/Discard supernatant
    a. Repeat 2x
    b. After 3rd spin, aspirate as much CHAPS Buffer as possible without removing beads.

5. Apply 150 mg of protein sample to washed agarose beads
    a. Fill to 300 ml with CHAPS Buffer **w/** protease inhibitors
    b. Rotate @ 4 °C for 1.0 hr

6. Centrifuge pre-clear @ 7,000 rpm for 5 min @ 4 °C
    a. Transfer pre-cleared lysate with a 200 ml pipette to pre-washed Streptavidin-agarose beads (see below)

b. Discard pre-clear Sepharose beads

bVAD isolation

7. Transfer 30 ml of Streptavidin-agarose beads into a fresh 500 ml microfuge tube.

8. Wash beads with 300 ml cold CHAPS Buffer **w/o** protease inhibitors; Centrifuge @ 7,000 rpm for 3 min @ 4 °C; Aspirate/Discard supernatant
    a. Repeat 2x
    b. After 3rd spin, aspirate as much CHAPS Buffer as possible without removing beads.

9. Apply **pre-cleared lysate** (from above) to washed Streptavidin-agarose beads
    a. Rotate at 4 °C overnight

10. Centrifuge sample @ 7,000 rpm for 5 min @ 4 °C
    a. Aspirate supernatant

11. Wash beads with 300 ml cold CHAPS Buffer w/o protease inhibitors; Centrifuge sample @ 5,000 rpm for 5 min @ 4 °C; Aspirate/discard supernatant
    a. Repeat 14x
    b. After the final wash remove as much CHAPS Buffer as possible with a 10 ml pipette

12. Add 25 ml of 1X Laemmli Sample Buffer w/o BME to beads
    a. Boil for 5 min in water bath
    b. Centrifuge sample @ 14,000 rpm for 10 min

13. Transfer supernatant to a fresh 500 ml tube
    a. Store at -20 °C until ready to run on SDS-PAGE
    b. On the day of electrophoresis, add 5% BME and boil for 5 min in water bath
    c. Discard Streptavidin beads

Protocol 2. With bVAD Lysis Buffer
bVAD administered prior to lysis (i.e. clysis).

Materials & Solutions:

a. *bVAD Lysis Buffer*[211]

- 10% Glycerol
- 150 mM NaCl
- 0.2% NP-40
- 20 mM Tris-HCl (pH 7.3)
- Roche Protease Inhibitor tablet or equivalent.

b. bVAD lysis buffer w/o protease inhibitors (50 ml)

c. Plain Agarose Resin (GE Life Science# 17-0120-01)

d. Streptavidin Agarose Resin (Invitrogen# SA100-04) or NeutrAvidin Agarose Resin (Pierce #29200)

e. 1x Laemmli Sample Buffer without reducing agent (100-200 ml)

Tissue Preparation:

1. Lyse tissue with pestle and 200 ml bVAD LYSIS Buffer w/ protease inhibitors
    a. Incubate on ice for 15 min

2. Isolate soluble fraction by centrifugation @ 13,000 rpm for 10 min
    a. Transfer supernatant to a new tube
        i. Discard pellet
    b. Measure protein concentration w/ Bio-Rad Bradford assay

Pre-clearing the lysate:

3. Transfer 40 ml of Plain Agarose Resin into a fresh 0.5-ml microfuge tube.
    a. Use a cut tip

4. Wash beads with 300 ml cold bVAD Lysis Buffer w/o protease inhibitors; Centrifuge @ 7,000 rpm for 3 min 4 °C; Aspirate/Discard supernatant
    a. Repeat 2x
    b. After 3rd spin, aspirate as much bVAD Lysis Buffer as possible without removing beads.

5. Apply 100 - 120 mg of sample protein to washed agarose beads
    a. Fill to 300 ml with bVAD Lysis Buffer **w/** protease inhibitors
    b. Rotate @ 4 °C for 1.0 hr

6. Centrifuge pre-clear @ 7,000 rpm for 5 min @ 4 °C
    a. Transfer pre-cleared lysate with a 200 ml pipette to pre-washed Streptavidin-agarose beads (see below)
    b. Discard pre-clear Sepharose beads

bVAD isolation

7. Transfer 40 ml of Streptavidin-agarose beads into a fresh 500 ml microfuge tube.

8. Wash beads with 300 ml cold bVAD Lysis Buffer **w/o** protease inhibitors; Centrifuge @ 7,000 rpm for 3 min @ 4 °C; Aspirate/Discard supernatant
    a. Repeat 2x
    b. After 3rd spin, aspirate as much bVAD Lysis Buffer as possible without removing beads.

9. Apply **pre-cleared lysate** (from above) to washed Streptavidin-agarose beads

a. Rotate at 4 °C overnight

10. Centrifuge sample @ 7,000 rpm for 3 min @ 4 °C
    a. Aspirate supernatant

11. Wash beads with 300 ml cold bVAD Lysis Buffer w/o protease inhibitors; Centrifuge sample @ 7,000 rpm for 5 min @ 4 °C; Aspirate/Discard supernatant
    a. Repeat 14x
    b. After the final wash remove as much bVAD Lysis Buffer as possible with a 10 ml pipette

12. Add 25 ml of 1X Laemmli Sample Buffer w/o BME to beads
    a. Boil for 5 min in water bath
    b. Centrifuge sample @ 14,000 rpm for 10 min

13. Transfer supernatant to a fresh 500 ml tube
    a. Store at -20 °C until ready to run on SDS-PAGE
    b. On the day of electrophoresis, add 5% BME and boil for 5 min in water bath
    c. Discard Streptavidin beads

Appendix III. Axon Flotation
Axon Flotation Method adapted for Rat tissue.

Solutions:

Isolation Buffer (Buffer A) pH 6.6

100 mM	NaCl (58.44 g/mol)
10 mM	phosphate buffer (0.0964% NaH_2PO_4-H_2O & 0.0808% Na_2HPO_4-$7H_2O$)
5 mM	EDTA (372.24 g/mol) (from 0.5 M EDTA stock solution)
0.85 M	sucrose (342.30 g/mol)

Demyelination Buffer (Buffer B) pH 6.6

100 mM	NaCl
10 mM	phosphate buffer
5 mM	EDTA
1%	Triton-X

Wash Buffer (Buffer C) pH 6.6

100 mM	NaCl
10 mM	phosphate buffer
5 mM	EDTA

Dissection:

1. After brain has been removed from skull/meninges, place brain in brain block
2. From bregma, place one razor 3 mm anterior and another razor 1 mm posterior (4 mm brain section
3. Carefully separate striatum, white matter tracts, and cortical matter
    a. Place in 1.5 ml Eppendorf tube and flash freeze with liquid nitrogen
    b. On day of axon isolation keep sections on dry ice until ready to put in Dounce homogenizer

Axon Isolation:

1. Place dissected piece into Dounce homogenizer.
2. Add **500 ml** of **Buffer A** and gently homogenize
    a. Wash homogenizer & pestle with 70% Ethanol followed by H_2O between each sample.
3. Centrifuge samples @ **10,000 x *g*** for **15 min**
    a. Transfer Myelin float **(200 µl)** to a new tube
    b. Transfer the remaining soluble fraction to a new tube
        i. **Label** "sol. frac."
        ii. This will be the **inputs** for western blotting
        iii. Optional: Save the pellet fraction (**label** pellet)
            1. Contains unmyelinated axons/nuclei/insoluble proteins
4. Add **500 ml** of **Buffer A** and repeat homogenization with myelin fraction in Dounce homogenizer

a. Centrifuge samples @ **10,000 x *g*** for **15 min**
b. Transfer myelin float **(200 µl)** to new tube
c. Do not save sol. frac or pellet
d. Repeat step 4 two more times

Demyelination and Washing:

5. Resuspend myelin float w/ **500 ml Buffer B**
a. Homogenize with Dounce homogenizer

6. Demyelinate by placing tube in rocker for **1hr** at **4 °C**

7. Pellet axoplasm proteins w/ **10,000 x *g*** for **15 min**

8. Remove as much supernatant as possible without disturbing the white pellet.

9. Wash and Pellet 3x with **500 ml Buffer C**
a. Pellet: Centrifuge at **10,000 x *g*** for **15 min**

10. Resuspend axons in **25 ml RIPA buffer with Roche protease inhibitors**

11. Measure Protein Concentration and run SDS-PAGE